THE UNIVERSITY OF ALBERTA

STRONG VISCOUS INTERACTIONS
IN
UNSTEADY HIGH SPEED FLOWS

BY

© ROOP NARAYAN GUPTA

A THESIS

SUBMITTED TO THE FACULTY OF GRADUATE STUDIES

IN PARTIAL FULFILMENT OF THE REQUIREMENTS FOR THE DEGREE

OF

DOCTOR OF PHILOSOPHY

DEPARTMENT OF MECHANICAL ENGINEERING

EDMONTON, ALBERTA

FALL, 1970

THE UNIVERSITY OF ALBERTA

STRONG VISCOUS INTERACTIONS
IN
UNSTEADY HIGH-SPEED FLOWS

BY

ROOP NARAYAN GUPTA

A THESIS

SUBMITTED TO THE FACULTY OF GRADUATE STUDIES

IN PARTIAL FULFILLMENT OF THE REQUIREMENTS FOR THE DEGREE

OF

DOCTOR OF PHILOSOPHY

DEPARTMENT OF MECHANICAL ENGINEERING

EDMONTON, ALBERTA

FALL, 1970

UNIVERSITY OF ALBERTA

FACULTY OF GRADUATE STUDIES

The undersigned certify that they have read, and recommend to the Faculty of Graduate Studies for acceptance, a thesis entitled "STRONG VISCOUS INTERACTIONS IN UNSTEADY HIGH SPEED FLOWS" submitted by ROOP NARAYAN GUPTA in partial fulfilment of the requirements for the degree of Doctor of Philosophy.

UNIVERSITY OF ALBERTA

FACULTY OF GRADUATE STUDIES

The undersigned certify that they have read, and recommend to the Faculty of Graduate Studies for acceptance, a thesis entitled "STRONG VISCOUS INTERACTIONS IN UNSTEADY HIGH SPEED FLOWS" submitted by ROOP NARAYAN GUPTA in partial fulfillment of the requirements for the degree of Doctor of Philosophy.

ABSTRACT

The hypersonic laminar two-dimensional flow over a stepwise-accelerated semi-infinite flat plate at zero angle of attack is analysed. The boundary layer governing momentum and energy equations are transformed in terms of the dimensionless stream function and the dimensionless total enthalpy (S). These coupled equations have been solved numerically for Prandtl number unity, pressure gradient parameter $\beta = 0.286$ and 0.4, $0 \leq S_w \leq 1$, and $0 \leq \xi \leq 0.3$ with $\xi = (1 + \bar{X}/V_e\bar{T})^{-1}$. The obtained solutions are utilized to compute the time-dependent displacement thickness which is subsequently used to obtain the strong interaction induced pressure (according to the Lighthill's Piston Theory) for $5 \leq M_e \leq 10$. For the same range of Mach numbers, the transient contributions to the boundary-layer velocity, the boundary-layer temperature and to the shear stress at the wall are also given.

ACKNOWLEDGEMENTS

The author wishes to express his deep appreciation to Dr. C.M. Rodkiewicz for his guidance and supervision of this thesis. His constant encouragement during the course of this investigation is thankfully acknowledged.

Mention must be made of the many fruitful discussions the author had with Dr. F.A. Baragar of the Department of Mathematics and Dr. J. Tartar of the Department of Computing Science.

The financial support in the form of fellowships from the University of Alberta and the National Research Council of Canada is gratefully acknowledged.

Additional thanks are extended to Miss M. Steinke who contributed in various ways. Her suggestions in the editing of the thesis are well appreciated. Mr. V. Srinivasan also helped in the editing and Mr. T.K. Chattodpadhyay assisted in proof reading the manuscript. Their assistance is well acknowledged. Thanks are also due to Miss H. Wozniuk for her excellent typing of the thesis.

Finally, the author would like to express his appreciation to his parents for their encouragement and consideration.

TABLE OF CONTENTS

TABLE OF CONTENTS (Continued)

TABLE OF CONTENTS (Continued)

LIST OF FIGURES

LIST OF FIGURES (Continued)

LIST OF FIGURES (Continued)

LIST OF SYMBOLS

a	velocity of sound
a	coefficient in difference eq. (A.12)
A	constant coefficient, defined by eq. (3.32a)
A	constant in eq. (4.26b)
A_1 A_2 A_3	constant coefficients, defined by eq. (3.28)
b	coefficient in difference eq. (A.12)
B	constant coefficient, defined by eq. (3.32b)
C	coefficient in difference eq. (A.12)
Cp	specific heat at constant pressure
C	$\mu T_o/\mu_o T$
C	coefficient, defined by eq. (A.32)
C_f	local skin friction coefficient, defined by eq. (4.29)
d	coefficient in difference eq. (A.12)
e	constant in eq. (2.42)
e	coefficient in difference eq. (A.12)
f	nondimensional stream function, defined by eq. (2.37)
$\overline{f}$	$= f-\eta$
Δf	$= f-f_2$
g	nondimensional local enthalpy ratio $= h/h_e$
h	local enthalpy

H	total enthalpy = $h + u^2/2$
H	interval of differencing in η-direction
I	integral, defined by eq. (4.11)
I*	integral, defined by eq. (4.13)
I**	integral, defined by eq. (4.14)
J	integral, defined by eq. (4.19)
k	thermal conductivity
k	bound in computer program on values of $\bar{f}'$
K	coefficient, defined by eq. (5.2)
m	exponent from $V_e = e\bar{X}^m$
m	an integer in numerical method
M	Mach number
n	an integer in numerical method
Nu	Nusselt number
p	thermodynamic pressure
Pr	Prandtl number
q	heat transfer
Q	count of successive solutions of the momentum equation in the procedure of solution
R	gas constant
R	coefficient, defined by eq. (A.31)
Re	Reynolds number
S	nondimensional total enthalpy ratio = H/H_e
$\bar{S}$	= S-1

t	time variable
$\bar{t}$, $\bar{\bar{t}}$	transformed time variables
T	temperature
$\bar{T}$, $\bar{\bar{T}}$	transformed time variables
T	interval of differencing in ξ-direction
T_1	interval of differencing in ξ-direction
u	x-component of velocity
U	free stream velocity
v	y-component of velocity
V	modified free stream velocity, defined by eq. (2.38)
W_p	piston velocity, defined by eq. (4.7)
x	coordinate along the wall
$\bar{x}$, $\bar{\bar{x}}$, $\bar{X}$, $\bar{\bar{X}}$	transformed coordinates along the wall
y	coordinate normal to the wall
$\bar{y}$, $\bar{\bar{y}}$, $\bar{Y}$, $\bar{\bar{Y}}$	transformed coordinates normal to the wall

β	pressure gradient parameter
γ	ratio of specific heats
δ^*	mass flow defect thickness, defined by eq. (4.3a)
δ_ρ	density defect thickness, defined by eq. (4.3b)
Δ	unsteady displacement thickness
ξ	modified similarity independent variable associated with time and space, defined by eq. (3.3)
η	similarity independent variable associated with space
μ	dynamic viscosity coefficient
ν	kinematic viscosity coefficient
ρ	density
τ	shear stress
τ	similarity independent variable associated with time and space
χ	hypersonic interaction parameter, defined by eq. (4.16)
ψ	stream function

Subscripts

e	evaluation in free stream ($y=y_e$)
ref	reference
w	evaluation at wall ($y=0$)
0	free stream stagnation value
1	condition just after the step-change in free stream velocity
2	final steady state

Superscripts

.	differentiation with respect to τ
'	differentiation with respect to η

CHAPTER I

INTRODUCTION AND DISCUSSION OF THE LITERATURE

1.1 Statement of the Unsteady Hypersonic Flow Problem

There are many situations where a quantitative description of the transient development of a boundary layer would be desirable and valuable; a few of these are aircraft and missiles in unsteady flight, oscillating wings, unsteady nozzle flow, blades rotating in non-uniform air streams, etc. In evaluating the forces acting on the components of aircraft and missiles during their maneuverability and control, viscous interactions have to be analysed. The viscous aspects of shock wave interaction phenomenon for such a case require the study of time-dependent boundary layers. The sharp-leading-edge bodies shall be considered for purposes of our investigation.

The problem to be discussed here, considers the interaction between the viscous and inviscid effects, when the high Mach number flow over a flat plate at zero angle of attack is stepwise-accelerated by a small amount in the direction of the initial flow. The induced pressure due to the viscous interactions will be obtained from the analysis of the temporal velocity and enthalpy boundary layers. Expressions will also be obtained for the transient shear-stress and heat transfer at the wall.

1.2 Review of the Associated Literature

The first treatment of the transient boundary layer was presented by Blasius [1] in 1908, who considered the "impulsive" start of bluff bodies such as cylinders. More recently, the review articles by Stewartson [2] and Rott [3] have covered the field in greater detail. Some of this literature, which has direct bearing to our work, will be discussed here.

Moore [4] considered the case of compressible laminar flow over a semi-infinite flat plate. In his analysis he found a group of parameters, whose magnitude determines the nature of flow unsteadiness for an arbitrary velocity U(t). Ostrach [5] extended Moore's work of zero wall heat transfer to the case of an isothermal surface. These are the asymptotic solutions for large times. In a recent paper Yang and Huang [6] supplemented the above with the solutions for small times. The boundary layer solutions of references [4], [5] and [6] have been utilized by Zien and Reshotko [7] to obtain the transient weak viscous interaction pressures. As a first approximation to the induced surface pressure, they have taken it equal to the acoustic pressure on a one-dimensional piston moving at a variable, but low, speed.

Stewartson [2,8], while considering the impulsive motion of a flat plate, gave an interesting explanation of how the initial Rayleigh solution, having no x-dependence, could possibly change over to the x-dependent but time-independent Blasius solution. He obtained two solutions, one for $\tau(= U_\infty t/x) > 1$ and the other for $\tau < 1$ with a singu-

larity at $\tau = 1$. He employed two different methods, namely, the Oseen's approximation and the momentum integral method to obtain these solutions. Stewartson argued that for $\tau << 1$, since a disturbance from the leading edge has not arrived yet, Rayleigh-type flow prevails; whereas, at $\tau = 1$ the leading edge effect is felt suddenly and the flow acquires its x-dependence through an essential singularity at this point. The existence of singularity was further supported by Smith [9] who generalized Stewartson's work for a wedge.

Lam and Crocco [10] investigated the boundary layer induced by a shock travelling down a semi-infinite flat plate. At time $t = 0$ the shock is at the leading edge of the plate, $x = 0$. For the special case of a very weak shock the problem becomes identical to Stewartson's impulsive plate problem. Using the Prandtl boundary layer equations under the Crocco transformation they give sufficient conditions for unique solution to the governing equations for the case $\rho\mu$ = constant and demonstrate the feasibility of enforcing two streamwise boundary conditions for such a problem. The boundary layer is divided in two parts:

(1) a region where the solution of Mirels [11] is valid ($\tau < 1$);

(2) the region, $\tau > 1$,

where both the leading edge effects and the effect of the shock solution downstream must be considered. The results are directly analogous to Stewartson's. In the region $\tau > 1$ the governing equations, although parabolic in nature, admit boundary conditions which are usually as-

sociated with elliptic equations. This type of behavior has been termed "singular parabolic" by Gevrey [12] and also Lam and Crocco [10]. It is in this second region that the "elliptic" boundary conditions must be enforced; i.e., boundary conditions must be given on $\tau = 1, \infty$ for $0 \leq \eta(= \frac{u}{U_\infty}) \leq 1$ and on $\eta = 0, 1$ for $1 \leq \tau \leq \infty$. Though the complete solution to the problem was not given by Lam and Crocco, the detailed discussion of the properties of the solution was provided.

Stewartson's singularity was also encountered by Cheng [13] who investigated the problem of a sharp-edged flat plate starting from rest and following a power law motion. Cheng expands the stream function in powers of quantity

$$\xi = \frac{x(n+1)}{At^{n+1}} \quad \text{with } U_o(t) = At^n \ .$$

He obtains a solution which is valid for large times (i.e. $\xi << 1$). For large ξ the solution is of the Rayleigh type. Later Cheng and Elliott [14] extended this to arbitrary plate velocity if the plate was started initially from rest.

Using the approximate momentum integral method Schuh [15] calculated unsteady boundary layers on bodies of arbitrary shape and for arbitrary variation with time, of the speed outside the boundary layer. He observed discontinuity in the slope of the skin friction distribution between $\frac{1}{\tau} = 0$ and $\frac{1}{\tau} = 1.0$ for the case of a flat plate. He attributed this to the failure of the boundary layer theory assumptions

near the leading edge. This will have to be resolved by using the Navier-Stokes equations in place of the boundary layer equations. With the complete Navier-Stokes equations the discontinuity would vanish at the leading edge and with it also the discontinuity in the slope of the skin friction distribution.

Schetz and Oh [16] also used the momentum integral technique to obtain the velocity field with a new type of profile. They have analysed the transient development of the boundary layer on a flat plate due to the impulsive start of motion of the surrounding fluid. They admit that their approximate solution, valid at every "x" station and for all times i.e. $0 < t < \infty$, tends to mask the detailed mathematical behavior of an exact solution. It cannot be expected to resolve the problem of "joining" at $\tau = 1$.

Tokuda [17] presented a solution to the Stewartson's problem [2,8] without having an essential singularity by "stretching" the co-ordinates. His erroneous conclusion that a power series solution exists about the Rayleigh solution for small times was corrected by Brown, Stewartson and Lam [18].

Recently Ban [19] has shown analytically the presence of an essential singularity at $\tau = 1$. He investigated the velocity and temperature boundary layers developed on a plane wall by the ideal shock-tube flow for the case of weak shock and expansion waves. Following Friedrichs theory [20] of symmetric positive linear differential equations Ban has provided the proof for the uniqueness and existence of his solutions to

the singular parabolic equations. As the basic character of the differential equations is different for $\tau > 1$ than for $\tau < 1$, he points out the necessity of an essential singularity for the problem to be properly posed. Murdock [21] developed an integral technique to solve a general class of shock-induced boundary layer problems including Ban's problem.

The difficulty at $\tau = 1$ was also experienced by Rodkiewicz and Reshotko [22] while dealing with the transient weak interactions. Their results for temporal shear stress, heat transfer and induced pressures cover the range $0 \leq \tau < 1$.

1.3 Choice of Variables

The literature survey pertinent to the present work suggests that in formulation of the transient boundary layer problem one of the independent variables should be of the type:

$$\tau = \frac{U_\infty t}{x} \quad .$$

The other independent variable has been chosen to be of the form:

$$\eta = \left[\frac{(m+1)\, U_\infty}{2\nu_o\, x}\right]^{\frac{1}{2}} \int_0^y \frac{\rho}{\rho_o}\, dy \quad .$$

The present problem has been formulated primarily to obtain the transient pressure distribution for the case of strong interaction (with non-zero pressure gradients). The weak interaction problem (with

initial zero pressure gradient) has been dealt with in references [22] and [23]. In the present analysis the equations have been developed with suitable distortion of the coordinates, which are especially suited for the study of flow with pressure gradients. The following hypersonic assumption has been made in the theory [22]

$$\frac{\partial U_e}{\partial t} = \frac{\partial h_e}{\partial t} = \frac{\partial H_e}{\partial t} = 0 \; ; \; H = h + \frac{u^2+v^2}{2} \simeq h + \frac{u^2}{2} \qquad (1.1)$$

i.e. the free stream adjusts itself instantaneously to the new conditions.

In a transient supersonic flow, there are three stages in the transient pressure distribution before the establishment of an Ackeret pressure distribution on the surface of an airfoil corresponding to the new free stream conditions. These three stages are:

(i) the time interval prior to arrival of the fastest signal from the leading edge;

(ii) the time interval between arrival of the fastest signal and the slowest signal from the leading edge;

(iii) and the final steady Ackeret pressure distribution after the arrival of the slowest signal from the leading edge.

With the increase in Mach number the time interval between arrival of the fastest signal and the slowest signal at a point on the body decreases approximately as $1/M^2$. Therefore, one may say that at very high Mach numbers the equivalent of the Ackeret pressure distribution is established (from a potential flow point of view) almost instantaneously.

1.4 Approach to the Strong Interaction Problem

The time-dependent two-dimensional boundary layer equations for a compressible fluid have been taken as the governing equations for the problem under consideration. These equations have been reduced to a coupled set of third order partial differential equations in two independent variables η and τ mentioned earlier. Next chapter gives a detailed account of the transformations employed for such a reduction. These coupled equations have been solved for the hypersonic pressure gradient

$$\beta = \frac{\gamma-1}{\gamma}$$

which corresponds to the strong interaction case. The numerical method, described in Chapter III, is an implicit finite difference technique which is inherently stable. This numerical method has been extensively used and produces results of high accuracy.

The solutions to the momentum and the energy equations give at once the shearing stress and heat transfer at the wall for a specified wall temperature. The relevant expressions have been obtained in section 4.3 of Chapter IV. In order to obtain the viscous interaction induced pressure, the boundary layer solutions of Chapter III have been utilized to obtain the displacement thickness. Employing Lighthill's concept [24] of a one-dimensional piston pushing into air the computed displacement thickness has been used to obtain the "piston velocity" and subsequently the strong interaction induced pressure over the plate

surface. The results for different values of Mach Number, wall heat transfer and the transient parameter $\xi(= \tau/\tau+1)$ have been displayed graphically for $\gamma = 1.4$ and $\gamma = 1.67$. The discussion of the results is included in the last chapter.

It should be mentioned that Lighthill's piston theory is accurate only for $M_e\sigma < 1$, where σ is the local inclination of the shock to the free stream. The changes in the entropy increase with $M_e\sigma$, and it becomes necessary to account for them in an adequate formulation for large $M_e\sigma$. We neglect the shock curvature and assume the flow to be isentropic except across the shock in order to avoid variations of entropy across the stream lines. Following Miles [25] we have used the extension of Lighthill's piston theory for large $M_e\sigma$. Miles has suggested that such an extension can be made simply by replacing the Lighthill's simple wave relations by the corresponding relations for an oblique shock. Expression (4.6) of Chapter IV represents the results of Mile's extension as applied to present work.

Generally the boundary layer in hypersonic flow is thick and doubts may arise regarding validity of the Prandtl's theory. Shen's [26] criterion of $\delta^*/x << 1$ has been met in order to justify the use of Prandtl's boundary-layer theory.

CHAPTER II

FLOW GOVERNING EQUATIONS

2.1 Boundary-Layer Equations

The unsteady, two-dimensional flow of a compressible viscous fluid along a semi-infinite flat plate will be considered. With the coordinate system fixed with reference to the plate and origin at the leading edge, the usual boundary layer approximation gives the following equations [29]:

Conservation of Momentum

$$\rho\left(\frac{\partial u}{\partial t} + u\frac{\partial u}{\partial x} + v\frac{\partial u}{\partial y}\right) = \rho\frac{\partial U_e}{\partial t} - \frac{\partial p}{\partial x} + \frac{\partial}{\partial y}\left(\mu\frac{\partial u}{\partial y}\right) \tag{2.1}$$

$$0 = \frac{\partial p}{\partial y} \tag{2.2}$$

Conservation of Energy

$$\rho\left(\frac{\partial h}{\partial t} + u\frac{\partial h}{\partial x} + v\frac{\partial h}{\partial y}\right) = \frac{\partial p}{\partial t} + u\frac{\partial p}{\partial x} + \frac{\partial}{\partial y}\left(\frac{\mu}{Pr}\frac{\partial h}{\partial y}\right) + \mu\left(\frac{\partial u}{\partial y}\right)^2 \tag{2.3}$$

Conservation of Mass

$$\frac{\partial \rho}{\partial t} + \frac{\partial}{\partial x}(\rho u) + \frac{\partial}{\partial y}(\rho v) = 0 \tag{2.4}$$

Outside the boundary layer where the effects of viscosity and heat conduction are neglected, velocity, pressure, temperature and density are functions of x and t only. The following relations are satisfied in the free-stream:

$$\rho_e\left(\frac{\partial U_e}{\partial t} + U_e \frac{\partial U_e}{\partial x}\right) = \rho_e \frac{\partial U_e}{\partial t} - \frac{\partial p_e}{\partial x} \tag{2.1a}$$

$$\rho_e\left(\frac{\partial h_e}{\partial t} + U_e \frac{\partial h_e}{\partial x}\right) = \frac{\partial p_e}{\partial t} + U_e \frac{\partial p_e}{\partial x} \tag{2.3a}$$

$$\frac{\partial \rho_e}{\partial t} + \frac{\partial}{\partial x}(\rho_e U_e) = 0 \tag{2.4a}$$

The boundary conditions are:

$$y = 0: \quad u = v = 0 \ , \ h = h_w(x,t) \tag{2.5}$$

$$y = y_e: \quad u = U_e(x,t) \ , \ h = h_e(x,t) \tag{2.6}$$

2.2 Transformed Boundary-Layer Equations

The equations of Section 2.1 suffer from several disadvantages: for example, they may be singular at x = 0, and the boundary layer thickness varies greatly with x near the leading edge (in the strong interaction regime). In this section they are transformed to a more convenient coordinate system by making a change of variables in the original boundary layer equations. Some of these new equations exhibit

much more clearly the role of certain parameters and of the viscosity law, as well as the relation to the incompressible case. They are also more suitable for numerical computations.

2.2a Dorodnitsyn-Howarth Transformation (in the restricted form)

In the case of zero pressure gradient, Dorodnitsyn-Howarth's restricted transformation is equivalent to the Howarth-Stewartson transformation to be introduced for non-zero pressure gradients. The purpose of this transformation is to remove the density ρ from the formal equations, and introduces the following new independent variables

$$\bar{t} \equiv t \ , \ \bar{x} \equiv x \ , \ \bar{y} = \int_0^y \frac{\rho}{\rho_o} \, dy \ . \tag{2.7}$$

The derivatives occurring in (2.1) through (2.4) become

$$\frac{\partial}{\partial t} = \frac{\partial}{\partial \bar{t}} + \frac{\partial}{\partial \bar{y}} \frac{\partial \bar{y}}{\partial t}$$

$$\frac{\partial}{\partial x} = \frac{\partial}{\partial \bar{x}} + \frac{\partial}{\partial \bar{y}} \frac{\partial \bar{y}}{\partial x} \tag{2.8}$$

$$\frac{\partial}{\partial y} = \frac{\rho}{\rho_o} \frac{\partial}{\partial \bar{y}} \ .$$

The equations (2.8 are now applied to (2.1) and (2.3) to give, respectively,

$$\rho\{\frac{\partial u}{\partial \bar{t}} + u\frac{\partial u}{\partial \bar{x}} + (\frac{\partial \bar{y}}{\partial t} + u\frac{\partial \bar{y}}{\partial x} + \frac{\rho}{\rho_o}v)\frac{\partial u}{\partial \bar{y}}\}$$

$$= -\frac{\partial p}{\partial \bar{x}} + \frac{\rho}{\rho_o}\frac{\partial}{\partial \bar{y}}(\frac{\mu\rho}{\rho_o}\frac{\partial u}{\partial \bar{y}}) \tag{2.9}$$

$$\rho\{(\frac{\partial H}{\partial \bar{t}} + \frac{\partial H}{\partial \bar{y}}\frac{\partial \bar{y}}{\partial t}) + u(\frac{\partial H}{\partial \bar{x}} + \frac{\partial H}{\partial \bar{y}}\frac{\partial \bar{y}}{\partial x}) + \frac{\rho}{\rho_o}v\frac{\partial H}{\partial \bar{y}}\}$$

$$= \frac{\rho}{\rho_o}\frac{\partial}{\partial \bar{y}}\{\frac{\mu\rho}{Pr\rho_o}\frac{\partial H}{\partial \bar{y}} + \frac{\mu\rho}{\rho_o}(1 - \frac{1}{Pr})u\frac{\partial u}{\partial \bar{y}}\} \tag{2.10}$$

(2.10) being derived from (2.1) and (2.3) for the new dependent variable H with the hypersonic assumption (1.1).

It is now convenient to introduce the stream function ψ such that

$$u = \frac{\partial \psi}{\partial \bar{y}} \tag{2.11}$$

$$v = -\frac{\rho_o}{\rho}\{\frac{\partial \psi}{\partial \bar{x}} + \frac{\partial \psi}{\partial \bar{y}}\frac{\partial \bar{y}}{\partial x} + \frac{\partial \bar{y}}{\partial t}\} \tag{2.12}$$

The continuity equation (2.4) is automatically satisfied by this definition of the stream function.

The momentum and the energy equations now become

$$\frac{\partial^2 \psi}{\partial \bar{y}\partial \bar{t}} + \frac{\partial \psi}{\partial \bar{y}}\frac{\partial^2 \psi}{\partial \bar{y}\partial \bar{x}} - \frac{\partial \psi}{\partial \bar{x}}\frac{\partial^2 \psi}{\partial \bar{y}^2} = -\frac{1}{\rho}\frac{\partial p}{\partial \bar{x}} + \frac{1}{\rho_o}\frac{\partial}{\partial \bar{y}}(\frac{\mu\rho}{\rho_o}\frac{\partial^2 \psi}{\partial \bar{y}^2}) \tag{2.13}$$

$$\frac{\partial H}{\partial \bar{t}} + \frac{\partial \psi}{\partial \bar{y}}\frac{\partial H}{\partial \bar{x}} - \frac{\partial H}{\partial \bar{y}}\frac{\partial \psi}{\partial \bar{x}} = \frac{1}{\rho_o}\frac{\partial}{\partial \bar{y}}\{\frac{\mu\rho}{Pr\rho_o}\frac{\partial H}{\partial \bar{y}} + \frac{\mu\rho}{\rho_o}(1-\frac{1}{Pr})\frac{\partial \psi}{\partial \bar{y}}\frac{\partial^2 \psi}{\partial \bar{y}^2}\} \tag{2.14}$$

2.2b Howarth-Stewartson Transformation

For the sake of convenience this transformation will be introduced in two steps.

First Step

The independent variables in this transformation are

$$\bar{\bar{t}} = \bar{t} \ , \ \bar{\bar{x}} = \bar{x} \ , \ \bar{\bar{y}} = \frac{a_e}{a_o} \bar{y} \tag{2.15}$$

The transformation equations for the derivatives are

$$\frac{\partial}{\partial \bar{t}} = \frac{\partial}{\partial \bar{\bar{t}}}$$

$$\frac{\partial}{\partial \bar{x}} = \frac{\partial}{\partial \bar{\bar{x}}} + \frac{\partial}{\partial \bar{\bar{y}}} \frac{\partial \bar{\bar{y}}}{\partial \bar{x}} \tag{2.16}$$

$$\frac{\partial}{\partial \bar{y}} = \frac{a_e}{a_o} \frac{\partial}{\partial \bar{\bar{y}}} \ .$$

Applying (2.16) to (2.13) and (2.14) we obtain

$$\frac{a_e}{a_o} \frac{\partial^2 \bar{\bar{\psi}}}{\partial \bar{\bar{t}} \partial \bar{\bar{y}}} + \left(\frac{a_e}{a_o}\right)^2 \frac{\partial \bar{\bar{\psi}}}{\partial \bar{\bar{y}}} \frac{\partial^2 \bar{\bar{\psi}}}{\partial \bar{\bar{y}} \partial \bar{\bar{x}}} + \frac{a_e}{a_o^2} \left(\frac{\partial \bar{\bar{\psi}}}{\partial \bar{\bar{y}}}\right)^2 \frac{\partial a_e}{\partial \bar{\bar{x}}} - \frac{\partial \bar{\bar{\psi}}}{\partial \bar{\bar{x}}} \left(\frac{a_e}{a_o}\right)^2 \frac{\partial^2 \bar{\bar{\psi}}}{\partial \bar{\bar{y}}^2}$$

$$= - \frac{1}{\rho} \frac{\partial p}{\partial \bar{\bar{x}}} + \frac{1}{\rho_o} \left(\frac{a_e}{a_o}\right)^3 \frac{\partial}{\partial \bar{\bar{y}}} \left(\frac{\mu \rho}{\rho_o} \frac{\partial^2 \bar{\bar{\psi}}}{\partial \bar{\bar{y}}^2}\right) \tag{2.17}$$

$$\frac{\partial H}{\partial \bar{\bar{t}}} + \frac{a_e}{a_o}\frac{\partial \psi}{\partial \bar{\bar{y}}}\frac{\partial H}{\partial \bar{\bar{x}}} - \frac{a_e}{a_o}\frac{\partial H}{\partial \bar{\bar{y}}}\frac{\partial \psi}{\partial \bar{\bar{x}}}$$

$$= \frac{1}{\rho_o}\left(\frac{a_e}{a_o}\right)^2 \frac{\partial}{\partial \bar{\bar{y}}}\left\{\frac{\mu\rho}{Pr\rho_o}\frac{\partial H}{\partial \bar{\bar{y}}} + \frac{\mu\rho}{\rho_o}\left(1 - \frac{1}{Pr}\right)\left(\frac{a_e}{a_o}\right)^2 \frac{\partial \psi}{\partial \bar{\bar{y}}}\frac{\partial^2 \psi}{\partial \bar{\bar{y}}^2}\right\} \qquad (2.18)$$

Second Step

The independent variables for the second step are:

$$\bar{\bar{T}} \equiv \bar{\bar{t}} \; ; \; \bar{\bar{X}} = \int_0^{\bar{\bar{x}}} C\left(\frac{a_e}{a_o}\right)\left(\frac{p_e}{p_o}\right) d\bar{\bar{x}} \; ; \; \bar{\bar{Y}} \equiv \bar{\bar{y}} \qquad (2.19)$$

where C is a proportionality factor in the linear viscosity law given by

$$C \equiv C(\bar{\bar{x}}) = \frac{\mu T_o}{\mu_o \bar{T}} \qquad (2.20)$$

Expression (2.20) is of the form taken by Chapman and Rubesin [30], except that the reference conditions (μ_o, T_o) are free stream stagnation values. The proportionality factor C serves to match the viscosity with the more exact Sutherland value at a desired station. If this station is taken to be the plate surface, assumed to be kept at constant temperature, the result is

$$C = \left(\frac{T_w}{T_o}\right)^{\frac{1}{2}} \left(\frac{T_o + S_1}{T_w + S_1}\right) \qquad (2.21)$$

where S_1 is a constant which for air has the value

$$S_1 = 110°K \ .$$

In view of (2.19) the following transformation equations may be used for the derivatives:

$$\frac{\partial}{\partial \bar{\bar{t}}} = \frac{\partial}{\partial \bar{\bar{T}}}$$

$$\frac{\partial}{\partial \bar{\bar{x}}} = C\left(\frac{a_e}{a_o}\right)\left(\frac{p_e}{p_o}\right) \frac{\partial}{\partial \bar{\bar{X}}} \tag{2.22}$$

$$\frac{\partial}{\partial \bar{\bar{y}}} = \frac{\partial}{\partial \bar{\bar{Y}}}$$

Using (2.22) in (2.17) and (2.18) we find, respectively,

$$\frac{a_e}{a_o} \frac{\partial^2 \psi}{\partial \bar{\bar{Y}} \partial \bar{\bar{T}}} + C\left(\frac{a_e}{a_o}\right)^3\left(\frac{p_e}{p_o}\right) \frac{\partial \psi}{\partial \bar{\bar{Y}}} \frac{\partial^2 \psi}{\partial \bar{\bar{X}} \partial \bar{\bar{Y}}} + C\left(\frac{a_e}{a_o}\right)^3\left(\frac{p_e}{p_o}\right) \frac{1}{a_e} \frac{\partial a_e}{\partial \bar{\bar{X}}} \left(\frac{\partial \psi}{\partial \bar{\bar{Y}}}\right)^2$$

$$- C\left(\frac{a_e}{a_o}\right)^3\left(\frac{p_e}{p_o}\right) \frac{\partial \psi}{\partial \bar{\bar{X}}} \frac{\partial^2 \psi}{\partial \bar{\bar{Y}}^2} = - \frac{C}{\rho} \left(\frac{a_e}{a_o}\right)\left(\frac{p_e}{p_o}\right) \frac{\partial p}{\partial \bar{\bar{X}}} + C\left(\frac{a_e}{a_o}\right)^3\left(\frac{p_e}{p_o}\right) \frac{\mu_o}{\rho_o} \frac{\partial^3 \psi}{\partial \bar{\bar{Y}}^3} \tag{2.23}$$

$$\frac{\partial H}{\partial \bar{\bar{T}}} + C\left(\frac{a_e}{a_o}\right)^2\left(\frac{p_e}{p_o}\right) \frac{\partial \psi}{\partial \bar{\bar{Y}}} \frac{\partial H}{\partial \bar{\bar{X}}} - C\left(\frac{a_e}{a_o}\right)^2\left(\frac{p_e}{p_o}\right) \frac{\partial \psi}{\partial \bar{\bar{X}}} \frac{\partial H}{\partial \bar{\bar{Y}}}$$

$$= \frac{1}{\rho_o} \left(\frac{a_e}{a_o}\right)^2 \frac{\partial}{\partial \bar{\bar{Y}}} \left\{\frac{\mu\rho}{Pr\rho_o} \frac{\partial H}{\partial \bar{\bar{Y}}} + \frac{\mu\rho}{\rho_o}\left(1 - \frac{1}{Pr}\right)\left(\frac{a_e}{a_o}\right)^2 \frac{\partial \psi}{\partial \bar{\bar{Y}}} \frac{\partial^2 \psi}{\partial \bar{\bar{Y}}^2}\right\} \tag{2.24}$$

where we have used the viscosity law of equations (2.20) and (2.21) along-

with the equation of state for a perfect gas

$$p = \rho RT \tag{2.25}$$

2.2c Final Transformation

Distorting the time-variable, the independent variables for the final transformation are

$$\bar{\bar{T}} = \int_0^{\bar{T}} C\left(\frac{a_e}{a_o}\right)^2\left(\frac{p_e}{p_o}\right) d\bar{T} \; ; \; \bar{X} \equiv \bar{\bar{X}} \; ; \; \bar{Y} \equiv \bar{\bar{Y}} \; . \tag{2.26}$$

Therefore,

$$\frac{\partial}{\partial \bar{T}} = C\left(\frac{a_e}{a_o}\right)^2\left(\frac{p_e}{p_o}\right) \frac{\partial}{\partial \bar{\bar{T}}}$$

$$\frac{\partial}{\partial \bar{X}} = \frac{\partial}{\partial \bar{X}} + \frac{\partial}{\partial \bar{T}} \frac{\partial \bar{T}}{\partial \bar{X}} \tag{2.27}$$

$$\frac{\partial}{\partial \bar{Y}} = \frac{\partial}{\partial \bar{Y}}$$

Use of the above transformation equations for the derivatives in (2.23) and (2.24) yields:

$$\frac{\partial^2 \psi}{\partial \bar{Y} \partial \bar{T}} + \frac{\partial \psi}{\partial \bar{Y}} \frac{\partial^2 \psi}{\partial \bar{Y} \partial \bar{X}} - \frac{\partial \psi}{\partial \bar{X}} \frac{\partial^2 \psi}{\partial \bar{Y}^2} - \frac{H}{H_e} a_o^2 M_e \frac{dM_e}{d\bar{X}}$$

$$+ \frac{\partial \bar{T}}{\partial \bar{X}} \left(\frac{\partial \psi}{\partial \bar{Y}} \frac{\partial^2 \psi}{\partial \bar{Y} \partial \bar{T}} - \frac{\partial \psi}{\partial \bar{T}} \frac{\partial^2 \psi}{\partial \bar{Y}^2} \right) = \nu_o \frac{\partial^3 \psi}{\partial \bar{Y}^3} \tag{2.28}$$

$$\frac{\partial H}{\partial \bar{T}} + \frac{\partial \psi}{\partial \bar{Y}} \frac{\partial H}{\partial \bar{X}} - \frac{\partial \psi}{\partial \bar{X}} \frac{\partial H}{\partial \bar{Y}} + \frac{\partial \bar{T}}{\partial \bar{X}} \left(\frac{\partial \psi}{\partial \bar{Y}} \frac{\partial H}{\partial \bar{T}} - \frac{\partial \psi}{\partial \bar{T}} \frac{\partial H}{\partial \bar{Y}} \right)$$

$$= \frac{\nu_o}{Pr} \frac{\partial}{\partial \bar{Y}} \left\{ \frac{\partial H}{\partial \bar{Y}} + (Pr - 1) \left(\frac{a_e}{a_o} \right)^2 \frac{\partial \psi}{\partial \bar{Y}} \frac{\partial^2 \psi}{\partial \bar{Y}^2} \right\} \tag{2.29}$$

where we have used

$$a_e^2 = (\gamma - 1) h_e \tag{2.30}$$

$$\frac{1}{a_e} \frac{\partial a_e}{\partial \bar{X}} \left(\frac{\partial \psi}{\partial \bar{Y}} \right)^2 = \left(\frac{a_o}{a_e} \right)^2 \frac{1}{h_e} \frac{\partial h_e}{\partial \bar{X}} \frac{u^2}{2} \tag{2.31}$$

$$\frac{1}{\rho} \left(\frac{a_o}{a_e} \right)^2 \frac{\partial p}{\partial \bar{X}} = \left(\frac{a_o}{a_e} \right)^2 \frac{h}{h_e} \frac{\partial h_e}{\partial \bar{X}} \tag{2.32}$$

$$\frac{U_e^2}{h_e} = (\gamma - 1) M_e^2 \tag{2.33}$$

$$\left(\frac{a_o}{a_e} \right)^2 \frac{1}{h_e} \frac{\partial h_e}{\partial \bar{X}} = - \frac{a_o^2}{H_e} M_e \frac{dM_e}{d\bar{X}} \tag{2.34}$$

and the hypersonic assumption (1.1).

Equations (2.28) and (2.29) represent the governing equations in terms of the new independent variables $\bar{T}$, $\bar{X}$ and $\bar{Y}$ which are related to the physical variables t, x and y by the following expression

$$\bar{T} = C\left(\frac{a_e}{a_o}\right)^2\left(\frac{p_e}{p_o}\right) t \; ; \; \bar{X} = \int_o^x C\left(\frac{a_e}{a_o}\right)\left(\frac{p_e}{p_o}\right) dx \; ; \; \bar{Y} = \frac{a_e}{a_o}\int_o^y \frac{\rho}{\rho_o} dy \quad (2.35)$$

2.2d Reduction to Similarity Form

The solution of equations (2.28) and (2.29) could be attempted by a number of different approaches. The approach chosen in this analysis is to use a similarity transformation. This type of transformation changes the two equations into a coupled set of partial differential equations in two independent variables η and τ. The velocity and the total enthalpy profiles at different plate surface locations and different times are the same as at any other location and time except for a scale factor.

We assume the following relations for this problem

$$\begin{aligned} \psi &= A\bar{X}^a V_e{}^p f(\eta,\tau) \\ \bar{Y} &= B\bar{X}^b V_e{}^q \eta \\ \bar{T} &= C\bar{X}^c V_e{}^r \tau \\ S \equiv S(\eta,\tau) &= \frac{H}{G(\bar{X},\bar{T})} \end{aligned} \quad (2.36)$$

where A, B, C, a, b, c, p, q and r are undetermined constants.

When equations (2.36) are used in the form

$$\psi = \left[\frac{2\nu_o \bar{X} V_e}{(m+1)}\right]^{1/2} f(\eta,\tau)$$

$$\eta = \left[\frac{(m+1)\, V_e}{2\nu_o\, \bar{X}}\right]^{1/2} \bar{Y} \qquad (2.37)$$

$$\tau = \frac{V_e \bar{T}}{\bar{X}}$$

$$S \equiv S(\eta,\tau) = \frac{H}{H_e}$$

with

$$V_e \equiv V_e(\bar{X}) = \frac{a_o}{a_e} U_e = a_o M_e(\bar{X}) \quad , \qquad (2.38)$$

we obtain from (2.28) and (2.29), respectively,

$$\frac{V_e^2}{\bar{X}} \dot{f}' + V_e f' \left[\{f' \frac{\partial V_e}{\partial \bar{X}} - \frac{1}{2}\sqrt{\frac{(m+1)}{2\nu_o}}\, \bar{X}^{-\frac{3}{2}} \bar{Y} V_e^{\frac{3}{2}} f'' + \frac{1}{2}\sqrt{\frac{(m+1)}{2\nu_o}}\, \bar{X}^{-\frac{1}{2}} \bar{Y} V_e^{\frac{1}{2}} f'' \frac{\partial V_e}{\partial \bar{X}}\right\}$$

$$+ V_e \dot{f}' \{-\frac{\tau}{\bar{X}} + \frac{\tau}{V_e}\frac{\partial V_e}{\partial \bar{X}}\}\Big] - \Big[\frac{1}{2}\sqrt{\frac{2\nu_o}{(m+1)}}\, \bar{X}^{-\frac{1}{2}} V_e^{\frac{1}{2}} f - \frac{1}{2}\bar{X}^{-1}\bar{Y} V_e f' + \frac{1}{2}\bar{Y} f' \frac{\partial V_e}{\partial \bar{X}}$$

$$+ \sqrt{\frac{2\nu_o}{(m+1)}}\, \bar{X}^{\frac{1}{2}} V_e^{\frac{1}{2}} \dot{f}\{-\frac{\tau}{\bar{X}} + \frac{\tau}{V_e}\frac{\partial V_e}{\partial \bar{X}}\} + \frac{1}{2}\sqrt{\frac{2\nu_o}{(m+1)}}\, \bar{X}^{\frac{1}{2}} V_e^{-\frac{1}{2}} f \frac{\partial V_e}{\partial \bar{X}}\Big]$$

$$\cdot\{\sqrt{\frac{(m+1)}{2\nu_o}}\, \bar{X}^{-\frac{1}{2}} V_e^{\frac{3}{2}} f''\} - \frac{H}{H_e} V_e \frac{\partial V_e}{\partial \bar{X}} - \bar{T}\left(\frac{2\gamma-1}{\gamma-1}\right)\frac{a_e^2}{H_e} M_e \frac{dM_e}{d\bar{X}}\{\frac{V_e^3}{\bar{X}} f'\dot{f}' - \frac{V_e^3}{\bar{X}} \dot{f} f''\}$$

$$= \nu_o\left(\frac{m+1}{2\nu_o}\right)\frac{V_e^2}{\bar{X}} f''' \qquad (2.39)$$

$$H_e \frac{V_e}{\bar{X}} \dot{S} + \tau H_e f' \dot{S}\left(\frac{\partial V_e}{\partial \bar{X}} - \frac{V_e}{\bar{X}}\right) + V_e f' S \frac{\partial H_e}{\partial \bar{X}} - \frac{1}{2} H_e f S'\left(\frac{\partial V_e}{\partial \bar{X}} + \frac{V_e}{\bar{X}}\right)$$

$$- \tau H_e \dot{f} S'\left(\frac{\partial V_e}{\partial \bar{X}} - \frac{V_e}{\bar{X}}\right) - \bar{T}\left(\frac{2\gamma-1}{\gamma-1}\right) \frac{a_e^2}{H_e} M_e \frac{dM_e}{d\bar{X}} \left(H_e f' \dot{S} \frac{V_e^2}{\bar{X}} - H_e \dot{f} S' \frac{V_e^2}{\bar{X}}\right)$$

$$= \left(\frac{m+1}{2}\right) \frac{H_e}{Pr} \frac{V_e}{\bar{X}} S'' + \left(\frac{m+1}{2}\right)\left(\frac{Pr-1}{Pr}\right)\left(\frac{a_e}{a_o}\right)^2 \frac{V_e^3}{\bar{X}} (f''^2 + f'f''') \quad (2.40)$$

where the following relations have been employed:

$$\frac{\partial \psi}{\partial \bar{Y}} = V_e f' \quad (2.41a)$$

$$\frac{\partial^2 \psi}{\partial \bar{Y} \partial \bar{T}} = \frac{V_e^2}{\bar{X}} \dot{f}' \quad (2.41b)$$

$$\frac{\partial^2 \psi}{\partial \bar{X} \partial \bar{Y}} = f' \frac{\partial V_e}{\partial \bar{X}} + \frac{1}{2} \sqrt{\frac{(m+1)}{2\nu_o}} \frac{V_e^{\frac{1}{2}}}{\bar{X}^{\frac{1}{2}}} \bar{Y} f'' \frac{\partial V_e}{\partial \bar{X}} - \frac{1}{2} \sqrt{\frac{(m+1)}{2\nu_o}} \frac{V_e^{\frac{3}{2}}}{\bar{X}^{\frac{3}{2}}} \bar{Y} f''$$

$$+ V_e \dot{f}' \left\{ - \frac{\tau}{\bar{X}} + \frac{\tau}{V_e} \frac{\partial V_e}{\partial \bar{X}} \right\} \quad (2.41c)$$

$$\frac{\partial \psi}{\partial \bar{X}} = \frac{1}{2} \bar{Y} f' \frac{\partial V_e}{\partial \bar{X}} - \frac{1}{2} \bar{Y} f' \frac{V_e}{\bar{X}} + \sqrt{\frac{2\nu_o}{(m+1)}} \frac{1}{\bar{X}^{\frac{1}{2}}} V_e^{\frac{1}{2}} \dot{f} \left\{ - \frac{\tau}{\bar{X}} + \frac{\tau}{V_e} \frac{\partial V_e}{\partial \bar{X}} \right\}$$

$$+ \frac{1}{2} \sqrt{\frac{2\nu_o}{(m+1)}} \frac{V_e^{\frac{1}{2}}}{\bar{X}^{\frac{1}{2}}} f + \frac{1}{2} \sqrt{\frac{2\nu_o}{(m+1)}} \frac{\bar{X}^{\frac{1}{2}}}{V_e^{\frac{1}{2}}} f \frac{\partial V_e}{\partial \bar{X}} \quad (2.41d)$$

$$\frac{\partial^2 \psi}{\partial \bar{Y}^2} = \sqrt{\frac{(m+1)}{2\nu_o}} \frac{V_e^{\frac{3}{2}}}{\bar{X}^{\frac{1}{2}}} f'' \tag{2.41e}$$

$$\frac{\partial^3 \psi}{\partial \bar{Y}^3} = \frac{(m+1)}{2\nu_o} \frac{V_e^2}{\bar{X}} f''' \tag{2.41f}$$

$$\frac{\partial \psi}{\partial \bar{T}} = \sqrt{\frac{2\nu_o}{(m+1)}} \frac{V_e^{\frac{3}{2}}}{\bar{X}^{\frac{1}{2}}} \dot{f} \tag{2.41g}$$

$$\frac{\partial \bar{T}}{\partial \bar{X}} = -\bar{T}\left(\frac{2\gamma-1}{\gamma-1}\right) \frac{a_e^2}{H_e} M_e \frac{dM_e}{d\bar{X}} \tag{2.41h}$$

$$\frac{\partial H}{\partial \bar{T}} = H_e \dot{S} \frac{V_e}{\bar{X}} \tag{2.41i}$$

$$\frac{\partial H}{\partial \bar{X}} = \sqrt{\frac{(m+1)}{2\nu_o}} H_e S' \left(\frac{1}{2} \frac{\bar{Y}}{\sqrt{(\bar{X} V_e)}} \frac{\partial V_e}{\partial \bar{X}} - \frac{1}{2} \bar{Y} \frac{V_e^{\frac{1}{2}}}{\bar{X}^{\frac{3}{2}}}\right)$$

$$+ H_e \dot{S}\left(-\frac{\tau}{\bar{X}} + \frac{\tau}{V_e} \frac{\partial V_e}{\partial \bar{X}}\right) + S \frac{\partial H_e}{\partial \bar{X}} \tag{2.41j}$$

$$\frac{\partial H}{\partial \bar{Y}} = \sqrt{\frac{(m+1)\, V_e}{2\nu_o\, \bar{X}}} H_e S' \tag{2.41k}$$

$$\frac{\partial^2 H}{\partial \bar{Y}^2} = \frac{(m+1)}{2\nu_o} H_e \frac{V_e}{\bar{X}} S'' \tag{2.41ℓ}$$

Let

$$V_e = e\bar{X}^m \tag{2.42}$$

and

$$\beta = \frac{2m}{m+1} . \tag{2.43}$$

Using (2.42) and (2.43) in (2.39) and (2.40) we obtain

$$\frac{V_e^2}{\bar{X}} \dot{f}' + m \frac{V_e^2}{\bar{X}} f'^2 - \frac{1}{2} \sqrt{\frac{(m+1)}{2\nu_o}} \frac{V_e^{\frac{5}{2}}}{\bar{X}^{\frac{3}{2}}} \bar{Y} f'f'' + \frac{m}{2} \sqrt{\frac{(m+1)}{2\nu_o}} \frac{V_e^{\frac{5}{2}}}{\bar{X}^{\frac{3}{2}}} \bar{Y} f'f''$$

$$- V_e^2 \frac{\tau}{\bar{X}} f'\dot{f}' + m V_e^2 \frac{\tau}{\bar{X}} f'\dot{f}' - [\frac{1}{2} \frac{V_e^2}{\bar{X}} ff'' - \frac{1}{2} \sqrt{\frac{(m+1)}{2\nu_o}} \frac{V_e^{\frac{5}{2}}}{\bar{X}^{\frac{3}{2}}} \bar{Y} f'f''$$

$$+ \frac{m}{2} \sqrt{\frac{(m+1)}{2\nu_o}} \frac{V_e^{\frac{5}{2}}}{\bar{X}^{\frac{3}{2}}} \bar{Y} f'f'' + V_e^2 \dot{f}f''\{- \frac{\tau}{\bar{X}} + m \frac{\tau}{\bar{X}}\} + \frac{m}{2} \frac{V_e^2}{\bar{X}} ff'']$$

$$- \frac{H}{H_e} m \frac{V_e^2}{\bar{X}} - m(\frac{2\gamma-1}{\gamma-1}) \tau \frac{U_e^2}{H_e} \frac{V_e^2}{\bar{X}} (f'\dot{f}' - \dot{f}f'')$$

$$= \frac{(m+1)}{2} \frac{V_e^2}{\bar{X}} f''' \tag{2.44}$$

$$H_e \frac{V_e}{\bar{X}} \dot{S} + (m-1) \tau H_e \dot{S} f' \frac{V_e}{\bar{X}} + V_e f'S \frac{\partial H_e}{\partial \bar{X}} - \frac{(m+1)}{2} H_e f S' \frac{V_e}{\bar{X}}$$

$$- (m-1) \tau H_e \dot{f} S' \frac{V_e}{\bar{X}} - m(\frac{2\gamma-1}{\gamma-1}) \tau \frac{U_e^2}{H_e} \frac{H_e V_e}{\bar{X}} (f'\dot{S} - \dot{f}S')$$

$$= \frac{(m+1)}{2} \frac{H_e}{Pr} \frac{V_e}{\bar{X}} S'' + \frac{(m+1)}{2} \frac{(Pr-1)}{Pr} \left(\frac{a_e}{a_o}\right)^2 \frac{V_e^3}{\bar{X}} (f''^2 + f'f''') \tag{2.45}$$

Noting that H_e does not vary with $\bar{X}$ and using

$$\frac{U_e^2}{H_e} = \frac{(\gamma-1) M_e^2}{1 + (\frac{\gamma-1}{2}) M_e^2} \tag{2.46}$$

in (2.44) and (2.45) we obtain after some algebraic manipulations

$$\left(\frac{2}{m+1}\right) \dot{f}' + \left(\frac{2m}{m+1}\right) f'^2 + \frac{2(m-1)}{(m+1)} \tau(f'\dot{f}' - \dot{f}f'') - ff''$$

$$- \left(\frac{2m}{m+1}\right) \frac{H}{H_e} - \left(\frac{2m}{m+1}\right) \left(\frac{2\gamma-1}{\gamma-1}\right) \tau \left\{\frac{(\gamma-1) M_e^2}{1 + \frac{(\gamma-1)}{2} M_e^2}\right\} (f'\dot{f}' - \dot{f}f'') = f''' \tag{2.47}$$

$$\dot{S}[1 - (1-m) \tau f'] - S'[\frac{(m+1)}{2} f - (1-m) \tau \dot{f}]$$

$$- m\left(\frac{2\gamma-1}{\gamma-1}\right) \tau \left\{\frac{(\gamma-1) M_e^2}{1 + (\frac{\gamma-1}{2}) M_e^2}\right\} (f'\dot{S} - \dot{f}S')$$

$$= \frac{(m+1)}{2} \frac{1}{Pr} S'' + \frac{(m+1)}{2} \frac{Pr-1}{Pr} \left\{\frac{(\gamma-1) M_e^2}{1 + \frac{(\gamma-1)}{2} M_e^2}\right\} (f''^2 + f'f''') \tag{2.48}$$

We may finally write (2.47) and (2.48) in the following form

$$(2-\beta)\,\dot{f}' + \beta(f'^2-S) + 2(\beta-1)\tau(f'\dot{f}' - \dot{f}f'') - ff'' - f'''$$

$$- \beta\left(\frac{2\gamma-1}{\gamma-1}\right)\tau \left\{\frac{(\gamma-1)\,M_e^2}{1 + \frac{(\gamma-1)}{2} M_e^2}\right\} (f'\dot{f}' - \dot{f}f'') = 0 \qquad (2.49)$$

$$\dot{S}\,Pr\,[(2-\beta) - 2(1-\beta)\tau f'] - S'' - S'Pr[f - 2(1-\beta)\tau\dot{f}]$$

$$-\beta\left(\frac{2\gamma-1}{\gamma-1}\right) Pr\tau \left\{\frac{(\gamma-1)\,M_e^2}{1 + \frac{(\gamma-1)}{2} M_e^2}\right\} (f'\dot{S} - \dot{f}S')$$

$$= (Pr-1) \left\{\frac{(\gamma-1)\,M_e^2}{1 + \frac{(\gamma-1)}{2} M_e^2}\right\} (f''^2 + f'f''') \qquad (2.50)$$

For steady state the above equations may be simplified to:

$$f''' + ff'' + \beta(S-f'^2) = 0 \qquad (2.51)$$

$$S'' + PrS'f = (1-Pr) \left\{\frac{(\gamma-1)\,M_e^2}{1 + \frac{(\gamma-1)}{2} M_e^2}\right\} (f''^2 + f'f''') \qquad (2.52)$$

Equations (2.51) and (2.52) have been obtained by Cohen and Reshotko [31] in a slightly different form.

Since M_e may, in general, depend on $\overline{X}$, the terms in equations (2.49) and (2.50) containing the factor in curly brackets are not yet functionally consistent with the rest of the terms in these two equations for arbitrary M_e and Pr. The functional consistency among the different

terms may be achieved by one of the following ways:

(1) The external Mach number may be a constant greater than zero.

(2) The external Mach number may be zero (the viscous dissipation and compressive-work terms are omitted in equation (2.3) for this case).

(3) The ratio of specific heats γ may equal 1 (for most gases, this assumption is physically unreasonable).

(4) The factor

$$\left\{ \frac{(\gamma-1)\, M_e^{\,2}}{1 + \frac{(\gamma-1)}{2} M_e^{\,2}} \right\}$$

may be approximately 2 corresponding to hypersonic flow.

It is the last assumption which would be reasonable for the present analysis. The treatment of hypersonic flow also requires the introduction of the effects of displacement thickness upon pressure gradient. For the flat plate, Lees [32] has shown that the induced hypersonic pressure gradient for the strong interaction case corresponds to

$$\beta = \frac{\gamma-1}{\gamma} \quad . \tag{2.53}$$

As a first order approximation we shall use (2.53) in our subsequent analysis.

Using the limiting value 2 of the quantity in curly brackets

of equations (2.49) and (2.50) alongwith the relation (2.53) we obtain:

$$\left(\frac{\gamma+1}{\gamma}\right)\dot{f}' + \left(\frac{\gamma-1}{\gamma}\right)(f'^2-S) - 4\tau(f'\dot{f}'-\dot{f}f'') - ff''-f''' = 0 \quad (2.54)$$

$$Pr\,\dot{S}\left[\left(\frac{\gamma+1}{\gamma}\right) - 4\tau f'\right] - S'' - S'Pr[f-4\tau\dot{f}] = 2(Pr-1)(f''^2+f'f''') \quad (2.55)$$

Letting Pr=1 further simplifies the energy equation (2.55) to

$$\dot{S}\left[\left(\frac{\gamma+1}{\gamma}\right) - 4\tau f'\right] - S'' - S'[f-4\tau\dot{f}] = 0 \quad (2.56)$$

2.3 Correlation with Reshotko-Rodkiewicz Equations [22] for Zero Pressure Gradient

Equations (2.49) and (2.50), when specialized for zero pressure gradient, yield, respectively,

$$2\dot{f}' + 2\tau(\dot{f}f''-f'\dot{f}') - ff''-f''' = 0 \quad (2.57)$$

$$2\dot{S}Pr[1-\tau f'] - S''-S'Pr[f-2\tau\dot{f}] = (Pr-1)\left\{\frac{(\gamma-1)\,M_e^2}{1+\frac{(\gamma-1)}{2}M_e^2}\right\}(f''^2 + f'f''') \quad (2.58)$$

For zero pressure gradient "e" condition may be taken as reference*, since the local "external" values are constant along the

*For non-zero pressure gradients, we have used free stream stagnation values as the reference conditions, since in the presence of pressure gradient the "e" values are not constant.

outer edge of the boundary layer. For this case

$$\frac{a_e}{a_{ref}} \to 1$$

consequently $$M_e\, a_{ref} \to U_e$$

$$\overline{Y} \to \overline{y} \tag{2.59}$$

$$\overline{X} \to \overline{x}$$

$$\overline{T} \to \overline{t}$$

and $$M_e \to \text{a constant} .$$

If we now use the relation

$$g(\eta,\tau) = (1 + \frac{(\gamma-1)}{2} M_e^2)\, S(\eta,\tau) - \frac{(\gamma-1)}{2} M_e^2 f'^2(\eta,\tau) \tag{2.60}$$

in (2.58) we find:

$$2Pr\, \dot{g}[1-\tau f'] - g'' - Pr\, g'[f-2\tau\dot{f}] - Pr(\gamma-1)\, M_e^2 f''^2$$

$$+ Pr(\gamma-1)\, M_e^2 f'\{2\dot{f}' + 2\tau(\dot{f}f''-f'\dot{f}') - ff''-f'''\} = 0$$

In view of (2.57) the last equation may be further simplified to

$$2Pr\ \dot{g}[1-\tau f'] - g''-Pr\ g'[f-2\tau\dot{f}] - Pr(\gamma-1)\ M_e^{\ 2} f''^2 = 0 \qquad (2.61)$$

Equations (2.57) and (2.61) have been obtained in reference [22].

From (2.60) we may also write down the following relations of interest:

(a) Static temperature T referred to the free stream stagnation temperature T_o

$$\frac{T}{T_o} = S(\eta,\tau) - \left\{\frac{\left(\frac{\gamma-1}{2}\right) M_e^{\ 2}}{1 + \frac{(\gamma-1)}{2} M_e^{\ 2}}\right\} f'^2(\eta,\tau) \qquad (2.62)$$

and

(b) flux density

$$\frac{\rho u}{\rho_e U_e} = \frac{f'(\eta,\tau)}{\left(1 + \frac{(\gamma-1)}{2} M_e^{\ 2}\right) S(\eta,\tau) - \frac{(\gamma-1)}{2} M_e^{\ 2} f'^2(\eta,\tau)} \qquad (2.63)$$

2.4 Boundary and Initial Conditions

When $y = y_e$, $\overline{Y} = \overline{Y}_e$, $\eta = \eta_e$, $u = U_{e2}$, and

$$f'(\eta_e,\tau) = \frac{1}{V_{e2}} \frac{a_o}{a_{e2}} u = \frac{u}{U_{e2}} = 1 \qquad (2.64)$$

When $y = 0$, $\overline{Y} = 0$, $\eta = 0$, $u = 0$, and

$$f'(0,\tau) = 0 \tag{2.65}$$

When $y = 0$, $\overline{Y} = 0$, $\eta = 0$, $\psi = 0$ and

$$f(0,\tau) = 0 \tag{2.66}$$

When $t = 0$, $\tau = 0$, $u = u_o + (U_{e2} - U_{e0})$* and

$$f' = f_0'(\eta_0)\,\frac{U_{e0}}{U_{e2}} + \left(1 - \frac{U_{e0}}{U_{e2}}\right) \tag{2.67}$$

When $y = y_e$, $\overline{Y} = \overline{Y}_e$, $\eta = \eta_e$, $H = H_{e2}$, and

$$S(\eta_e,\tau) = 1 \tag{2.68}$$

When $y = 0$, $\overline{Y} = 0$, $\eta = 0$, $H = h_w$, and

$$S(0,\tau) = \frac{h_w}{H_{e2}} \tag{2.69}$$

or for the case of no wall heat transfer

$$S'(0,\tau) = 0 \tag{2.70}$$

---

*$u_0 = u(\eta,\tau<0)$; $u_1 = u(\eta,\tau=0)$; $u_2 = u(\eta,\tau=\infty)$

When $t = 0$, $\tau = 0$, $H = H_1$, and

$$S(\eta,0) = \frac{H_1}{H_{e2}} \tag{2.71}$$

CHAPTER III

SOLUTION TO THE GOVERNING EQUATIONS

3.1 General Approach

The problem formulated in Chapter II requires the solution of a third order partial differential equation(2.54) which is coupled to a second order partial differential equation (2.56). Equations (2.54) and (2.56) are the pertinent equations for the strong interaction case. As a closed form solution of these two coupled differential equations could not be found, a suitable numerical method had to be adopted.

3.2 Introduction to the Numerical Method

The method of solution adopted here, has been developed by Clutter and Smith [33] for the solution of compressible laminar boundary layer equations with transverse curvature effect. In this method of solution the partial derivatives with respect to the modified similarity variable ξ, associated with time and space,are replaced by finite differences. The derivatives with respect to the similarity variable η, associated with space,are retained. In this way the partial differential equations become approximated by ordinary differential equations at any particular value of ξ.

The particular choice of this method is based on the following reasons: the requirement that the method should solve both accurately

and rapidly any problem for which the boundary layer equations are valid, seems to call for an implicit finite difference technique which is inherently stable and is also exact in the limit. The method chosen here comes in this category and has the additional advantage of reducing the equation to an ordinary differential equation. Questions regarding the existence of the solution, the nature of the solution, and the error propagation are much better understood for ordinary differential equations than they are for the conventional finite difference methods used for the partial differential equations. A final reason for the choice of the Clutter-Smith technique is that it is known to produce accurate results, has been well explored and does not involve any kind of linearization* used in reference [22].

The round-off errors in the computer program can be reduced by substitution of $\bar{f}' = f'-1$ in the momentum equation (2.54). The reason for this is that in equation (2.54) all terms approach zero as η approaches η_e; both S and f'^2 approach unity and the round-off error is primarily introduced when taking their difference. The substitution of

$$\begin{aligned} \bar{f} &= f - \eta \\ \bar{f}' &= f' - 1 \\ \bar{f}'' &= f'' \\ \bar{f}''' &= f''' \end{aligned} \tag{3.1}$$

*See appendix A for linearized solutions.

in (2.54) gives

$$\left(\frac{\gamma+1}{\gamma}\right)\dot{\bar{f}}' + \left(\frac{\gamma-1}{\gamma}\right)\{(\bar{f}'+1)^2 - S\} - 4\tau\{(\bar{f}'+1)\dot{\bar{f}}' - \dot{\bar{f}}\bar{f}''\}$$

$$- (\bar{f}+\eta)\bar{f}'' - \bar{f}''' = 0 \qquad (3.2)$$

In terms of the Euler's transformation [30]

$$\xi = \frac{\tau}{\tau+1} \qquad (3.3)$$

we may rewrite equation (3.2) as

$$\left(\frac{\gamma+1}{\gamma}\right)(1-\xi)^2 \frac{\partial^2\bar{f}}{\partial\eta\partial\xi} + \left(\frac{\gamma-1}{\gamma}\right)\{\left(\frac{\partial\bar{f}}{\partial\eta} + 1\right)^2 - S\} - 4\xi(1-\xi)$$

$$\cdot \{\left(\frac{\partial\bar{f}}{\partial\eta} + 1\right)\frac{\partial^2\bar{f}}{\partial\eta\partial\xi} - \frac{\partial\bar{f}}{\partial\xi}\frac{\partial^2\bar{f}}{\partial\eta^2}\} - (\bar{f}+\eta)\frac{\partial^2\bar{f}}{\partial\eta^2} - \frac{\partial^3\bar{f}}{\partial\eta^3} = 0 \qquad (3.4)$$

Introduction of the Euler's transformation improves the convergence rate of the numerical method.

A function $\bar{S}$ may now be introduced in the energy equation (2.56) for similar reasons that $\bar{f}$ was introduced in the momentum equation. $\bar{S}$ is defined as

$$\bar{S} = S - 1 . \qquad (3.5)$$

Its substitution, alongwith the Euler's transformation, in the energy equation (2.56) gives

$$(1-\xi)\frac{\partial \bar{S}}{\partial \xi}\left[(1-\xi)\left(\frac{\gamma+1}{\gamma}\right) - 4\xi\left(\frac{\partial \bar{f}}{\partial \eta} + 1\right)\right] - \frac{\partial^2 \bar{S}}{\partial \eta^2}$$

$$- \frac{\partial \bar{S}}{\partial \eta}\left[(\bar{f}+\eta) - 4\xi(1-\xi)\frac{\partial \bar{f}}{\partial \xi}\right] = 0 \ . \qquad (3.6)$$

Also, S in the momentum equation (3.4) may be replaced by $\bar{S}+1$, giving

$$\left(\frac{\gamma+1}{\gamma}\right)(1-\xi)^2 \frac{\partial^2 \bar{f}}{\partial \eta \partial \xi} + \left(\frac{\gamma-1}{\gamma}\right)\left\{\left(\frac{\partial \bar{f}}{\partial \eta} + 1\right)^2 - (\bar{S} + 1)\right\} - 4\xi(1-\xi)$$

$$\cdot \left\{\left(\frac{\partial \bar{f}}{\partial \eta} + 1\right)\frac{\partial^2 f}{\partial \eta \partial \xi} - \frac{\partial \bar{f}}{\partial \xi}\frac{\partial^2 \bar{f}}{\partial \eta^2}\right\} - (\bar{f}+\eta)\frac{\partial^2 \bar{f}}{\partial \eta^2} - \frac{\partial^3 \bar{f}}{\partial \eta^3} = 0 \qquad (3.7)$$

3.3 Finite-Difference Representation of ξ-derivatives

This fundamental idea of replacing the ξ-derivatives by finite differences to approximate the partial differential equation was first advanced by Hartree and Womersley [34] and subsequently used by Clutter and Smith [33]. It may be noted that all of the ξ-derivatives appearing in the momentum and the energy equations are of the first order only.

In replacing the ξ-derivatives at a point by their finite differencè equivalents, one may use two-point or more accurate three-point finite differences. Whereas usually three-point finite differences have been used, at the start of a solution only two points are available and the two-point form must be used there.

Since the momentum equation and the energy equation are parabolic in ξ, the problem must be solved by marching in the direction of ξ. When the solution has been obtained at all previous stations up to and including ξ_{m-1}, the problem is to find the solution at the new station ξ_m. The notation system for the finite-difference approximation of ξ-derivatives is shown in the figures 1a and 1b.

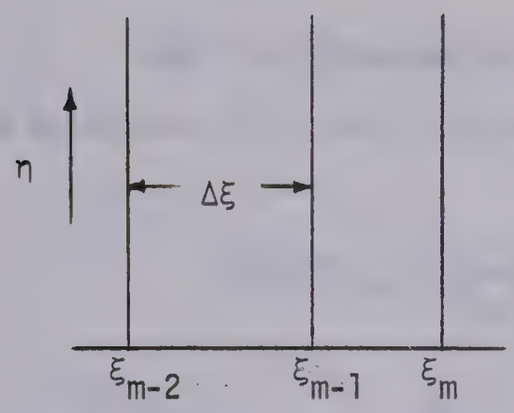

Figure 1a

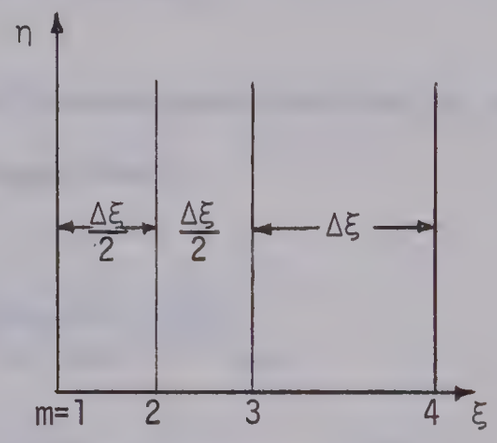

Figure 1b

Notation System for Finite-Difference Representation of ξ-derivatives

Using a two-point finite difference approximation in the ξ-direction, the momentum equation (3.7) and the energy equation (3.6) may be written, respectively, as

$$\left(\frac{\gamma+1}{\gamma}\right)(1-\xi_m)^2\left\{\frac{\left.\frac{\partial \bar{f}}{\partial \eta}\right|_{m,n} - \left.\frac{\partial \bar{f}}{\partial \eta}\right|_{m-1,n}}{\xi_m-\xi_{m-1}}\right\} + \left(\frac{\gamma-1}{\gamma}\right)\left\{\left(\left.\frac{\partial \bar{f}}{\partial \eta}\right|_{m,n}+1\right)^2-(\bar{S}_{m,n}+1)\right\}$$

$$- 4\xi_m(1-\xi_m)\left\{\left(\left.\frac{\partial \bar{f}}{\partial \eta}\right|_{m,n}+1\right)\left(\frac{\left.\frac{\partial \bar{f}}{\partial \eta}\right|_{m,n} - \left.\frac{\partial \bar{f}}{\partial \eta}\right|_{m-1,n}}{\xi_m-\xi_{m-1}}\right)-\left(\frac{\bar{f}_{m,n}-f_{m-1,n}}{\xi_m-\xi_{m-1}}\right)\left.\frac{\partial^2 f}{\partial \eta^2}\right|_{m,n}\right\}$$

$$- (\bar{f}_{m,n}+\eta_n) \left.\frac{\partial^2 \bar{f}}{\partial \eta^2}\right|_{m,n} - \left.\frac{\partial^3 \bar{f}}{\partial \eta^3}\right|_{m,n} = 0 \qquad (3.8)$$

$$(1-\xi_m)\left\{\frac{\bar{S}_{m,n}-\bar{S}_{m-1}}{\xi_m-\xi_{m-1}}\right\} \quad \left[(1-\xi_m)\left(\frac{\gamma+1}{\gamma}\right) - 4\xi_m\left(\left.\frac{\partial \bar{f}}{\partial \eta}\right|_{m,n}+1\right)\right] - \left.\frac{\partial^2 \bar{S}}{\partial \eta^2}\right|_{m,n}$$

$$- \left.\frac{\partial \bar{S}}{\partial \eta}\right|_{m,n} \cdot \left[(\bar{f}_{m,n}+\eta_n) - 4\xi_m(1-\xi_m)\left\{\frac{\bar{f}_{m,n}-\bar{f}_{m-1,n}}{\xi_m-\xi_{m-1}}\right\}\right] = 0 \ . \qquad (3.9)$$

When the three-point finite difference approximation is used, the equations (3.7) and (3.6) become, respectively,

$$\left(\frac{\gamma+1}{\gamma}\right)(1-\xi_m)^2\left\{\left[\frac{1}{(\xi_m-\xi_{m-1})} + \frac{1}{(\xi_m-\xi_{m-2})}\right] \left.\frac{\partial \bar{f}}{\partial \eta}\right|_{m,n}\right.$$

$$-\left[\frac{(\xi_m-\xi_{m-2})}{(\xi_m-\xi_{m-1})(\xi_{m-1}-\xi_{m-2})}\right] \left.\frac{\partial \bar{f}}{\partial \eta}\right|_{m-1,n} + \left[\frac{(\xi_m-\xi_{m-1})}{(\xi_m-\xi_{m-2})(\xi_{m-1}-\xi_{m-2})}\right] \left.\frac{\partial \bar{f}}{\partial \eta}\right|_{m-2,n} \Bigg\}$$

$$+ \left(\frac{\gamma-1}{\gamma}\right)\left\{\left(\left.\frac{\partial \bar{f}}{\partial \eta}\right|_{m,n} + 1\right)^2 - (\bar{S}_{m,n}+1)\right\} - 4\xi_m(1-\xi_m)$$

$$\cdot \left\langle \left(\left.\frac{\partial \bar{f}}{\partial \eta}\right|_{m,n}+1\right)\left\{\left[\frac{1}{(\xi_m-\xi_{m-1})} + \frac{1}{(\xi_m-\xi_{m-2})}\right] \left.\frac{\partial \bar{f}}{\partial \eta}\right|_{m,n}\right.\right.$$

$$-\left[\frac{(\xi_m-\xi_{m-2})}{(\xi_m-\xi_{m-1})(\xi_{m-1}-\xi_{m-2})}\right] \left.\frac{\partial \bar{f}}{\partial \eta}\right|_{m-1,n} + \left[\frac{(\xi_m-\xi_{m-1})}{(\xi_m-\xi_{m-2})(\xi_{m-1}-\xi_{m-2})}\right] \left.\frac{\partial \bar{f}}{\partial \eta}\right|_{m-2,n} \Bigg\}$$

$$- \left.\frac{\partial^2 \bar{f}}{\partial \eta^2}\right|_{m,n} \left\{\left[\frac{1}{(\xi_m-\xi_{m-1})} + \frac{1}{(\xi_m-\xi_{m-2})}\right] \bar{f}_{m,n} - \left[\frac{(\xi_m-\xi_{m-2})}{(\xi_m-\xi_{m-1})(\xi_{m-1}-\xi_{m-2})}\right]\bar{f}_{m-1,n}\right.$$

$$+\left[\frac{(\xi_m-\xi_{m-1})}{(\xi_m-\xi_{m-2})(\xi_{m-1}-\xi_{m-2})}\right]\bar{f}_{m-2,n}\Big\}\Big\rangle-(\bar{f}_{m,n+\eta_n})\left.\frac{\partial^2\bar{f}}{\partial\eta^2}\right|_{m,n}-\left.\frac{\partial^3\bar{f}}{\partial\eta^3}\right|_{m,n}=0 \tag{3.10}$$

$$(1-\xi_m)\left\{\left[\frac{1}{(\xi_m-\xi_{m-1})}+\frac{1}{(\xi_m-\xi_{m-2})}\right]\bar{S}_{m,n}-\left[\frac{(\xi_m-\xi_{m-2})}{(\xi_m-\xi_{m-1})(\xi_{m-1}-\xi_{m-2})}\right]\bar{S}_{m-1,n}\right.$$

$$\left.+\left[\frac{(\xi_m-\xi_{m-1})}{(\xi_m-\xi_{m-2})(\xi_{m-1}-\xi_{m-2})}\right]\bar{S}_{m-2,n}\right\}\left[(1-\xi_m)\left(\frac{\gamma+1}{\gamma}\right)-4\xi_m\left(\left.\frac{\partial\bar{f}}{\partial\eta}\right|_{m,n}+1\right)\right]$$

$$-\left.\frac{\partial^2\bar{S}}{\partial\eta^2}\right|_{m,n}-\left.\frac{\partial\bar{S}}{\partial\eta}\right|_{m,n}\Big\langle(\bar{f}_{m,n+\eta_n})-4\xi_m(1-\xi_m)\left\{\left[\frac{1}{(\xi_m-\xi_{m-1})}+\frac{1}{(\xi_m-\xi_{m-2})}\right]\bar{f}_{m,n}\right.$$

$$\left.-\left[\frac{(\xi_m-\xi_{m-2})}{(\xi_m-\xi_{m-1})(\xi_{m-1}-\xi_{m-2})}\right]\bar{f}_{m-1,n}+\left[\frac{(\xi_m-\xi_{m-1})}{(\xi_m-\xi_{m-2})(\xi_{m-1}-\xi_{m-2})}\right]\bar{f}_{m-2,n}\right\}\Big\rangle=0 \tag{3.11}$$

Equations (3.8) through (3.11) are ordinary differential equations in η with the variable quantities $\bar{f}$, $\bar{f}'$, and $\bar{S}$ at the m-1 and m-2 stations. It may be noted that step size $\Delta\xi$, which need not be constant, is not a primary parameter; instead, $\xi/\Delta\xi$ is. The errors* in the two-point and three-point formulation, respectively, are

$$\left(\frac{\xi_m-\xi_{m-1}}{2}\right)\frac{\partial^2 F}{\partial\xi^2}\text{ and }\frac{(\xi_m-\xi_{m-1})(\xi_m-\xi_{m-2})}{6}\frac{\partial^3 F}{\partial\xi^3} \tag{3.12}$$

which, for the equal stepsize in ξ-direction, reduce to

$$\frac{\Delta\xi}{2}\frac{\partial^2 F}{\partial\xi^2}\text{ and }\frac{(\Delta\xi)^2}{3}\frac{\partial^3 F}{\partial\xi^3} \tag{3.13}$$

---

*The absolute magnitude of the maximum error in the two-point and three-point formulation is given in Appendix E.

This means that to have the same accuracy in the solution at all stations the stepsize at the second station, i.e. m = 2, must be suitably reduced. In the present numerical computations the stepsize at the second and third stations was taken half the value used at subsequent stations.

3.4 Boundary Conditions Associated with the Equations of Section 3.3

When $\eta = \eta_e$, $f'(\eta_e,\xi) = 1$, and

$$\frac{\partial \bar{f}}{\partial \eta}\Big|_{\eta_e,\xi} = 0 \tag{3.14}$$

When $\eta = 0$, $f'(0,\xi) = 0$, and

$$\frac{\partial \bar{f}}{\partial \eta}\Big|_{\eta=0,\xi} = -1 \tag{3.15}$$

When $\eta = 0$, $f(0,\xi) = 0$, and

$$\bar{f}(0,\xi) = 0 \tag{3.16}$$

When $\tau = 0$, $\xi = 0$, $f' = f_0'(\eta_0)\,\frac{U_{e0}}{U_{e2}} + (1 - \frac{U_{e0}}{U_{e2}})$, and

$$\frac{\partial \bar{f}}{\partial \eta}\Big|_{\eta_2>0,\xi=0} = \frac{U_{e0}}{U_{e2}}\,\frac{\partial \bar{f}_0}{\partial \eta} \tag{3.17}$$

When $\eta = \eta_e$, $S(\eta_e,\xi) = 1$, and

$$\bar{S}(\eta_e,\xi) = 0 \tag{3.18}$$

When $\eta = 0$, $S(0,\xi) = \frac{h_w}{H_{e2}}$, and

$$\bar{S}(0,\xi) = \frac{h_w}{H_{e2}} - 1 \tag{3.19}$$

or for the case of no wall heat transfer

$$\left.\frac{\partial \bar{S}}{\partial \eta}\right|_{\eta=0,\xi} = 0 \tag{3.20}$$

When $\tau = 0$, $\xi = 0$, $S(\eta,0) = \frac{H_1}{H_{e2}}$, and

$$\bar{S}(\eta,0) = \frac{H_1}{H_{e2}} - 1 \tag{3.21}$$

We now specify [35] H_1 such that $\left.\frac{\partial \bar{S}}{\partial \xi}\right|_{\eta,\xi=0} = 0$; thus the $\bar{S}$-distribution at $\xi=0$ may be obtained from

$$\frac{\partial^2 \bar{S}}{\partial \eta^2} + \frac{\partial \bar{S}}{\partial \eta}\left(\bar{f}_{\xi=0}+\eta\right) = 0$$

which upon integration gives

$$\bar{S}(\eta,0) = (-\bar{S}_w)\frac{\int_0^{\eta} e^{-\int_0^{\eta}(\bar{f}_{\xi=0}+\eta)\,d\eta}\,d\eta}{\int_0^{\infty} e^{-\int_0^{\eta}(\bar{f}_{\xi=0}+\eta)\,d\eta}\,d\eta} + \bar{S}_w \qquad (3.21a)$$

This expression has been evaluated using the numerical values of $\bar{f}_{\xi=0}$ obtained from (3.17). See appendix B for details of the numerical integration.

3.5 Simplifications for an Adiabatic Wall

The momentum equation is, in general, coupled with the energy equation. For the case of an adiabatic wall, however, this coupling can be removed.

The solution to the energy equation (2.55) for the case of zero heat transfer at the wall and Pr=1 may be written as

$$H = h + \frac{u^2}{2} = \text{constant} = h_{e2} + \frac{U_{e2}^2}{2} = H_{e2} \qquad (3.22)$$

For the problem under consideration the external flow has instantaneously acquired the new free steam conditions whereas the boundary layer itself is non-stationary.

We may rewrite (3.22) in terms of the dimensionless enthalpy as

$$S = 1 \qquad (3.23)$$

which is the desired solution for the case of an insulated wall. Using

(3.23) in (2.54) we notice that the momentum equation is uncoupled from the energy equation (2.56) for this particular case. A solution to the uncoupled equation (2.54) is now easily obtained from the Clutter-Smith numerical technique.

The static temperature T_1 at any point in the boundary layer after the jump in the free stream velocity may be obtained from

$$S(\eta,0) = \frac{H_1}{H_{e2}} = 1$$

Rewriting the last expression as

$$h_1 + \frac{u_1^2}{2} = h_{e2} + \frac{U_{e2}^2}{2}$$

we find, after some simplifications,

$$g_1 = \frac{T_1}{T_{e2}} = 1 + \frac{(\gamma-1)}{2} M_{e2}^2 \{1 - f'^2(\eta,0)\} \qquad (3.24)$$

3.6 Procedure for Solving the Momentum and the Energy Equations Simultaneously

After the ξ-derivatives in the momentum and energy equations are replaced by finite differences, so that the partial differential equations are approximated by ordinary differential equations, the problem of solution is essentially to find the unknown boundary conditions at the wall that satisfy the known outer boundary conditions. The procedure

for doing this is given in the following sections. The two equations (3.6) and (3.7) are coupled and must be solved simultaneously.

In order to get a first solution of the momentum equation we assume $\bar{S} = 0$ at all points in the boundary layer. (As pointed out earlier $\bar{S} = 0$ or $S = 1$ is the solution of the energy equation for zero heat transfer at the wall). This gives us $\bar{f}$-distribution as a function of η and ξ. Solution to the momentum equation is now used to solve the energy equation with the appropriate boundary conditions for finite wall heat transfer. With the new solution to the energy equation we go back to solve the momentum equation again and obtain new $\bar{f}$-distribution. This $\bar{f}$-distribution may now be used to obtain improved solution to the energy equation. This procedure is continued until convergence of the solution to the momentum equation is obtained to a specified accuracy. The details of the method are given in the following paragraphs.

First the momentum equation is solved for $2 \leq m \leq m^*$[+] with known values of $\bar{f}$ from station m-1 and $\bar{S} = 0$. The values of $\bar{f}$ and their derivatives from this solution are used to solve the energy equation for the same range of m. Thus the $\bar{S}$-distribution is obtained, which may now be used to replace the earlier $\bar{S}$-distribution ($\bar{S}$=0). The iterative procedure is continued until convergence of the solution to the momentum equation is obtained.

In the iterative procedure let $Q = i, m\big|_2^{m^*}$ denote the solution of the momentum equation with accompanying solution of the energy equation

---

[+]No convergence was obtained beyond $m^*=8$(for $\gamma=1.4$) and beyond $m^*=7$ (for $\gamma = 1.67$).

for stations m=2 to m=m*. With i representing the i-th iteration of the momentum equation, the procedure is as given below:

$\underline{Q = 0, m|_2^{m^*}}$

(a) The momentum equation is solved for m=2 to m=m* with $\bar{S}$=0 and the values of $\bar{f}$ and its derivatives from station m-1. At each station m, it is solved by the cut-and-try and interpolating procedure to be described in next section. The solution may be denoted by $\bar{f}_0$.

(b) The solutions $\bar{f}_0$, the values of $\bar{S}$ and their derivatives from station m-1 are used to solve the energy equation for m=2 to m=m*. The solution is denoted by $\bar{S}_0$. The method now proceeds to the Q=1 solution.

$\underline{Q = 1, m|_2^{m^*}}$

(a) The momentum equation is solved a second time by using $\bar{S}_0$ and the solution is denoted by $\bar{f}_1$.

(b) Step (b) in $Q = 0, m|_2^{m^*}$ is repeated to obtain $\bar{S}_1$.

$\underline{Q > 1, m|_2^{m^*}}$

The procedure in $Q = 1, m|_2^{m^*}$ is repeated, always with the latest values of $\bar{f}$ and $\bar{S}$ until

$$Q = Q_{max}$$

When this condition is met, the $\overline{f}$ and $\overline{S}$ distributions are the required solutions of the momentum and the energy equations. Q_{max} was chosen to be 6 to give the values of $\overline{f}'$ from two consecutive iterations within 10^{-7}.

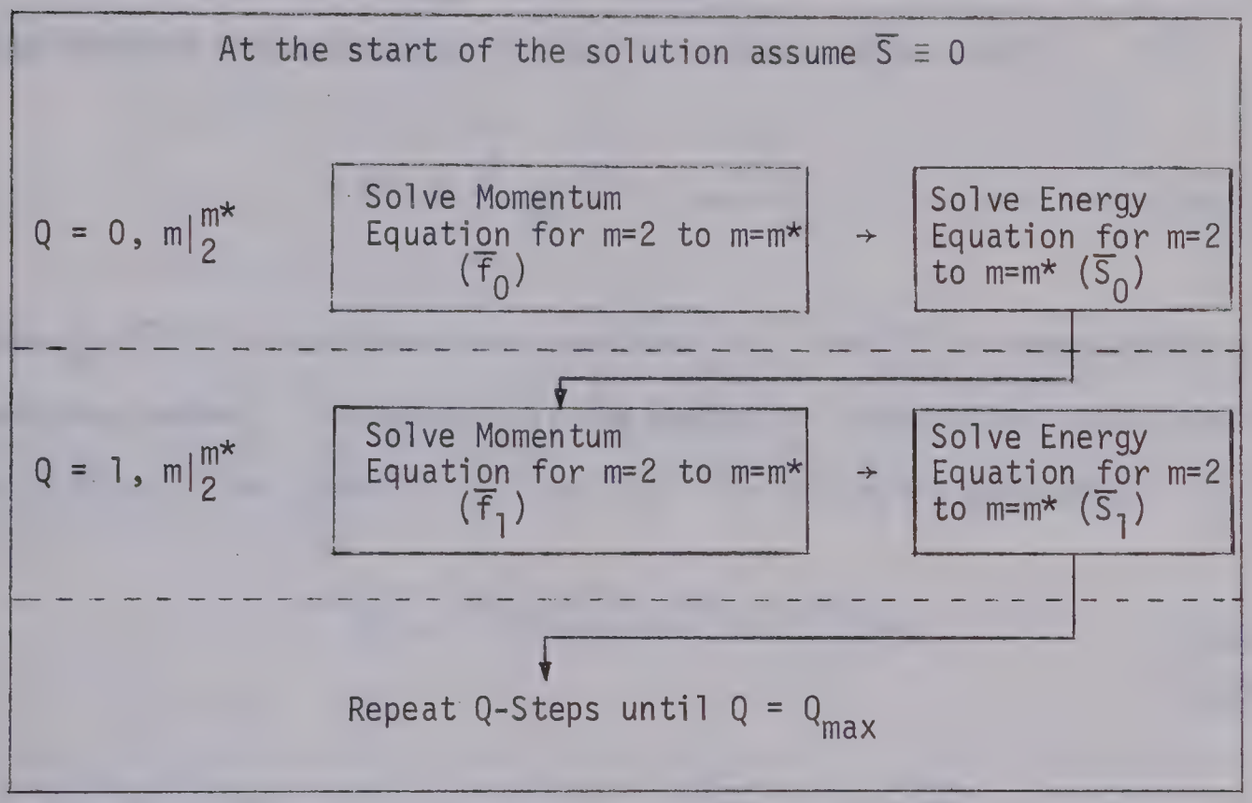

Figure 2 Flow Diagram for Solving Boundary-Layer Equations

3.7 Method of Solution of Momentum Equation at a Particular ξ-Station

As explained in section 3.3, the replacement of the ξ-derivatives by finite differences results in an ordinary differential equation at each ξ-station. Each of these third order non-linear ordinary differential equations are to be solved step by step as the solution proceeds in the ξ-direction. In this method of solution equation (3.7) is solved

as an initial value problem with trial values of $\overline{f}''_w$ as a third boundary condition. A search is then made through the possible values of $\overline{f}''_w$ to find the one that satisfies the outer boundary condition that $\overline{f}'$ approaches zero asymptotically as η approaches η_e. Before describing the procedure for making the search of $\overline{f}''_w$, the solution of the equation as an initial value problem is considered. It may first be written that

$$\overline{f}'' = \int_0^{\eta} \frac{\partial}{\partial \eta} (\overline{f}'') \, d\eta + \overline{f}''_w \tag{3.25}$$

where $\frac{\partial}{\partial \eta} (\overline{f}'')$ is obtained from equation (3.7) and $\overline{f}''_w$ is found by the searching method. The details of the method of integration to be used in (3.25) will be given in section 3.9. The following expressions

$$\overline{f}' = \int_0^{\eta} \overline{f}'' d\eta - 1 \; ; \; \overline{f} = \int_0^{\eta} \overline{f}' d\eta \tag{3.26a}$$

$$\tag{3.26b}$$

give other quantities required in the solution of (3.7).

The steps for searching the correct value of $\overline{f}''_w$ are given below:

(i) A trial value of $\overline{f}''_w$ (it was the value at the previous station for this particular problem) is used to integrate outward from the wall and a check is made to find whether or not $\overline{f}'_{trial}$ exceeds $\overline{f}' = 0$.

(ii) If $\overline{f}'_{trial}$ exceeds 0, the trial value of $\overline{f}''_w$ is high and a second solution is sought with reduced $\overline{f}''_w$. This procedure

is repeated to yield a high and a low value of $\overline{f}_w''$.

(iii) With these high and low values of $\overline{f}_w''$, the bounds on the correct value of f_w'' are further narrowed by splitting the difference between the upper and lower bounds and seeking the solution again.

(iv) This splitting-the-difference procedure is used until three solutions are obtained such that $\overline{f}_e'$ at η_e is between the bounds of $-k \leq \overline{f}'(\eta_e) \leq k$. At least one of the three solutions must be high and one must be low.

A three-point interpolation procedure, described below, is then used to determine the correct solution that satisfies the outer boundary condition $\overline{f}'(\eta_e) = 0$.

If the three trial solutions are

1st Solution	$\overline{f}_1$	$\overline{f}_1'$	$\overline{f}_1''$	$\overline{f}_1'''$
2nd Solution	$\overline{f}_2$	$\overline{f}_2'$	$\overline{f}_2''$	$\overline{f}_2'''$
3rd Solution	$\overline{f}_3$	$\overline{f}_3'$	$\overline{f}_3''$	$\overline{f}_3'''$

the desired solution is obtained from

$$\overline{f}(\eta) = A_1\overline{f}_1(\eta) + A_2\overline{f}_2(\eta) + A_3\overline{f}_3(\eta) \qquad (3.27)$$

where Lagrangian three-point interpolation is used to determine the solution that satisfies the outer boundary condition $\overline{f}'(\eta_e) = 0$. Similar

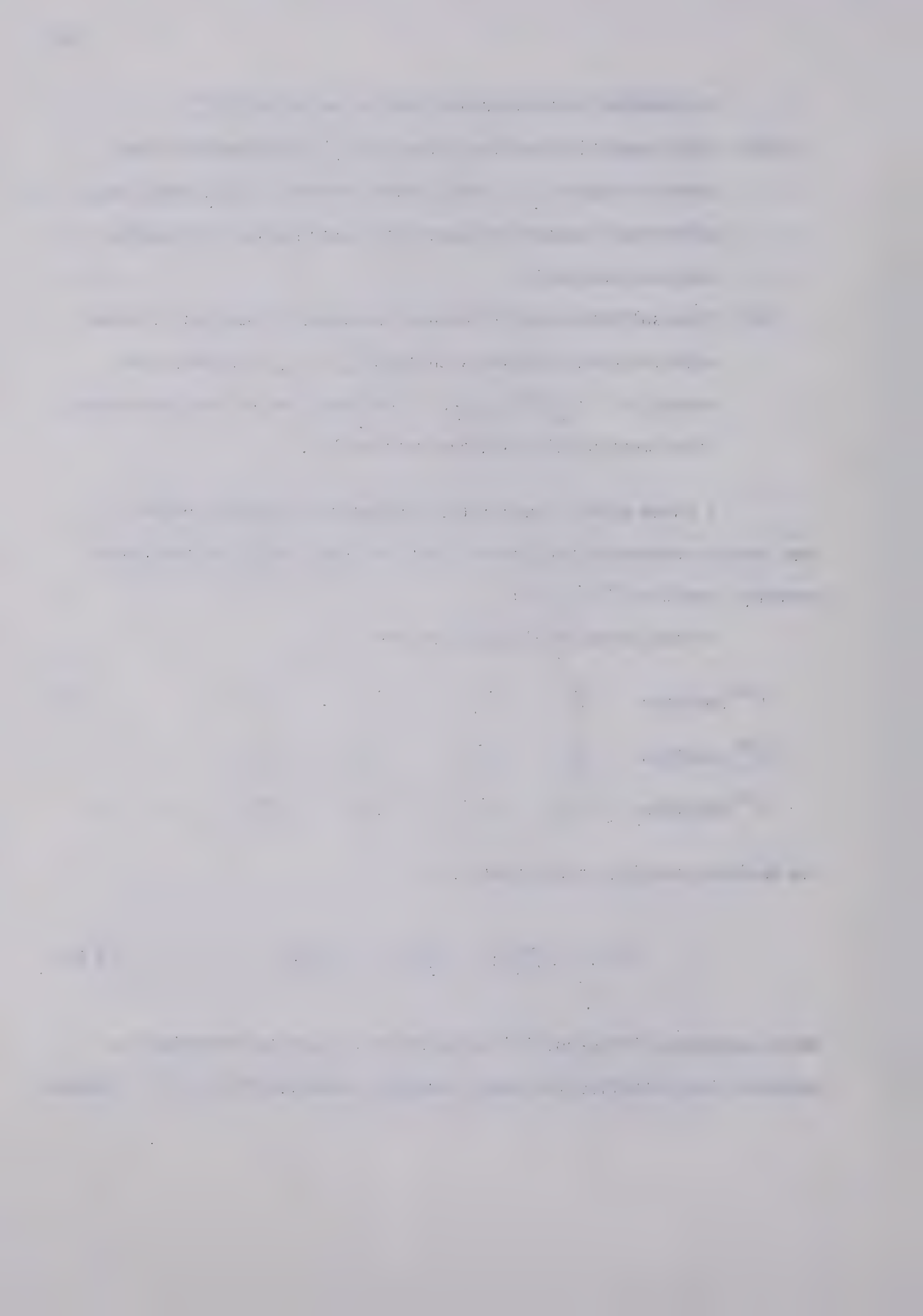

relations can be written for $\bar{f}'$, $\bar{f}''$ and $\bar{f}'''$ with the coefficients A_1, A_2 and A_3 given by

$$A_1 = \frac{\bar{f}_2'(\eta_e)\ \bar{f}_3'(\eta_e)}{\{\bar{f}_1'(\eta_e) - \bar{f}_2'(\eta_e)\}\{\bar{f}_1'(\eta_e) - \bar{f}_3'(\eta_e)\}}$$

$$A_2 = \frac{\bar{f}_1'(\eta_e)\ \bar{f}_3'(\eta_e)}{\{\bar{f}_2'(\eta_e) - \bar{f}_1'(\eta_e)\}\{\bar{f}_2'(\eta_e) - \bar{f}_3'(\eta_e)\}} \qquad (3.28)$$

$$A_3 = \frac{\bar{f}_1'(\eta_e)\ \bar{f}_2'(\eta_e)}{\{\bar{f}_3'(\eta_e) - \bar{f}_1'(\eta_e)\}\{\bar{f}_3'(\eta_e) - \bar{f}_2'(\eta_e)\}}$$

Accuracy of the solution can be improved by restricting the values of the bounds k.

It may be mentioned in passing that the Lagrangian technique is oscillatory in nature and must be used with care: for the problem treated here the smooth nature of the function permits its discriminatory use.

3.8 Method of Solution of Energy Equation at a Particular ξ-Station

The following procedure is adopted for the inetgration of the energy equation. $\bar{S}''$ is obtained from (3.6). Then $\bar{S}'$ can be determined from

$$\bar{S}' = \int_0^\eta \frac{\partial}{\partial\eta}(\bar{S}')\, d\eta + \bar{S}_w' \qquad (3.29)$$

$\bar{S}'_w$ is found by a search technique similar to the one used for solving the momentum equation. ($\bar{S}_w$ is supposed to be specified here).

Now $\bar{S}'$ can be integrated to find $\bar{S}$

$$\bar{S} = \int_0^\eta \bar{S}' d\eta + \bar{S}_w \tag{3.30}$$

With $\bar{S}_w$ specified, the procedure for searching the correct value of $\bar{S}'_w$ is as outlined below:

(i) Equation (3.6) is first solved by using a trial value of $\bar{S}'_w$ (which may be taken to be the value at the previous station). This solution is stored as $\bar{S}_1(\eta)$.

(ii) Depending on whether $\bar{S}_1(\eta_e)$ is greater than zero or less than zero, a lower or higher value, respectively, of $\bar{S}'_w$ is tried. The second solution is stored as $\bar{S}_2(\eta)$.

The two solutions can now be added to give the most general solution since the energy equation (3.6) is linear in $\bar{S}$. The general solution, which can be made to satisfy the outer boundary condition, is

$$\bar{S}(\eta) = A\,\bar{S}_1(\eta) + B\,\bar{S}_2(\eta) \tag{3.31}$$

When the outer boundary condition

$$\bar{S}(\eta_e) = A\,\bar{S}_1(\eta_e) + B\,\bar{S}_2(\eta_e) = 0$$

is used along with the condition

$$\bar{S}(0) \equiv \bar{S}_w = A\,\bar{S}_1(0) + B\,\bar{S}_2(0)$$

at $\eta = 0$ and

$$\bar{S}(0) = \bar{S}_1(0) = \bar{S}_2(0)$$

equation (3.31) gives

$$A = \frac{-\bar{S}_2(\eta_e)}{\bar{S}_1(\eta_e) - \bar{S}_2(\eta_e)} \qquad (3.32a)$$

with

$$B = 1 - A \qquad (3.32b)$$

In order to obtain more accurate results a bound k_1 on $\bar{S}(\eta_e)$, similar to k on $\bar{f}'(\eta_e)$, has been used.

3.9 Details of the Method of Integration

The overall procedure for the solution of the two coupled equations (3.6) and (3.7) has been described in the previous sections. This section is intended to give the details of integration of these equations. With the replacement of the ξ-derivatives by finite differences, the problem of solution is essetnially one of integration of a

set of ordinary differential equations. The method of integration is a predictor-corrector multistep method that uses the Falkner multiple-integration extrapolation formulae and the Adams-type multiple-integration interpolation formulae, which are described on pages 116-131 of reference [36]. The four point form of these formulae is used. The multistep method used here requires considerably less computation compared with the one-step Runge-Kutta method to produce results of comparable accuracy.

A special procedure is required to start the integration near the wall, the details are given in appendix C. We consider the general situation (away from the wall) where the equations have been integrated up to η_n and we are interested to obtain the values of $\bar{f}$ and $\bar{S}$ and their derivatives at $\eta_{n+1} (= \eta_n + \Delta\eta)$. The extrapolation and interpolation formulae are used to approximate the integration indicated in (3.25) and (3.26) for the momentum equation. The two-step procedure used in the integration is:

(i) The extrapolation formulae are used first, with the values of $\bar{f}'''$ and $\bar{f}''$ at the stations n, n-1, n-2 and n-3, to obtain the values of $\bar{f}$, $\bar{f}'$, $\bar{f}''$, and $\bar{f}'''$ at station n+1. The formulae employed are

$$\bar{f}''_{n+1)_E} = \bar{f}''_n + \frac{\Delta\eta}{24} [55\, \bar{f}'''_n - 59\, \bar{f}'''_{n-1} + 37\, \bar{f}'''_{n-2} - 9\, \bar{f}'''_{n-3}] \quad (3.33)$$

$$\bar{f}'_{n+1)_E} = \bar{f}'_n + \frac{\Delta\eta}{24} [55\, \bar{f}''_n - 59\, \bar{f}''_{n-1} + 37\, \bar{f}''_{n-2} - 9\, \bar{f}''_{n-3}] \quad (3.34)$$

$$\bar{f}_{n+1)_E} = \bar{f}_n + \Delta\eta\bar{f}'_n + \frac{(\Delta\eta)^2}{360}[323\bar{f}''_n - 264\bar{f}''_{n-1} + 159\bar{f}''_{n-2} - 38\bar{f}''_{n-3}] \qquad (3.35)$$

where the subscript E denotes "extrapolated". The errors in these equations are proportional to $(\Delta\eta)^5$ or $(\Delta\eta)^6$. (For their exact form, see reference [33])*. The value of $\bar{f}'''$ at station n+1 may now be obtained from the momentum equation (3.7) using the extrapolated values of $\bar{f}''$, $\bar{f}'$ and $\bar{f}$. This is denoted by

$$\bar{f}'''_{n+1)_E} = F(\bar{f}''_{n+1)_E}, \bar{f}'_{n+1)_E}, \bar{f}_{n+1)_E})$$

(ii) The interpolation formulae may now be used to obtain more accurate values of $\bar{f}''$, $\bar{f}'$, $\bar{f}$ and $\bar{f}'''$ at the n+1 station. These formulae are:

$$\bar{f}''_{n+1} = \bar{f}''_n + \frac{\Delta\eta}{24}[9\bar{f}'''_{n+1)_E} + 19\bar{f}'''_n - 5\bar{f}'''_{n-1} + \bar{f}'''_{n-2}] \qquad (3.36)$$

$$\bar{f}'_{n+1} = \bar{f}'_n + \frac{\Delta\eta}{24}[9\bar{f}''_{n+1)_E} + 19\bar{f}''_n - 5\bar{f}''_{n-1} + \bar{f}''_{n-2}] \qquad (3.37)$$

$$\bar{f}_{n+1} = \bar{f}_n + \Delta\eta\bar{f}'_n + \frac{(\Delta\eta)^2}{360}[360\bar{f}''_{n+1} + 171\bar{f}''_n - 36\bar{f}''_{n-1} + 7\bar{f}''_{n-2}] \qquad (3.38)$$

These interpolated values are finally used in the momentum equation (3.7) to obtain the value of $\bar{f}'''_{n+1}$

$$\bar{f}'''_{n+1} = F(\bar{f}''_{n+1}, \bar{f}'_{n+1}, \bar{f}_{n+1}).$$

---

*A brief listing of these errors is provided in Appendix E.

The errors in the interpolation formulae are much smaller in their magnitude as compared to those in the extrapolation formulae. Also, they are opposite in sign. Therefore the exact value of the variable in question, say $\overline{f}'$, must lie within the bounds of the extrapolated and interpolated values. This provides a check on the procedure and the solution can be made more exact by choosing a small enough stepsize in η.

It may be indicated here that the predictor-corrector technique was used only once to obtain the values of $\overline{f}$ and $\overline{S}$ at a point in question. A more efficient method will be to use predictor once and vary the stepsize in η such that the corrector is used once or if necessary twice to obtain the required accuracy. For the problem under consideration, however, it was found that for a five-place accuracy in the values of $\overline{f}$ and $\overline{S}$, the use of corrector was necessary once only. A standard stepsize of $\Delta\eta=0.1$ was maintained.

The formulae for performing the integrations required in the energy equation are similar to those for the momentum equation integration (refer appendix D for details).

CHAPTER IV

APPLICATION OF THE SOLUTIONS

4.1 Time-Dependent Displacement Thickness

The displacement thickness for the time-dependent boundary layer may be obtained from the following equation [37]

$$\nabla \cdot [\rho_e \vec{U}_e \Delta - \int_0^\infty (\rho_e \vec{U}_e - \rho u)\, dy] + \frac{\partial}{\partial t} [\rho_e \Delta - \int_0^\infty (\rho_e - \rho)\, dy] = 0 \,. \tag{4.1}$$

For a two-dimensional boundary layer their result may be written as

$$\rho_e[(U_e \frac{\partial \Delta}{\partial x} + \frac{\partial \Delta}{\partial t}) - (U_e \frac{\partial \delta^*}{\partial x} + \frac{\partial \delta_\rho}{\partial t})] + (\Delta - \delta^*) \frac{\partial}{\partial x} (\rho_e U_e) + (\Delta - \delta_\rho) \frac{\partial \rho_e}{\partial t} = 0 \tag{4.2}$$

where

$$\delta^* = \int_0^e (1 - \frac{\rho u}{\rho_e U_e})\, dy \tag{4.3a}$$

and

$$\delta_\rho = \int_0^e (1 - \frac{\rho}{\rho_e})\, dy \tag{4.3b}$$

Expressions (4.3) can be written in terms of the transformed variables of Chapter II, namely,

$$\delta^* = \left(\frac{\rho_o}{\rho_e}\right)\left(\frac{a_o}{a_e}\right) \int_o^e \left(\frac{T}{T_e} - \frac{u}{U_e}\right) d\bar{Y}$$

$$= \left(\frac{a_o}{a_e}\right)^{\frac{3\gamma-1}{\gamma-1}} \left[\frac{2\nu_o \bar{X}}{(m+1)V_e}\right]^{\frac{1}{2}} \int_o^e \left[S - f'^2 - \left(1 + \frac{\gamma-1}{2} M_e^2\right)^{-1}(f' - f'^2)\right] d\eta \quad (4.4a)$$

$$\delta_\rho = \left(\frac{\rho_o}{\rho_e}\right)\left(\frac{a_o}{a_e}\right) \int_o^e \left(\frac{T}{T_e} - 1\right) d\bar{Y}$$

$$= \left(\frac{a_o}{a_e}\right)^{\frac{3\gamma-1}{\gamma-1}} \left[\frac{2\nu_o \bar{X}}{(m+1)V_e}\right]^{\frac{1}{2}} \int_o^e \left[S - f'^2 - \left(1 + \frac{\gamma-1}{2} M_e^2\right)^{-1}(1 - f'^2)\right] d\eta \quad (4.4b)$$

Under our hypersonic assumption of $\frac{\partial \rho_e}{\partial t} = 0$, the continuity equation (2.4a) gives

$$\frac{\partial}{\partial x}(\rho_e U_e) = 0$$

and consequently, expression (4.2) is simplified to

$$U_e \frac{\partial \Delta}{\partial x} + \frac{\partial \Delta}{\partial t} - U_e \frac{\partial \delta^*}{\partial x} - \frac{\partial \delta_\rho}{\partial t} = 0 \quad (4.5)$$

4.2 Strong Pressure Interactions

If we denote the shock angle by σ, then for the condition that $M_e \gg 1$ and $\sigma \ll 1$ such that $M_e\sigma \gg 1$, the pressure on the surface of the plate may be expressed [25,38] as

$$\frac{p}{p_\infty} = 1 + \frac{\gamma(\gamma+1)}{2}\left(\frac{W_p}{a_\infty}\right)^2 \tag{4.6}$$

where W_p is the piston velocity.

The normal velocity of the displacement surface (piston velocity) is given [24,25] by

$$W_p = \frac{\partial \Delta}{\partial t} + U_e \frac{\partial \Delta}{\partial x} \tag{4.7}$$

and using (4.5) we obtain

$$\begin{aligned}\frac{W_p}{a_\infty} &= \frac{a_e}{a_\infty}\left(\frac{1}{a_e}\frac{\partial \delta_\rho}{\partial t} + M_e \frac{\partial \delta^*}{\partial x}\right) \\ &\simeq \frac{1}{a_e}\frac{\partial \delta_\rho}{\partial t} + M_e \frac{\partial \delta^*}{\partial x}\end{aligned} \tag{4.8}$$

where a_e/a_∞ has been approximated as unity.

Introducing (4.8) in (4.6) we get

$$\frac{p-p_\infty}{p_\infty} = \frac{\gamma(\gamma+1)}{2}\left(\frac{1}{a_e}\frac{\partial \delta_\rho}{\partial t} + M_e \frac{\partial \delta^*}{\partial x}\right)^2 \tag{4.9}$$

Now differentiating (4.4a) we find

$$\frac{\partial \delta^*}{\partial x} = C\left(\frac{a_e}{a_o}\right)^{\frac{3\gamma-1}{\gamma-1}} \frac{\partial}{\partial \bar{X}} \left\{\left(\frac{a_o}{a_e}\right)^{\frac{3\gamma-1}{\gamma-1}} \left[\frac{2\nu_o \bar{X}}{(m+1)V_e}\right]^{\frac{1}{2}}\right.$$

$$\left. \cdot \int_o^e [S - f'^2 - (1 + \frac{\gamma-1}{2} M_e^2)^{-1}(f' - f'^2)]d\eta \right\} + C\left(\frac{a_e}{a_o}\right)^{\frac{3\gamma-1}{\gamma-1}}$$

$$\cdot \frac{\partial}{\partial \bar{T}} \left\{\left(\frac{a_o}{a_e}\right)^{\frac{3\gamma-1}{\gamma-1}} \left[\frac{2\nu_o \bar{X}}{(m+1)V_e}\right]^{\frac{1}{2}} \int_o^e [S - f'^2 - (1 + \frac{\gamma-1}{2} M_e^2)^{-1}(f' - f'^2)]d\eta \right\} \cdot \frac{\partial \bar{T}}{\partial \bar{\bar{X}}}$$

or

$$\frac{\partial \delta^*}{\partial x} = C\left(\frac{a_e}{a_o}\right)^{\frac{3\gamma-1}{\gamma-1}} \frac{\partial}{\partial \bar{X}} \left\{\left(\frac{a_o}{a_e}\right)^{\frac{3\gamma-1}{\gamma-1}} \left[\frac{2\nu_o \bar{X}}{(m+1)V_e}\right]^{\frac{1}{2}} I(\xi)\right\}$$

$$+ C\left(\frac{a_e}{a_o}\right)^{\frac{3\gamma-1}{\gamma-1}} \frac{\partial}{\partial \bar{T}} \left\{\left(\frac{a_o}{a_e}\right)^{\frac{3\gamma-1}{\gamma-1}} \left[\frac{2\nu_o \bar{X}}{(m+1)V_e}\right]^{\frac{1}{2}} I(\xi)\right\} \frac{\partial \bar{T}}{\partial \bar{\bar{X}}} \qquad (4.10)$$

where

$$I = \int_o^e [S - f'^2 - (1 + \frac{\gamma-1}{2} M_e^2)^{-1}(f' - f'^2)]d\eta \qquad (4.11)$$

Simplification of (4.10) gives

$$\frac{\partial \delta^*}{\partial x} = C\left(\frac{a_e}{a_o}\right)^{\frac{3\gamma-1}{\gamma-1}} \left[\left(\frac{a_o}{a_e}\right)^{\frac{3\gamma-1}{\gamma-1}} \left(\frac{2\nu_o}{m+1}\right)^{\frac{1}{2}} \left\{I \frac{\partial}{\partial \bar{X}} \left(\sqrt{\frac{\bar{X}}{V_e}}\right)\right.\right.$$

$$\left.\left. + \sqrt{\frac{\bar{X}}{V_e}} \frac{\partial I^*}{\partial \bar{X}} - \sqrt{\frac{\bar{X}}{V_e}} \frac{\partial}{\partial \bar{X}} \left(\frac{I^{**}}{1 + \frac{\gamma-1}{2} M_e^2}\right)\right\} + \left\{\frac{2\nu_o \bar{X}}{(m+1)V_e}\right\}^{\frac{1}{2}} I\right.$$

$$\cdot \frac{\partial}{\partial \bar{X}} \{(\frac{a_o}{a_e})^{\frac{3\gamma-1}{\gamma-1}}\}] + C(\frac{a_e}{a_o})^{\frac{3\gamma-1}{\gamma-1}} [(\frac{a_o}{a_e})^{\frac{3\gamma-1}{\gamma-1}} \{\frac{2\nu_o \bar{X}}{(m+1)V_e}\}^{\frac{1}{2}} \frac{\partial I}{\partial \bar{T}} \frac{\partial \bar{T}}{\partial \bar{X}}] \quad (4.12)$$

where

$$I^* = \int_o^e (S - f'^2) d\eta \quad (4.13)$$

and

$$I^{**} = \int_o^e (f' - f'^2) d\eta \quad (4.14)$$

Expressions (4.11), (4.13) and (4.14) are functions of ξ only, and

$$\frac{\partial \delta^*}{\partial x} = C(\frac{a_e}{a_o})^{\frac{3\gamma-1}{\gamma-1}} [(\frac{a_o}{a_e})^{\frac{3\gamma-1}{\gamma-1}} (\frac{2\nu_o}{m+1})^{\frac{1}{2}} \{I \frac{\partial}{\partial \bar{X}} (\sqrt{\frac{\bar{X}}{V_e}}) + \sqrt{\frac{\bar{X}}{V_e}} \frac{\partial I^*}{\partial \xi} \frac{\partial \xi}{\partial \tau} \frac{\partial \tau}{\partial \bar{X}}$$

$$- \sqrt{\frac{\bar{X}}{V_e}} \frac{\partial}{\partial \xi} (\frac{I^{**}}{1 + \frac{\gamma-1}{2} M_e^2}) \frac{\partial \xi}{\partial \tau} \frac{\partial \tau}{\partial \bar{X}}\} + \{\frac{2\nu_o \bar{X}}{(m+1)V_e}\}^{\frac{1}{2}} I$$

$$\cdot \frac{\partial}{\partial \bar{X}} \{(\frac{a_o}{a_e})^{\frac{3\gamma-1}{\gamma-1}}\}] + C(\frac{a_e}{a_o})^{\frac{3\gamma-1}{\gamma-1}} [(\frac{a_o}{a_e})^{\frac{3\gamma-1}{\gamma-1}} \{\frac{2\nu_o \bar{X}}{(m+1)V_e}\}^{\frac{1}{2}}$$

$$\cdot \frac{\partial I}{\partial \xi} \frac{\partial \xi}{\partial \tau} \frac{\partial \tau}{\partial \bar{T}} \cdot \frac{\partial \bar{T}}{\partial \bar{X}}]$$

$$= C \sqrt{\frac{2\nu_o}{(m+1)V_e \bar{X}}} [\frac{(1-m)}{2} I - \xi(1-\xi) \frac{\partial I^*}{\partial \xi} + \frac{\xi(1-\xi)}{(1 + \frac{\gamma-1}{2} M_e^2)} \frac{\partial I^{**}}{\partial \xi}$$

$$+ \frac{m(\gamma-1) M_e^2}{(1 + \frac{\gamma-1}{2} M_e^2)^2} I^{**} + \frac{m(3\gamma-1) M_e^2}{(1 + \frac{\gamma-1}{2} M_e^2)} \frac{I}{2} + \frac{(2-4\gamma)}{(\gamma+1)} \xi(1-\xi) \frac{\partial I}{\partial \xi}] \quad (4.15)$$

To be consistent with the steady state results let us define an interaction parameter χ by

$$\chi = M_e^3 C \sqrt{\frac{\nu_o}{V_e \bar{X}}} \tag{4.16}$$

Then from (4.15) we obtain

$$M_e \frac{\partial \delta^*}{\partial x} = \sqrt{\frac{2}{(m+1)}} \frac{\chi}{M_e^2} \left[\frac{(1-m)}{2} I - \xi(1-\xi) \frac{\partial I^*}{\partial \xi} + \frac{\xi(1-\xi)}{(1 + \frac{\gamma-1}{2} M_e^2)} \frac{\partial I^{**}}{\partial \xi}\right.$$

$$\left. + \frac{m(\gamma-1) M_e^2}{(1 + \frac{\gamma-1}{2} M_e^2)^2} I^{**} + \frac{m(3\gamma-1) M_e^2}{(1 + \frac{\gamma-1}{2} M_e^2)} \frac{I}{2} + (\frac{2-4\gamma}{\gamma+1})\xi(1-\xi) \frac{\partial I}{\partial \xi}\right] \tag{4.17}$$

Similarly differentiating (4.4b) we have

$$\frac{1}{a_e} \frac{\partial \delta_\rho}{\partial t} = \frac{1}{a_e} (\frac{a_o}{a_e})^{\frac{3\gamma-1}{\gamma-1}} \left[\frac{2\nu_o \bar{X}}{(m+1)V_e}\right]^{\frac{1}{2}} \frac{\partial}{\partial t}\{\int_o^e [S-f'^2-(1 + \frac{\gamma-1}{2} M_e^2)^{-1}(1-f'^2)]d\eta\}$$

or

$$\frac{1}{a_e} \frac{\partial \delta_\rho}{\partial t} = \frac{1}{a_e} (\frac{a_o}{a_e})^{\frac{3\gamma-1}{\gamma-1}} \left[\frac{2\nu_o \bar{X}}{(m+1)V_e}\right]^{\frac{1}{2}} \frac{\partial J}{\partial t} \tag{4.18}$$

where

$$J = \int_o^e [S-f'^2-(1 + \frac{\gamma-1}{2} M_e^2)^{-1}(1-f'^2)]d\eta \tag{4.19}$$

Expression (4.19) is a function of ξ only, and

$$\frac{1}{a_e} \frac{\partial \delta_\rho}{\partial t} = \frac{1}{a_e} (\frac{a_o}{a_e})^{\frac{3\gamma-1}{\gamma-1}} \left[\frac{2\nu_o \bar{X}}{(m+1)V_e}\right]^{\frac{1}{2}} C(\frac{a_e}{a_o})^{\frac{4\gamma-2}{\gamma-1}} \frac{\partial J}{\partial \xi} \frac{\partial \xi}{\partial \tau} \frac{\partial \tau}{\partial \bar{t}}$$

$$= C \sqrt{\frac{2\nu_o}{(m+1)V_e \overline{X}}} M_e (1-\xi)^2 \frac{\partial J}{\partial \xi} \tag{4.20}$$

Using (4.16) in (4.20) we obtain

$$\frac{1}{a_e} \frac{\partial \delta_\rho}{\partial t} = \sqrt{\frac{2}{m+1}} \frac{\chi}{M_e^2} (1-\xi)^2 \frac{\partial J}{\partial \xi} \tag{4.21}$$

Substitution of the pertinent quantities from (4.17) and (4.21) in (4.9) finally gives

$$\frac{p-p_\infty}{p_\infty} = \frac{\gamma(\gamma+1)}{(m+1)} \frac{\chi^2}{M_e^4} \left[(1-\xi)^2 \frac{\partial J}{\partial \xi} + \left\{(1-m) + \frac{m(3\gamma-1) M_e^2}{(1 + \frac{\gamma-1}{2} M_e^2)}\right\} \frac{I}{2}\right.$$

$$\left. - \xi(1-\xi) \left\{\frac{\partial I^*}{\partial \xi} - \frac{1}{(1 + \frac{\gamma-1}{2} M_e^2)} \frac{\partial I^{**}}{\partial \xi} - \left(\frac{2-4\gamma}{\gamma+1}\right) \frac{\partial I}{\partial \xi}\right\} + \frac{m(\gamma-1) M_e^2}{(1 + \frac{\gamma-1}{2} M_e^2)^2} I^{**}\right]^2$$

$$= \frac{1}{2} \left[\frac{(\gamma+1)\chi}{M_e^2}\right]^2 \left[(1-\xi)^2 \frac{\partial J}{\partial \xi} + \left\{\left(\frac{2}{\gamma+1}\right) + \left(\frac{\gamma-1}{\gamma+1}\right) \frac{(3\gamma-1) M_e^2}{(1 + \frac{\gamma-1}{2} M_e^2)}\right\} \frac{I}{2}\right.$$

$$\left. - \xi(1-\xi) \left\{\frac{\partial I^*}{\partial \xi} - \frac{1}{(1 + \frac{\gamma-1}{2} M_e^2)} \frac{\partial I^{**}}{\partial \xi} - \left(\frac{2-4\gamma}{\gamma+1}\right) \frac{\partial I}{\partial \xi}\right\} + \frac{(\gamma-1)^2 M_e^2}{(\gamma+1)(1 + \frac{\gamma-1}{2} M_e^2)^2} I^{**}\right]^2 \tag{4.22}$$

From (4.22) we may also write, for the final steady state,

$$\frac{p_2-p_\infty}{p_\infty} = \frac{1}{2} \left[\frac{(\gamma+1)\chi}{M_e^2}\right]^2 \left[\left\{\left(\frac{2}{\gamma+1}\right) + \left(\frac{\gamma-1}{\gamma+1}\right) \frac{(3\gamma-1) M_e^2}{(1 + \frac{\gamma-1}{2} M_e^2)}\right\} \frac{I_2}{2}\right.$$

$$+ \frac{(\gamma-1)^2 M_e^2}{(\gamma+1)(1 + \frac{\gamma-1}{2} M_e^2)^2} I_2^{**}]^2 \qquad (4.23)$$

where

$$I_2 = \int_0^e [S_2 - f_2'^2 - (1 + \frac{\gamma-1}{2} M_e^2)^{-1}(f_2' - f_2'^2)]d\eta \qquad (4.24)$$

and

$$I_2^{**} = \int_0^e (f_2' - f_2'^2)d\eta \qquad (4.25)$$

From (4.22) and (4.23) we may obtain the expression for the strong interaction induced pressure referenced to the final steady state

$$\frac{p-p_2}{p_\infty} = \frac{1}{2}\left[\frac{(\gamma+1)\chi}{M_e^2}\right]^2 \Bigg\langle \left[(1-\xi)^2 \frac{\partial J}{\partial \xi} + \left\{\left(\frac{2}{\gamma+1}\right) + \left(\frac{\gamma-1}{\gamma+1}\right) \frac{(3\gamma-1) M_e^2}{(1 + \frac{\gamma-1}{2} M_e^2)}\right\} \frac{I}{2}\right.$$

$$- \xi(1-\xi) \left\{\frac{\partial I^*}{\partial \xi} - \frac{1}{(1 + \frac{\gamma-1}{2} M_e^2)} \frac{\partial I^{**}}{\partial \xi} - \left(\frac{2-4\gamma}{\gamma+1}\right) \frac{\partial I}{\partial \xi}\right\}$$

$$+ \frac{(\gamma-1)^2 M_e^2}{(\gamma+1)(1 + \frac{\gamma-1}{2} M_e^2)^2} I^{**}]^2 - \left[\left\{\left(\frac{2}{\gamma+1}\right) + \left(\frac{\gamma-1}{\gamma+1}\right) \frac{(3\gamma-1) M_e^2}{(1 + \frac{\gamma-1}{2} M_e^2)}\right\} \frac{I_2}{2}\right.$$

$$\left. + \frac{(\gamma-1)^2 M_e^2}{(\gamma+1)(1 + \frac{\gamma-1}{2} M_e^2)^2} I_2^{**}]^2 \right\rangle \qquad (4.26)$$

4.3 Shear Stress at the Wall

The shear stress at the wall may be obtained from

$$\tau_w = \mu_w \left.\frac{\partial u}{\partial y}\right|_{y=0} \tag{4.27}$$

Using the transformations of Chapter II we find

$$\tau_w = \frac{\mu_w \rho_w}{\rho_o} \left(\frac{a_e}{a_o}\right)^2 \frac{\partial^2 \psi}{\partial \bar{Y}^2}$$

$$= \frac{\mu_w \rho_w}{\rho_o} \left(\frac{a_e}{a_o}\right)^2 \left[\frac{(m+1)}{2\nu_o \bar{X}}\right]^{\frac{1}{2}} V_e^{\frac{3}{2}} f''(0,\xi) \tag{4.28}$$

Now the local skin friction coefficient may be defined as

$$C_f = \frac{\tau_w}{\frac{1}{2} \rho_w U_e^2} \tag{4.29}$$

Substituting for τ_w from (4.28) we get

$$C_f = \frac{2\mu_w}{\rho_o U_e^2} \left(\frac{a_e}{a_o}\right)^2 \left[\frac{(m+1)}{2\nu_o \bar{X} V_e}\right]^{\frac{1}{2}} V_e^2 f''(0,\xi)$$

$$= 2\mu_w \left[\frac{(m+1)}{2\nu_o \bar{X} V_e \rho_o^2}\right]^{\frac{1}{2}} f''(0,\xi) \tag{4.30}$$

Using the viscosity law (2.20), we may rewrite (4.30) in the following form

$$C_f = 2C\ S_w \sqrt{\frac{(m+1)\nu_o}{2\bar{X}\ V_e}}\ f''(0,\xi) \tag{4.31}$$

We now introduce a Reynolds number based on fluid properties evaluated at the wall temperature

$$Re_w = \frac{U_e x}{\nu_w} \tag{4.32}$$

and expression (4.31) becomes

$$C_f = 2C\ S_w \sqrt{\frac{(m+1)}{2Re_w}} \cdot \sqrt{\frac{\nu_o\ x\ a_e}{\nu_w\ \bar{X}\ a_o}}\ f''(0,\xi)$$

or

$$\frac{C_f \sqrt{Re_w}}{2} = \sqrt{\left[\frac{(m+1)}{2}\ \frac{d\ln\bar{X}}{d\ln x}\right]} f''(0,\xi) \tag{4.33}$$

The advantage of evaluating fluid properties at the wall temperature can now be seen from the fact that for the case of $\beta = 0$ the right hand side of equation (4.33) becomes independent of x and $\bar{X}$ and is a function of ξ alone.

4.4 Heat Transfer at the Wall

The heat transfer at the wall can be found from

$$q_w = -\ k_w \left.\frac{\partial T}{\partial y}\right|_{y=0} \tag{4.34}$$

or

$$q_w = - k_w \left[\frac{(m+1)\, V_e}{2\nu_o \bar{X}}\right]^{\frac{1}{2}} \left(\frac{a_e}{a_o}\right)\left(\frac{\rho_w}{\rho_o}\right) \left.\frac{\partial T}{\partial \eta}\right|_{\eta=0}$$

$$= - k_w \left[\frac{(m+1)\, V_e}{2\nu_o \bar{X}}\right]^{\frac{1}{2}} \left(\frac{a_e}{a_o}\right)\left(\frac{\rho_w}{\rho_o}\right) \frac{h_e}{c_p} \left(1 + \frac{\gamma-1}{2} M_e^2\right) S'(0,\xi) \quad (4.35)$$

Defining Nusselt number as

$$Nu = \frac{x\left(\frac{\partial T}{\partial y}\right)_w}{T_o - T_w} = - \frac{x\, q_w}{(T_o - T_w)\, k_w} \quad (4.36)$$

we obtain, after substituting for q_w from (4.35),

$$Nu = \frac{\left[\frac{(m+1)}{2} Re_w\right]}{(T_o - T_w)} \sqrt{\frac{a_e \nu_o}{a_o \nu_w} \frac{x}{\bar{X}}} \left(\frac{\nu_w}{\nu_o}\right)\left(\frac{\rho_w}{\rho_o}\right) \frac{h_e}{c_p} \left(1 + \frac{\gamma-1}{2} M_e^2\right) S'(0,\xi)$$

$$= \sqrt{\left[\frac{(m+1)}{2} Re_w \frac{d\ln \bar{X}}{d\ln x}\right]} \left(\frac{T_e}{T_o - T_w}\right) \left(1 + \frac{\gamma-1}{2} M_e^2\right) S'(0,\xi)$$

$$= \sqrt{Re_w} \cdot \sqrt{\left[\frac{(m+1)}{2} \frac{d\ln \bar{X}}{d\ln x}\right]} \frac{S'(0,\xi)}{(1-S_w)} \quad (4.37)$$

From (4.33) and (4.37) a simple modified Reynold's analogy parameter is obtained

$$\frac{C_f\, Re_w}{Nu} = \frac{2f''(0,\xi)}{\left(\frac{S'(0,\xi)}{1-S_w}\right)} \quad (4.38)$$

The numerical results for the transient contributions to the shear stress and heat transfer at the wall and to the interaction pressure are displayed in appendix F.

CHAPTER V

RESULTS AND CONCLUSIONS

5.1 Discussion of the Results

Using the Prandtl boundary-layer equations for a time-dependent two-dimensional compressible fluid flow, the strong interaction problem has been analysed. The earlier work of reference [22] investigated the weak interaction problem. The numerical method adopted there, requires the linearization of the governing equations. For this linearization to be valid, the free stream velocity change was restricted to about 1%. The numerical method adopted here eliminates this restriction. The governing equations, under the suggested transformations of Chapter II, are more suitable for analysing the strong interaction case. One of the contributions of the present work lies in obtaining equations (2.49) and (2.50) which are a coupled set of partial differential equations in two independent variables for large Mach numbers. As a limit for weak interactions, the present equations reduce to those obtained in reference [22]. These coupled equations have been solved for $\beta = (\gamma-1)/\gamma$, with $\gamma = 1.4$ and 1.67. The induced pressure results are, therefore, obtained according to the strong interaction theory. Another important contribution of the present work is in obtaining the transient strong-interaction induced pressure along with the time-dependent wall shear and wall heat transfer for an insulated and non-insulated wall.

The distribution of the transient contribution to the velocity function f_2' is given in Figures 3 through 10 for different values of wall heat transfer and for $\beta = 0.286$ and 0.4. These distributions have been obtained corresponding to 1% change in the free stream velocity. It may be noticed from these figures that the numerical results have been obtained for $0 \leq \xi \leq 0.3$ only, since the method of solution becomes unstable for $\xi > 0.3$. This instability may be explained qualitatively if we examine equation (3.7). The leading derivative terms in this equation are

$$\frac{\partial^2(\bar{f}')}{\partial\eta^2} = \{(\frac{\gamma+1}{\gamma})(1-\xi)^2 - 4\xi(1-\xi)(\bar{f}'+1)\} \frac{\partial}{\partial\xi}(\bar{f}') + \ldots$$

or

$$\frac{\partial(\bar{f}')}{\partial\xi} = K \frac{\partial^2(\bar{f}')}{\partial\eta^2} + \ldots \qquad (5.1)$$

The above expression has the character of the conduction heat equation with the equivalent coefficient of conductivity given by

$$K = \frac{1}{(1-\xi)^2\{(\frac{\gamma+1}{\gamma}) - \frac{4\xi}{(1-\xi)}(\bar{f}'+1)\}} \qquad (5.2)$$

In expression (5.1) K will have different signs for $0 < \xi < (\gamma+1)/(4\gamma\bar{f}'+5\gamma+1)$ and $(\gamma+1)/(4\gamma\bar{f}'+5\gamma+1) < \xi < 1$. At $\xi = (\gamma+1)/(4\gamma\bar{f}'+5\gamma+1)$, K becomes infinite. It seems that the discontinuity in the $\bar{f}'$-distribution occurs upon approaching the neighbourhood of $\xi = (\gamma+1)/(4\gamma\bar{f}'+5\gamma+1)$.

At the outer edge of the boundary layer, where $\overline{f}' = 0$ and the discontinuity first appears, ξ has the value of 0.3 for $\gamma = 1.4$.

In the discussion of literature in section 1.2 Stewartson's singularity at $\tau=1$(or $\xi=0.5$) has been described in detail. If the highest order derivative terms in equation (2.49) are considered with $\beta=0$, the relationship between the singularities at $\xi=0.3$ (for $\beta=0.286$) and at $\xi=0.5$(for$\beta=0$) becomes clearer. The highest order and the mixed derivative terms are

$$\frac{\partial^2(f')}{\partial\eta^2} = 2\{1-\tau f'\} \frac{\partial(f')}{\partial\tau} + \ldots \qquad (5.3)$$

The coefficient of the mixed derivative (5.3) will have different signs for $0 < \tau < \frac{1}{f'}$ and $\frac{1}{f'} < \tau < \infty$. Once again this coefficient will be 0 or the equivalent coefficient of conduction will be ∞ at $\tau = \frac{1}{f'}$. This seems to imply that the discontinuity in the solutions will set in for $\tau = 1$ at the outer edge of the boundary layer where $f' = 1$. Thus $\tau=1$(or $\xi=0.5$) is the singularity for $\beta=0$, which corresponds to $\xi=0.3$ for $\beta=0.286$.

The curves of Figure 3 through 10 indicate the beginning of a monotonic approach to the final steady state. For $\beta = 0.286$, Figures 3 through 6 also show that the approach towards the steady state is faster when the wall is kept at a higher temperature as compared to the case when the wall is at a lower temperature. (In all these cases the flow of heat is always from the fluid to the wall). One possible interpretation for this trend is related to the effect of wall temperature on

the mean density of the fluid within the boundary layer. For the hot wall, the boundary-layer density is less than that for the cold wall, rendering the hot-wall boundary layer more susceptible to thermodynamic changes than the cold-wall boundary layer. This implies that a hot-wall boundary layer would approach the steady state faster than the cold-wall boundary layer.

Figures 7 through 10 indicate a similar behavior of $(f'-f_2')$ for $\beta = 0.4$. A comparison of these figures with those for $\beta = 0.286$ indicates that the approach towards the final steady state is faster for $\beta = 0.4$ for a given value of the wall temperature.

The transient distribution of the shear function f_w'' is given in Figure 11. This figure shows that the approach of the shear function towards its steady state value is rapid and monotonic. It may also be noted that heating the surface and larger pressure gradients increase the wall shear.

The distribution of the transient contribution to the boundary-layer temperature is shown in Figures 12 through 19. The negative values in (g_w-g) distribution for small η's may be explained if we consider an approximate solution to the energy equation (2.56). Such a solution for $S_w \simeq 0$ may be written down as

$$S(\eta,\tau) = S_w + (1-S_w)\, f'(\eta,\tau) \qquad (5.4a)$$

This may be used for $S_w \simeq 0$ and small values of β, since the contri-

bution of $\beta(f'^2-S)$ to the momentum equation is negligible as compared to the other terms. For $S_w = 0$ we obtain from (5.4a)

$$S = f' \tag{5.4b}$$

For large Mach numbers expression (2.60) also gives

$$(g_2-g) = \frac{(\gamma-1)}{2} M_e^2 (S_2-f_2'^2-S+f'^2) \tag{5.5a}$$

Using (5.4b) in (5.5a) we obtain, for $S_w = 0$,

$$(g_2-g) = \frac{(\gamma-1)}{2} M_e^2 (f'-f_2')\{(f'+f_2') - 1\} \tag{5.5b}$$

For the problem under consideration $(f'-f_2')$ is always positive. However, the expression in the curly bracket is negative for small η's and positive for large η's. This gives the qualitative explanation for the "peculiar" behavior of (g_2-g) at small η's. In order to explain this physically we consider the viscous dissipation close to the plate. The slope of the velocity profile which is a measure of the shear stress, changes very fast for small values of η's and ξ's. This means that there is substantial viscous dissipation for this range of η and ξ. This raises the temperature of the fluid next to the plate higher than the final steady state temperature. For large values of η's however, the velocity profile is less steep and accordingly the viscous dissipation is not very significant. Therefore, the temperature of that part of the boundary-

layer fluid is smaller than the final steady state temperature. As time increases (i.e for large values of ξ's) the heat transfer in the boundary layer helps to bring the temperature of the fluid towards the final steady state temperature for all values of η's. Figure 12 through 19 also indicate that for a given Mach number and wall temperature, the transient contribution to the temperature in the boundary layer is larger for $\beta = 0.4$ as compared with $\beta = 0.286$.

The linearized solutions for the transient contribution to the wall shear, boundary-layer temperature and the velocity function for the case of an adiabatic wall and $\gamma = 1.4$ have been presented in appendix A. It has been found that the wall shear predicted by the linearized solutions is about 1% lower than the one obtained without linearization using the Clutter-Smith technique. The values for the transient boundary-layer temperature are smaller by about 1/2% using the linearized solutions. The agreement between the linearized and the non-linearized solutions appears to be very good for the 1% change in the plate velocity. For larger changes in the plate velocity the linearized solutions are expected to be in more error as compared to the non-linearized solutions.

The transient distribution of Reynolds analogy parameter is given in Figure 20. These curves resemble the $f''(0,\xi)$ curves (Fig. 11) because of the relatively small variation in magnitude of $S'(0,\xi)/(1-S_w)$ compared with that of $f''(0,\xi)$. Utilizing expression (4.38) and Figure 11 we may easily obtain the heat transfer at the wall from Figure 20 for any particular case in question.

The strong-interaction transient contribution to the pressure distribution for the different values of wall temperature and Mach numbers is given in Figures 21 through 26. We notice from these figures that for a given Mach number and the pressure gradient parameter β, the transient contribution is larger for a hot wall as compared to that for a cold wall. We may thus conclude that cooling the surface tends to induce a smaller pressure rise in the interaction zone.

With the increase in Mach number the transient contribution goes down for fixed values of S_w and β. For a given S_w and Mach number, the transient contribution is smaller for $\beta = 0.286$ as compared with $\beta = 0.4$.

Some of the induced pressure results have been further analysed in Figure 27 for $M_e = 5$ and $\chi = 6$. This figure indicates that the transient contribution decreases faster for large values of β and wall temperature.

The numerical results pertinent to expression (4.22) reveal that for most of the cases under consideration, the following approximate expression may be used:

$$\frac{p-p_\infty}{p_\infty} = \frac{1}{2}\left[\frac{(\gamma+1)\,\chi}{M_e^2}\right]^2\left[\left\{\left(\frac{2}{\gamma+1}\right)+\left(\frac{\gamma-1}{\gamma+1}\right)\frac{(3\gamma-1)\,M_e^2}{\left(1+\frac{\gamma-1}{2}M_e^2\right)}\right\}\frac{I}{2}\right.$$

$$\left.+\frac{(\gamma-1)^2\,M_e^2}{(\gamma+1)\left(1+\frac{\gamma-1}{2}M_e^2\right)^2}\,I^{**}\right]^2 \qquad (5.6)$$

5.2 Concluding Remarks

The present results may be utilized to obtain the history of the temperature distribution at the wall, the transient drag force (obtained through the integration of the shear stresses at various times), and the transient induced pressure over the wall.

In order to extend the present solutions beyond $\xi = (\gamma+1)/(4\gamma\bar{f}'+5\gamma+1)$, a different approach should be adopted. Ban's [19] method of solution appears to be more plausible for this region. Equation (2.54) although parabolic in nature, may be subjected to the "elliptic" boundary conditions in the region $(\gamma+1)/(4\gamma\bar{f}'+5\gamma+1) < \xi < 1$. The present solutions evaluated at $\xi = 0.3$ (for $\gamma = 1.4$) may be used to provide one set of boundary conditions.

Once the solutions for the above range of ξ have been completed it would be desirable to extent the analysis to cases of Prandtl number other than unity. Similar investigations for other airfoil profiles like an inclined flat plate, circular cone etc. should also be of interest.

BIBLIOGRAPHY

[1] Blasius, H., "Grenzschicten in Flussigkeiten mit kleiner Reibung", Math. and Phys., Vol. 56, p. 1, 1908.

[2] Stewartson, K., "The Theory of Unsteady Laminar Boundary Layers", in Advances in Applied Mechanics, Vol. 6, pp. 1-37, Academic Press, 1960.

[3] Rott, N., "Theory of Time-dependent Laminar Flows", in Theory of Laminar Flows, High Speed Aerodynamics and Jet Propulsion, Vol. 4, Princeton University Press, pp. 395-438, 1964.

[4] Moore, F.K., "Unsteady Laminar Boundary Layer Flow", NACA TN 2471, 1951.

[5] Ostrach, S., "Compressible Laminar Boundary Layer and Heat Transfer for Unsteady Motions of a Flat Plate", NACA TN 3569, 1955.

[6] Yang, W.J. and Huang, H.S., "Unsteady Compressible Laminar Boundary-Layer Flow over a Flat Plate", AIAA Journal, Vol. 7, No. 1, pp. 100-105, Jan. 1969.

[7] Zien, T.F. and Reshotko, E., "Boundary-Layer Induced Pressures on a Flat Plate in Unsteady Hypersonic Flight", AIAA Journal, Vol. 8, No. 1, pp. 158-160, Jan. 1970.

[8] Stewartson, K., "On the Impulsive Motion of a Flat Plate in a Viscous Fluid", Quart. Appl. Math. and Mech., 4, pp. 182-198, 1951.

[9] Smith, S.H., "The Impulsive Motion of a Wedge in a Viscous Fluid", Z. angew. Math. Phys., 18, pp. 508-522, 1967.

[10] Lam, S.H. and Crocco, L., "Shock Induced Unsteady Laminar Compressible Boundary Layer on a Semi-Infinite Flat Plate", Princeton University Report No. 428, AFOSR TN 58-581, September, 1958.

[11] Mirels, H., "Laminar Boundary Layer Behind Shock Advancing into Stationary Fluid", NACA TN 3401, 1955.

[12] Gevrey, M., "Sur les Equations aux Derivees Partielles du Type Parabolique", Journ. de Math., Series 6, Vol. 10, pp. 105-142, 1914.

[13] Cheng, S.I., "Some Aspects of Unsteady Laminar Boundary Layer Flows", Quart. Appl. Math., Vol. 14, No. 4, Jan. 1957.

[14] Cheng, S.I. and Elliott, D., "The Unsteady Laminar Boundary Layer on a Flat Plate", Princeton University, Aero. Eng. Report 318, 1955.

[15] Schuh, H., "Calculation of Unsteady Boundary Layers in Two-dimensional Flow", Zeitschr. Flugw., Vol. 1, pp.122-131, 1953.

[16] Schetz, J.A. and Oh, S.K., "Approximate Analysis of Transient Laminar Boundary-Layer Development", J. Heat Transfer, Trans. ASME, Nov. 1968.

[17] Tokuda, N., "On the Impulsive Motion of a Flat Plate in a Viscous Fluid", J. Fluid Mech., Vol. 33, part 4, pp. 657-672, 1968.

[18] Corrigenda, J. Fluid Mech., Vol. 35, part 4, pp. 828-829, 1969.

[19] Ban, S.D., "Interaction Region in the Boundary Layer of a Shock Tube", Scientific Report AFOSR 67-1286, Case Inst. of Tech., FTAS/TR-67-20, June 1967.

[20] Friedrichs, K., "Symmetric Positive Linear Differential Equations", Comm. Pure Appl. Math., Vol. 11, pp. 333-418, 1958.

[21] Murdock, J.W., "A Solution of Shock-Induced Boundary Layer Problems by an Integral Method" , Aerospace Corp. Tech. Rept. No. TR-0158, San Benardino, California, 1969.

[22] Rodkiewicz, C.M. and Reshotko, E., "Time-Dependent Hypersonic Viscous Interactions", Scientific Report AFOSR 67-2451, Case Inst. of Tech., FTAS/TR-67-28, Nov. 1967.

[23] Reshotko, E. and Rodkiewicz, C.M., "Pressure Induced by Weak Interaction with Unsteady Hypersonic Boundary Layers", AIAA Journal, Vol. 7, No. 8, pp.1609-1610, August 1969.

[24] Lighthill, M.J., "Oscillating Airfoils at High Mach Number", Journal Aero. Sci., Vol. 20, No. 6, pp. 402-406, June 1953.

[25] Miles, J.W., "Unsteady Flow at Hypersonic Speeds", in Hypersonic Flow, Butterworths Scientific Publications, London, pp. 185-197, 1960.

[26] Shen, S.F., "On the Boundary Layer Equations in Hypersonic Flow", Journal Aero. Sci., Vol. 19, pp. 500-501, July 1952.

[27] Landahl, M.T., "Unsteady Flow Around Thin Wings at High Mach Numbers", Journal Aero. Sci., Vol. 24, No. 1, pp. 33-38, Jan. 1957.

[28] Raymond, J.L., "Piston Theory Applied to Strong Shocks and Unsteady Flow", RAND Corp. Rept. p. 1398, 1958.

[29] Stewartson, K., "The Theory of Laminar Boundary Layers in Compressible Fluids", Oxford Mathematical Monographs, Oxford University Press, pp. 122-142, 1964.

[30] Chapman, D.R. and Rubesin, M.W., "Temperature and Velocity Profiles in the Compressible Laminar Boundary Layer with Arbitrary Distribution of Surface Temperature", Journal Aero. Sci., Vol. 16, No. 9, pp. 547-565, 1949.

[31] Cohen, C.B. and Reshotko, E., "Similar Solutions for the Compressible Laminar Boundary Layer with Heat Transfer and Pressure Gradient", NACA Report 1293, 1956.

[32] Lees, L., "On the Boundary Layer Equations in Hypersonic Flow and Their Approximate Solutions", Journal Aero. Sci., Vol. 20, No. 5, pp. 143-145, May 1953.

[33] Clutter, W.D. and Smith, A.M.O., "Solutions of the General Boundary-Layer Equations for Compressible Laminar Flow Including Transverse Curvature", Report No. LB31088, Douglas Aircraft Co., Feb. 1963; Revised October, 1964, Also AIAA Journal, Vol. 3, pp. 639-647, 1965.

[34] Hartree, D.R. and Womersley, J.R., "A Method for the Numerical or Mechanical Solution of Certain Types of Partial Differential Equations", Proc. Royal Soc., Series A, Vol. 161, No. 906, p. 353, August 1937.

[35] Luft, B., "The Weak Viscous Interactions in the Unsteady High Mach Number Flow", M.Sc. Thesis to be submitted at the University of Alberta, 1970.

[36] Collatz, L., "The Numerical Treatment of Differential Equations", Springer-Verlag, 1960.

[37] Moore, F.K. and Ostrach, S., "Displacement Thickness of the Unsteady Boundary Layer", Journal Aero. Sci., January 1957.

[38] King, W.S., "Low Frequency, Large Amplitude Fluctuations of the Laminar Boundary Layer", AIAA Journal, Vol. 4, No. 6, June 1966.

[39] Hays, W.D. and Probstein, R.F., "Hypersonic Flow Theory", Academic Press, 1959.

[40] Van Dyke, M.D., "Perturbation Methods in Fluid Mechanics", Academic Press, New York, 1964.

[41] Wachspress, E.L., "Iterative Solution of Elliptic Systems", Prentice Hall, Inc., 1966.

[42] Hartree, D.R., "On an Equation Occurring in Falkner and Skan's Approximate Treatment of the Equations of the Boundary Layer", Proc. Cambridge Phil. Soc., Vol. 33, p. 237, 1937.

[43] Dorrance, W.H., "Viscous Hypersonic Flow", McGraw-Hill Book Co., In., 1962.

[44] Goldstein, S. and Rosenhead, L., "Boundary Layer Growth", Proc. Cambridge Phil. Soc., Vol. 32, p. 392, 1936.

[45] Orlik-Ruckemann, K.J., "Stability Derivatives of Sharp Wedges in Viscous Hypersonic Flow", AIAA Journal, Vol. 4, No. 6, 1966.

[46] Van Dyke, M., "Applications of Hypersonic Small-Disturbance Theory", Journal Aero. Sci., 21, pp. 179-186, 1954.

[47] Mollo-Christensen, E. and Ashley, H., "Applicability of Piston Theory to the Flow Around Wings in Unsteady Motion", Journal Aero. Sci., 21, pp. 779-80, 1954.

[48] Landahl, M., Ashley, H. and Mollo-Christensen, E., "On Approximate Solutions for the Compressible Flow Around Oscillating Thin Wings", Journal Aero. Sci., 22, pp. 581-582, 1955.

[49] Hamaker, F. and Wong, T., "The Similarity Law for Unsteady Hypersonic Flows and Requirements for the Dynamical Similarity of Related Bodies in Free Flight", NACA TN 2631, 1952.

[50] Miles, J.W., "Panel Flutter in the Presence of a Boundary Layer", Journal Aero. Sci., 26, pp. 81-93, 1959.

[51] Lomax, H., Heaslet, M.A., Fuller, F.B. and Sluder, L., "Two and Three Dimensional Unsteady Lift Problems in High Speed Flight", NACA Report 1077, 1952.

[52] Garrick, I.E., "Nonsteady Wing Characteristics", in High Speed Aerodynamics and Jet Propulsion, Vol. VII, Princeton University Press, pp. 658,793, 1957.

[53] Richtmyer, R.D., "Difference Methods for Initial Value Problems", Interscience Publishers, Inc., 1957.

[54] Allen, D.N.G., "Relaxation Methods in Engineering and Science", McGraw-Hill Book Compl., Inc., 1954.

[55] Rolston, A. and Wilf, H.S., "Mathematical Methods for Digital Computers, John Wiley and Sons, Inc., 1965.

[56] Lees, L. and Probstein, R.F., "Hypersonic Flows of a Viscous Fluid", U.S. Air Force Contract No. AF 33(038)-250, Project No. 1363, 1953.

[57] Carnahan, B., Luther, H.A. and Wilkes, J.O., "Applied Numerical Methods", John Wiley & Sons, Inc., 1969.

[58] Li, T.Y. and Nagamatsu, H.T., "Similar Solutions of Compressible Boundary Layer Equations", Journal Aero. Sci., Vol. 22, No. 9, pp. 607-616, Sept. 1955.

[59] Li, T.Y. and Nagamatsu, H.T., "Hypersonic Viscous Flow on Non-insulated Flat Plate", Proc. Fourth Midwestern Conf. Fluid Mech., pp. 273-287, Purdue University, 1955.

[60] Rodkiewicz, C.M. and Gupta, R.N., "Time-Dependent Strong-Interaction Shear Stress and Temperature Distribution over an Insulated Flat Plate", submitted for publication.

APPENDIX A

LINEARIZED SOLUTIONS FOR AN INSULATED SURFACE

A.1 Linearized Form of the Problem

Let

$$f(\eta,\tau) = f_2(\eta) + \Delta f(\eta,\tau) \tag{A.1}$$

where f_2 satisfies the steady state momentum equation, namely,

$$f_2''' + f_2 f_2'' - \beta(f_2'^2 - S_2) = 0 \tag{A.2}$$

The momentum equation (2.54), after omitting small terms of the second order, becomes

$$\left(\frac{\gamma+1}{\gamma}\right)\dot{\Delta f}' + 2\left(\frac{\gamma-1}{\gamma}\right) f_2'\Delta f' - 4\tau(f_2'\dot{\Delta f}' - \dot{\Delta f} f_2'')$$

$$- f_2\Delta f'' - f_2''\Delta f - \Delta f''' + \left(\frac{\gamma-1}{\gamma}\right)f_2'^2 - f_2 f_2'' - f_2''' - \left(\frac{\gamma-1}{\gamma}\right)S = 0 \tag{A.3}$$

However, if we prescribe H, so that $S(\eta,0) = 1$ then [60]

$$S = 1 \tag{A.4}$$

satisfies the energy equation (2.56) with its space conditions, and consequently the linearized momentum equation becomes

$$(\frac{\gamma+1}{\gamma})\ \dot{\Delta f}' + 2(\frac{\gamma-1}{\gamma})\ f_2'\Delta f' - 4\tau(f_2'\dot{\Delta f}' - f_2''\dot{\Delta f}) - f_2\Delta f''$$

$$- f_2''\Delta f - \Delta f''' = 0 \qquad (A.5)$$

with its steady state counterpart

$$f_2''' + f_2 f_2'' - (\frac{\gamma-1}{\gamma})(f_2'^2 - 1) = 0 \qquad (A.6)$$

In terms of the Euler's transformation (3.3) we may rewrite expression (A.5) as:

$$(\frac{\gamma+1}{\gamma})\ \frac{\partial(\Delta f')}{\partial\xi} + 2(\frac{\gamma-1}{\gamma})\ f_2'\Delta f' - 4\xi(1-\xi)\{f_2'\ \frac{\partial(\Delta f')}{\partial\xi} - f_2''\frac{\partial(\Delta f)}{\partial\xi}\}$$

$$- f_2\Delta f'' - f_2''\Delta f - \Delta f''' = 0 \qquad (A.7)$$

The boundary conditions associated with equation (A.7) are

$$(\Delta f)'(\eta_e,\xi) = 0 \qquad (A.8)$$

$$(\Delta f)'\ (0,\xi) = 0 \qquad (A.9)$$

$$(\Delta f)\ (0,\xi) = 0 \qquad (A.10)$$

$$(\Delta f)'(\eta>0,0) = f_0' \frac{U_{e0}}{U_{e2}} + \left(1 - \frac{U_{e0}}{U_{e2}}\right) - f_2' \qquad (A.11)$$

A.2 Numerical Solution to the Linearized Equation

The solution to equation (A.7) with the boundary conditions (A.8) through (A.11) has been obtained using the numerical method described by Rodkiewicz and Reshotko [22] with certain modifications in the computational molecule. In the numerical computations of reference [22] the 7-point computational molecule, indicated in Figure A.1, was used for all values of $\xi(\text{or}\tau)$. In order to obtain more accurate results in the present work the 7-point computational molecule was used only for the first step in ξ-direction. For the subsequent values the 10-point computational molecule indicated in Figure A.2 was used with variable stepsize in ξ-direction.

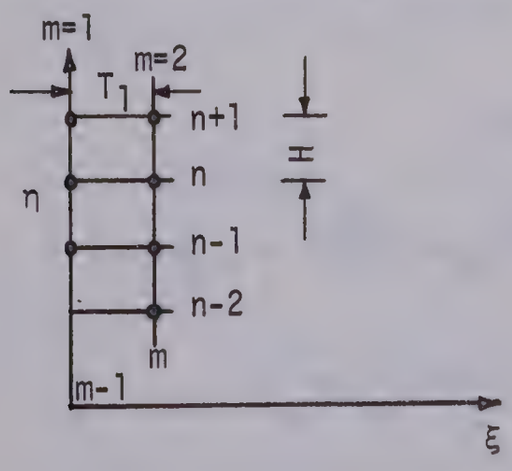

Figure A.1 The 7-point Computational Molecule; H = 0.05, T_1 = 0.025

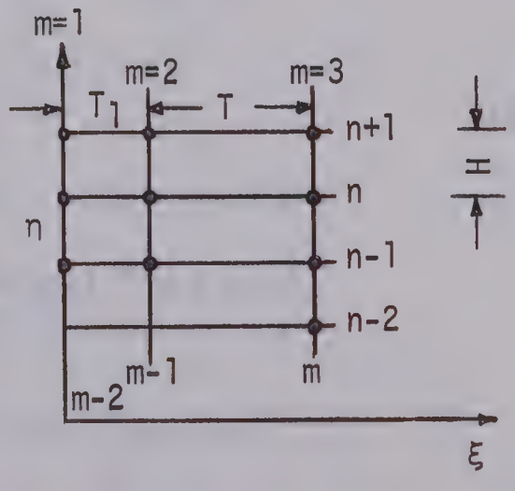

Figure A.2 The 10-point Computational Molecule; H = 0.05, T = 0.05, T_1 = 0.025

The momentum equation (A.7) may be written in the finite difference approximation as:

$$a_{m,n}\,\Delta f_{m,n+1} + b_{m,n}\,\Delta f_{m,n} + c_{m,n}\,\Delta f_{m,n-1} + d_{m,n}\,\Delta f_{m,n-2} = e_{m,n} \quad (A.12)$$

where for the case of 7-point computational molecule we have:

$$a_{m,n} = \left(\frac{\gamma+1}{\gamma}\right)(1-\xi_m)^2H^2 - 4\xi_m(1-\xi_m)H^2f_2'(n) - 2HT_1f_2(n)$$

$$- 2T_1 + 2\left(\frac{\gamma-1}{\gamma}\right)H^2T_1f_2'(n) \quad (A.13)$$

$$b_{m,n} = 8\xi_m(1-\xi_m)H^3f_2''(n) + 4HT_1f_2(n) + 6T_1 - 2H^3T_1f_2''(n) \quad (A.14)$$

$$c_{m,n} = -\left(\frac{\gamma+1}{\gamma}\right)(1-\xi_m)^2H^2 + 4\xi_m(1-\xi_m)H^2f_2'(n)$$

$$- 2HT_1f_2(n) - 6T_1 - 2\left(\frac{\gamma-1}{\gamma}\right)H^2T_1f_2'(n) \quad (A.15)$$

$$d_{m,n} = 2T_1 \quad (A.16)$$

$$e_{m,n} = \left(\frac{\gamma+1}{\gamma}\right)(1-\xi_m)^2H^2(\Delta f_{m-1,n+1} - \Delta f_{m-1,n-1})$$

$$- 4\xi_m(1-\xi_m)H^2f_2'(n)(\Delta f_{m-1,n+1} - \Delta f_{m-1,n-1})$$

$$+ 8\xi_m(1-\xi_m)H^3f_2''(n)\Delta f_{m-1,n} \quad (A.17)$$

While for the case of the 10-point computational molecule we get

$$a_{m,n} = (\frac{\gamma+1}{\gamma})(1-\xi_m)^2H^2T_1(2T+T_1) - 4\xi_m(1-\xi_m)H^2T_1(2T+T_1)f_2'(n)$$

$$- 2HTT_1(T+T_1)f_2(n) - 2TT_1(T+T_1) + 2(\frac{\gamma-1}{\gamma})H^2TT_1(T+T_1)f_2'(n) \quad (A.18)$$

$$b_{m,n} = 8\xi_m(1-\xi_m)H^3T_1(2T+T_1)f_2''(n) - 2H^3TT_1(T+T_1)f_2''(n)$$

$$+ 4HTT_1(T+T_1)f_2(n) + 6TT_1(T+T_1) \quad (A.19)$$

$$c_{m,n} = -(\frac{\gamma+1}{\gamma})(1-\xi_m)^2H^2T_1(2T+T_1) + 4\xi_m(1-\xi_m)$$

$$\cdot H^2T_1(2T+T_1)\, f_2'(n) \quad (A.20)$$

$$d_{m,n} = 2TT_1(T+T_1) \quad (A.21)$$

$$e_{m,n} = (\frac{\gamma+1}{\gamma})(1-\xi_m)^2[H^2(T+T_1)^2\{\Delta f_{m-1,n+1} - \Delta f_{m-1,n-1}\}$$

$$- H^2T^2\{\Delta f_{m-2,n+1} - \Delta f_{m-2,n-1}\}] - 4\xi_m(1-\xi_m)\, f_2'(n)$$

$$\cdot [H^2(T+T_1)^2\{\Delta f_{m-1,n+1} - \Delta f_{m-1,n-1}\} - H^2T^2\{\Delta f_{m-2,n+1} - \Delta f_{m-2,n-1}\}]$$

$$+ 4\xi_m(1-\xi_m)f_2''(n)[2H^3(T+T_1)^2\Delta f_{m-1,n} - 2H^3T^2\Delta f_{m-2,n}] \quad (A.22)$$

In the foregoing the following finite difference approximations have been used.

For 7-Point Computational Molecule:

$$\frac{\partial(\Delta f)}{\partial \xi} = \frac{1}{T_1}\left[\Delta f_{m,n} - \Delta f_{m-1,n}\right] \tag{A.23}$$

$$\frac{\partial(\Delta f)}{\partial \eta} = \frac{1}{2H}\left[\Delta f_{m,n+1} - \Delta f_{m,n-1}\right] \tag{A.24}$$

$$\frac{\partial^2(\Delta f)}{\partial \eta \partial \xi} = \frac{1}{2HT_1}\left[\Delta f_{m,n+1} - \Delta f_{m,n-1} - \Delta f_{m-1,n+1} + \Delta f_{m-1,n-1}\right] \tag{A.25}$$

$$\frac{\partial^2(\Delta f)}{\partial \eta^2} = \frac{1}{H^2}\left[\Delta f_{m,n+1} - 2\Delta f_{m,n} + \Delta f_{m,n-1}\right] \tag{A.26}$$

$$\frac{\partial^3(\Delta f)}{\partial \eta^3} = \frac{1}{H^3}\left[\Delta f_{m,n+1} - 3\Delta f_{m,n} + 3\Delta f_{m,n-1} - \Delta f_{m,n-2}\right] \tag{A.27}$$

For 10-Point Computational Molecule:

$$\frac{\partial(\Delta f)}{\partial \xi} = \frac{(2T+T_1)}{T(T+T_1)}\Delta f_{m,n} - \frac{(T+T_1)}{TT_1}\Delta f_{m-1,n} + \frac{T}{(T+T_1)T_1}\Delta f_{m-2,n} \tag{A.28}$$

$$\frac{\partial^2(\Delta f)}{\partial \eta \partial \xi} = \frac{(2T+T_1)}{2HT(T+T_1)}\left\{\Delta f_{m,n+1} - \Delta f_{m,n-1}\right\} - \frac{(T+T_1)}{2HTT_1}\left\{\Delta f_{m-1,n+1} - \Delta f_{m-1,n-1}\right\} + \frac{T}{2HT_1(T+T_1)}\left\{\Delta f_{m-2,n+1} - \Delta f_{m-2,n-1}\right\} \tag{A.29}$$

Expressions for $\frac{\partial(\Delta f)}{\partial \eta}$, $\frac{\partial^2(\Delta f)}{\partial \eta^2}$ and $\frac{\partial^3(\Delta f)}{\partial \eta^3}$ are similar to those for the 7-point computational molecule.

Equation (A.12) may also be written in the form

$$\Delta f_{m,n} = R_{m,n}\Delta f_{m,n+1} + C_{m,n} \tag{A.30}$$

which was obtained by considering the boundary conditions (A.9) and (A.10) with $R_{m,n}$ and $C_{m,n}$ defined respectively as:

$$R_{m,n} = \frac{-a_{m,n}}{(b_{m,n} + c_{m,n}R_{m,n-1} + d_{m,n}R_{m,n-1}R_{m,n-2})} \tag{A.31}$$

$$C_{m,n} = \frac{e_{m,n} - (c_{m,n}C_{m,n-1}+d_{m,n}R_{m,n-2}C_{m,n-1}+d_{m,n}C_{m,n-2})}{(b_{m,n}+c_{m,n}R_{m,n-1}+d_{m,n}R_{m,n-1}R_{m,n-2})} \tag{A.32}$$

where

$$R_{m,1} = C_{m,1} = C_{m,2} = 0 \ , \ R_{m,2} = 0.25 \ .$$

Letting n = N in the free stream (where the 'e' condition prevails), we may write, from the boundary condition (A.8), the following

$$\left.\frac{\partial(\Delta f)}{\partial \eta}\right|_{\eta=\eta_e} = \frac{1}{2\Delta\eta}\left(-3\Delta f_{m,N}+4\Delta f_{m,N-1}-\Delta f_{m,N-2}\right) = 0 \tag{A.33}$$

Further using expression (A.30) for $\Delta f_{m,N-1}$ and $\Delta f_{m,N-2}$ in relation (A.33), we obtain

$$\Delta f_{m,N} = \frac{C_{m,N-1} - \dfrac{C_{m,N-2}}{4-R_{m,N-2}}}{\dfrac{3}{4-R_{m,N-2}} - R_{m,N-1}} \qquad (A.34)$$

Expression (A.34) may be utilized at the boundary-layer edge (i.e. at n=N) as the starting point in the use of recurrence relation (A.30).

In actual computations the following procedure is used. First we calculate the coefficients $R_{m,n}$ and $C_{m,n}$. It may be noted that expressions (A.31) and (A.32), when specialized to station m, require the knowledge of the values of function Δf at station m-1. The Δf-distribution for zero-time(m=1) is known from expression (A.11) and consequently we may calculate the coefficients $R_{m,n}$ and $C_{m,n}$ for the station m=2. Once these are found for all values of n we may obtain $\Delta f_{2,n}$ from expression (A.30) by incorporating expression (A.34) at the outer edge. This procedure was repeated at other values of m covering the range $0 \leq \xi \leq 0.3$ (for $\gamma = 1.4$). For $\xi > 0.3$, the method became unstable.

The Δf-solutions were used to obtain the transient contribution to the velocity function ($\Delta f'$). The distribution of ($\Delta f'$) is shown in Figure A.3. It may be noted that each curve has an inflection point which penetrates into the region of higher values of η as ξ increases.

The time-dependent shearing stress at the wall is presented in Figure A.4. Figure A.5 gives the transient contribution to the boundary-layer temperature for various values of ξ and for M_e = 5, 8

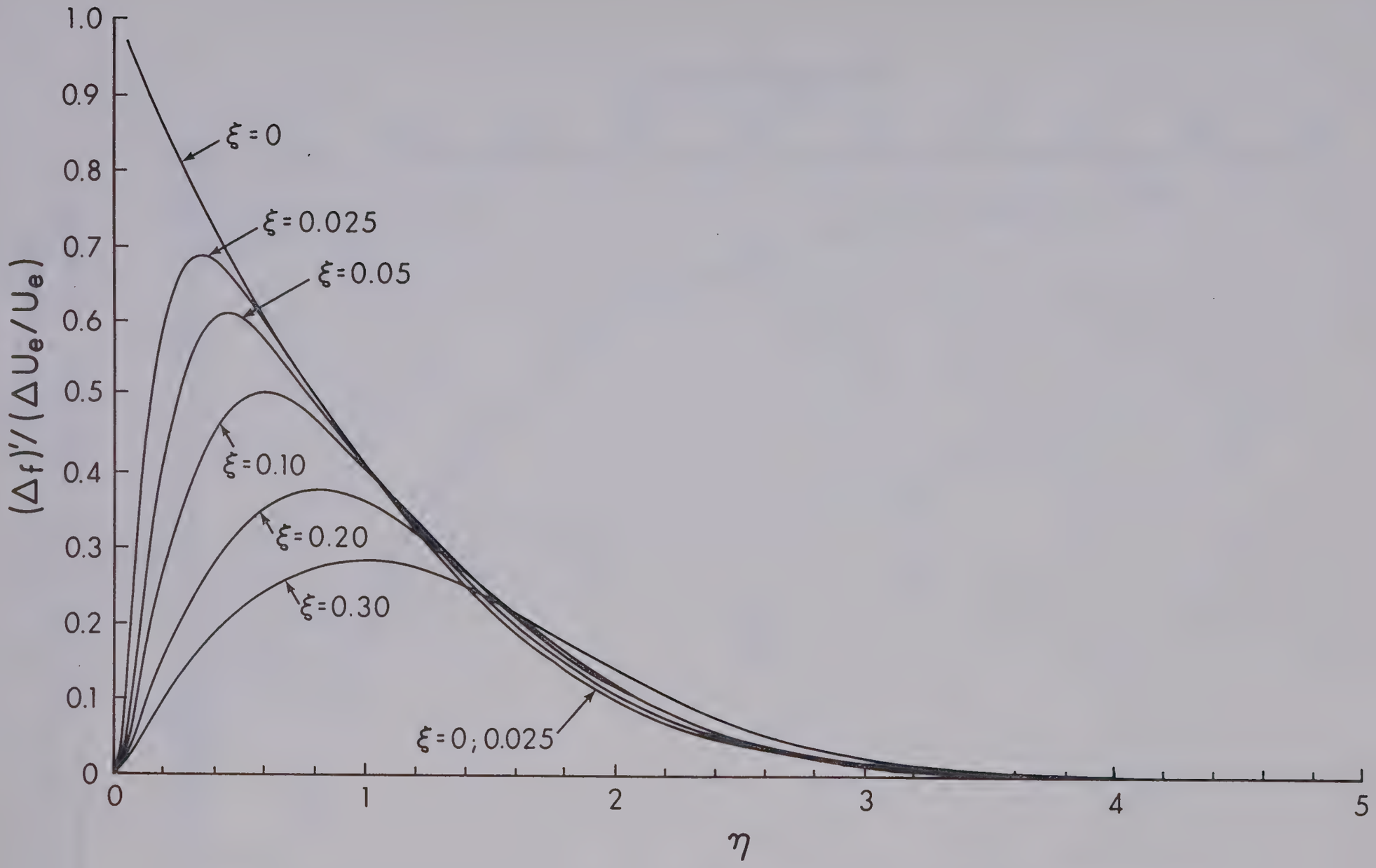

Figure A.3 Distribution of the transient contribution to the velocity-function for $\beta = 0.286$ (γ=1.4) and no wall heat transfer

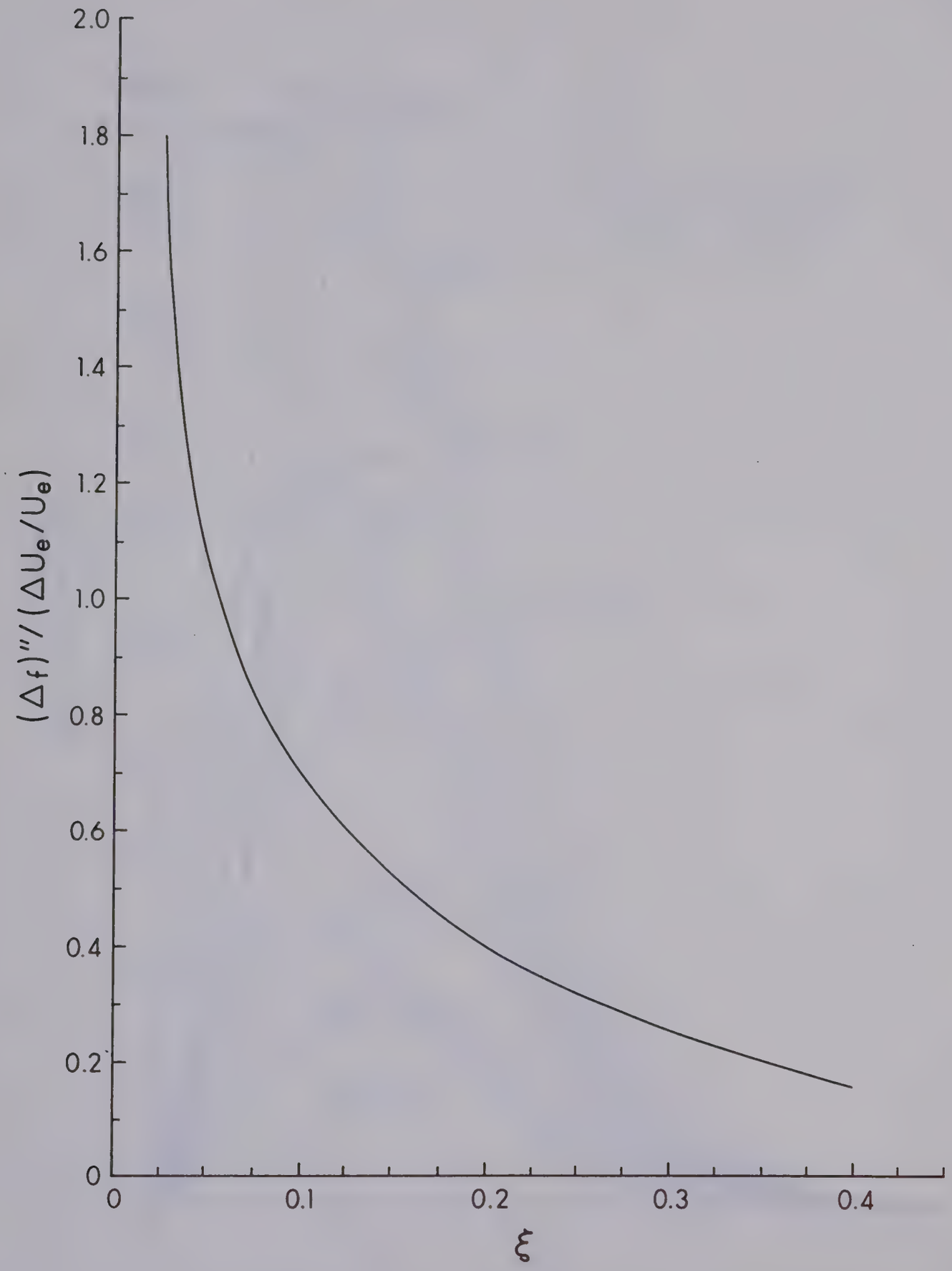

Figure A.4 Distribution of the transient contribution to the shear-stress for $\beta = 0.286$ and no wall heat transfer

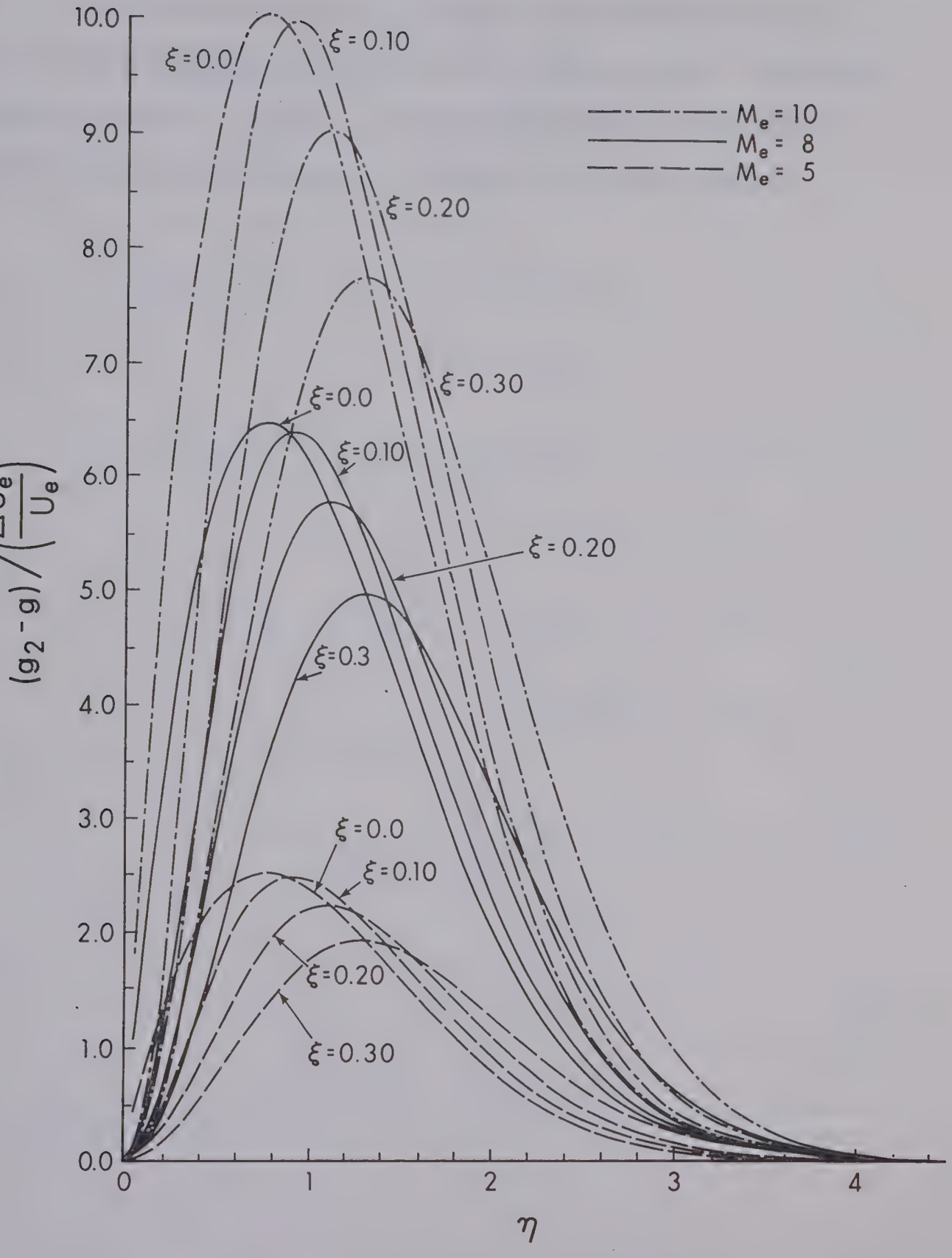

Figure A.5 Distribution of the transient contribution to the temperature distribution for $\beta = 0.286$ and no wall heat transfer

and 10.

The linearization used to solve the momentum equation requires that the change in the free stream velocity should not be too large (say, about 1 to 1.5%). A comparison between the linearized and non-linearized solutions is indicated in the last chapter.

APPENDIX B

NUMERICAL INTEGRATION TO SPECIFY INITIAL CONDITION ON TOTAL ENTHALPY

B.1 Details of the Numerical Integration

In order to evaluate the expression

$$\bar{S}(\eta,0) = (-\bar{S}_w)\frac{\int_0^{\eta} e^{-\int_0^{\eta}(\bar{f}_{\xi=0}+\eta)\,d\eta}\,d\eta}{\int_0^{e} e^{-\int_0^{\eta}(\bar{f}_{\xi=0}+\eta)\,d\eta}\,d\eta} + \bar{S}_w \qquad (B.1)$$

with the numerical values of $\bar{f}_{\xi=0}$ obtained from (3.17), we write

$$\bar{S}'(\eta,0) = \bar{S}'(0,0)\, e^{-\int_0^{\eta}(\bar{f}_{\xi=0}+\eta)\,d\eta}$$

$$= \bar{S}'(0,0)\, F_{\xi=0}(\eta) \qquad (B.2)$$

where

$$F_{\xi=0}(\eta) = e^{-\int_0^{\eta}(\bar{f}_{\xi=0}+\eta)\,d\eta} \qquad (B.3)$$

From (B.2) we may also write

$$\bar{S}'(0,0) = -\frac{\bar{S}_w}{\int_0^e F_{\xi=0}(\eta)\,d\eta} \qquad (B.4)$$

Now,

$$\int_0^e F_{\xi=0}(\eta)\,d\eta$$

may be evaluated numerically by the trapezoidal integration formula. Therefore, we write

$$\int_0^e F(\eta)\,d\eta = \frac{F(0)+F(1)}{2}\Delta\eta + \frac{F(1)+F(2)}{2}\Delta\eta + \ldots + \frac{F(N-1)+F(N)}{2}\Delta\eta \qquad (B.5)$$

with

$$F(0) = e^{-\int_0^0 (\bar{f}+\eta)\,d\eta} = 1$$

$$F(1) = e^{-\int_0^{\Delta\eta} (\bar{f}+\eta)\,d\eta} = F(0)\, e^{-\{\frac{\bar{f}(0)+\bar{f}(1)}{2} + \frac{\eta(0)+\eta(1)}{2}\}\Delta\eta}$$

$$F(2) = e^{-\int_0^{2\Delta\eta} (\bar{f}+\eta)\,d\eta} = F(1)\, e^{-\{\frac{\bar{f}(1)+\bar{f}(2)}{2} + \frac{\eta(1)+\eta(2)}{2}\}\Delta\eta} \qquad (B.6)$$

.

.

.

$$F(N) = F(N-1)\, e^{-\{\frac{\bar{f}(N-1)+\bar{f}(N)}{2} + \frac{\eta(N-1)+\eta(N)}{2}\}\Delta\eta}$$

Here $\Delta\eta$ denotes the stepsize ($=\eta(n) - \eta(n-1)$) in the η-direction. Subscript $\xi=0$ has been dropped from the function $F(\eta)$ for the sake of convenience.

Furthermore, we may write

$$\bar{S}(\eta,0) = \int_0^{\eta} \bar{S}'(\eta,0)\, d\eta + \bar{S}_w \tag{B.7}$$

or

$$\bar{S}(N^*,0) = \bar{S}_{\xi=0}(N^*) = \int_0^{N^*\Delta\eta} \bar{S}'_{\xi=0}\, d\eta + \bar{S}_w \tag{B.8a}$$

Using the trapezoidal rule for integration we obtain

$$\bar{S}_{\xi=0}(N^*) = \left\{\frac{\bar{S}'_{\xi=0}(0)+\bar{S}'_{\xi=0}(1)}{2}\Delta\eta + \frac{\bar{S}'_{\xi=0}(1)+\bar{S}'_{\xi=0}(2)}{2}\Delta\eta \right.$$

$$\left. \ldots + \frac{\bar{S}'_{\xi=0}(N^*-1)+\bar{S}'_{\xi=0}(N^*)}{2}\Delta\eta\right\} + \bar{S}_w \tag{B.8b}$$

where, we have from (B.2) and (B.4),

$$\begin{aligned}
\bar{S}'_{\xi=0}(0) &= (-\bar{S}_w)\,\frac{F_{\xi=0}(0)}{\int_0^e F_{\xi=0}(\eta)d\eta} \\
\bar{S}'_{\xi=0}(1) &= (-\bar{S}_w)\,\frac{F_{\xi=0}(1)}{\int_0^e F_{\xi=0}(\eta)d\eta} \\
&\vdots \\
\bar{S}'_{\xi=0}(N^*) &= (-\bar{S}_w)\,\frac{F_{\xi=0}(N^*)}{\int_0^e F_{\xi=0}(\eta)\, d\eta}
\end{aligned} \tag{B.9}$$

Expressions (B.9) may be used to evaluate expression (B.8b) which gives $\overline{S}(\eta,0)$ distribution represented by expression (B.1). This is the initial condition used on $\overline{S}$ in the numerical solution.

APPENDIX C

STARTING PROCEDURE FOR THE INTEGRATION OF THE GOVERNING DIFFERENTIAL EQUATIONS

C.1 Starting the Solution near the Wall

The extrapolation-interpolation formulae in section 3.9 of Chapter III require values of the variables at four previous η-stations. To start the integration at the wall Taylor's series has been employed. For $\overline{f}''$ we may write

$$\overline{f}''_{\Delta\eta} = \overline{f}''_{w} + \Delta\eta\, \overline{f}'''_{w} + \frac{(\Delta\eta)^2}{2}\, \overline{f}^{iv}_{w} + \ldots \qquad (C.1)$$

In the present computations, only two terms of this expansion have been used. In order to have the same accuracy as in the extrapolation and interpolation formulae, however, much shorter steps in η are to be used in the Taylor's series. The study made in reference [33] shows that a five-place accuracy in the values of $\overline{f}$ and $\overline{S}$ can be maintained by using the Taylor's series to obtain these values at only $\eta = \frac{\Delta\eta}{16}$ from the wall. Here $\Delta\eta$ denotes the stepsize used in the extrapolation-interpolation formulae. The numerical value of $\Delta\eta$ used in the computations is 0.1. The two-point and three-point extrapolation formulae are used to build the values up to the full length step size $\Delta\eta$. Again the accuracy requirements call for step sizes of $\frac{\Delta\eta}{4}$ and $\frac{\Delta\eta}{2}$

to be used for the two-point and three-point forms respectively. The expressions to be used with different step sizes are summarized below.

(i) Immediately next to the wall (i.e. at $\eta = \Delta\eta/16$) Taylor's series is used with the step size $\Delta\eta/16$:

$$\bar{f}''_{\Delta\eta/16} = \bar{f}''_w + \frac{\Delta\eta}{16}\,\bar{f}'''_w \tag{C.2}$$

$$\bar{f}'_{\Delta\eta/16} = -1 + \frac{\Delta\eta}{16}\,\bar{f}''_w \tag{C.3}$$

$$\bar{f}_{\Delta\eta/16} = \bar{f}_w - \frac{\Delta\eta}{16} + \frac{(\Delta\eta)^2}{512}\,\bar{f}''_w \tag{C.4}$$

$$\bar{S}'_{\Delta\eta/16} = \bar{S}'_w + \frac{\Delta\eta}{16}\,\bar{S}''_w \tag{C.5}$$

$$\bar{S}_{\Delta\eta/16} = \bar{S}_w + \frac{\Delta\eta}{16}\,\bar{S}'_w \tag{C.6}$$

(ii) At $\eta = \Delta\eta/8$, 2-point extrapolation formulae are used with the step size $\Delta\eta/16$:

$$\bar{f}''_{\Delta\eta/8} = \bar{f}''_{\Delta\eta/16} + \frac{\Delta\eta}{32}\left[3\,\bar{f}'''_{\Delta\eta/16} - \bar{f}'''_w\right] \tag{C.7}$$

$$\bar{f}'_{\Delta\eta/8} = \bar{f}'_{\Delta\eta/16} + \frac{\Delta\eta}{32}\left[3\bar{f}''_{\Delta\eta/16} - \bar{f}''_w\right] \tag{C.8}$$

$$\bar{f}_{\Delta\eta/8} = \bar{f}_{\Delta\eta/16} + \frac{\Delta\eta}{16}\,\bar{f}'_{\Delta\eta/16} + \frac{(\Delta\eta)^2}{1536}\left[4\bar{f}''_{\Delta\eta/16} - \bar{f}''_w\right] \tag{C.9}$$

$$\bar{S}'_{\Delta\eta/8} = \bar{S}'_{\Delta\eta/16} + \frac{\Delta\eta}{32}\left[3\bar{S}''_{\Delta\eta/16} - \bar{S}''_{w}\right] \tag{C.10}$$

$$\bar{S}_{\Delta\eta/8} = \bar{S}_{\Delta\eta/16} + \frac{\Delta\eta}{32}\left[3\bar{S}'_{\Delta\eta/16} - \bar{S}'_{w}\right] \tag{C.11}$$

(iii) At $\eta = \Delta\eta/4$, 2-point extrapolation formulae are employed with the step size $\Delta\eta/8$:

$$\bar{f}''_{\Delta\eta/4} = \bar{f}''_{\Delta\eta/8} + \frac{\Delta\eta}{16}\left[3\bar{f}'''_{\Delta\eta/8} - \bar{f}'''_{w}\right] \tag{C.12}$$

$$\bar{f}'_{\Delta\eta/4} = \bar{f}'_{\Delta\eta/8} + \frac{\Delta\eta}{16}\left[3\bar{f}''_{\Delta\eta/8} - \bar{f}''_{w}\right] \tag{C.13}$$

$$\bar{f}_{\Delta\eta/4} = \bar{f}_{\Delta\eta/8} + \frac{\Delta\eta}{8}\bar{f}'_{\Delta\eta/8} + \frac{(\Delta\eta)^2}{384}\left[4\bar{f}''_{\Delta\eta/8} - \bar{f}''_{w}\right] \tag{C.14}$$

$$\bar{S}'_{\Delta\eta/4} = \bar{S}'_{\Delta\eta/8} + \frac{\Delta\eta}{16}\left[3\bar{S}''_{\Delta\eta/8} - \bar{S}''_{w}\right] \tag{C.15}$$

$$\bar{S}_{\Delta\eta/4} = \bar{S}_{\Delta\eta/8} + \frac{\Delta\eta}{16}\left[3\bar{S}'_{\Delta\eta/8} - \bar{S}'_{w}\right] \tag{C.16}$$

(iv) At $\eta = \Delta\eta/2$, $\eta = \frac{3}{4}\Delta\eta$ and $\eta = \Delta\eta$, 2-point extrapolation formulae are used with the step size $\Delta\eta/4$:

$$\bar{f}''_{n+1} = \bar{f}''_{n} + \frac{\Delta\eta}{8}\left[3\bar{f}'''_{n} - \bar{f}'''_{n-1}\right] \tag{C.17}$$

$$\bar{f}'_{n+1} = \bar{f}'_{n} + \frac{\Delta\eta}{8}\left[3\bar{f}''_{n} - \bar{f}''_{n-1}\right] \tag{C.18}$$

$$\bar{f}_{n+1} = \bar{f}_n + \frac{\Delta\eta}{4}\bar{f}'_n + \frac{(\Delta\eta)^2}{96}[4\bar{f}''_n - \bar{f}''_{n-1}] \tag{C.19}$$

$$\bar{S}'_{n+1} = \bar{S}'_n + \frac{\Delta\eta}{8}[3\bar{S}''_n - \bar{S}''_{n-1}] \tag{C.20}$$

$$\bar{S}_{n+1} = \bar{S}_n + \frac{\Delta\eta}{8}[3\bar{S}'_n - \bar{S}'_{n-1}] \tag{C.21}$$

(v) At $\eta = \frac{3}{2}\Delta\eta$, $\eta = 2\Delta\eta$, $\eta = \frac{5}{2}\Delta\eta$ and $\eta = 3\Delta\eta$, 3-point extrapolation formulae are used with the step size $\Delta\eta/2$:

$$\bar{f}''_{n+1} = \bar{f}''_n + \frac{\Delta\eta}{24}[23\bar{f}'''_n - 16\bar{f}'''_{n-1} + 5\bar{f}'''_{n-2}] \tag{C.22}$$

$$\bar{f}'_{n+1} = \bar{f}'_n + \frac{\Delta\eta}{24}[23\bar{f}''_n - 16\bar{f}''_{n-1} + 5\bar{f}''_{n-2}] \tag{C.23}$$

$$\bar{f}_{n+1} = \bar{f}_n + \frac{\Delta\eta}{2}\bar{f}'_n + \frac{(\Delta\eta)^2}{96}[19\bar{f}''_n - 10\bar{f}''_{n-1} + 3\bar{f}''_{n-2}] \tag{C.24}$$

$$\bar{S}'_{n+1} = \bar{S}'_n + \frac{\Delta\eta}{24}[23\bar{S}''_n - 16\bar{S}''_{n-1} + 5\bar{S}''_{n-2}] \tag{C.25}$$

$$\bar{S}_{n+1} = \bar{S}_n + \frac{\Delta\eta}{24}[23\bar{S}'_n - 16\bar{S}'_{n-1} + 5\bar{S}'_{n-2}] \tag{C.26}$$

For $\eta \geq 4\Delta\eta$, the 4-point extrapolation-interpolation formulae of section (3.9) are used with the regular step size of $\Delta\eta$.

Use of Taylor's series to start the integration near the wall has the advantage that it can be checked in a simple and effective manner for accuracy. If Runge-Kutta integration technique were used

as a starting method, the error estimation and checking for accuracy would be difficult.

APPENDIX D

INTEGRATION FORMULAE FOR THE ENERGY EQUATION

D.1 Extrapolation-Interpolation Formulae

The 4-point extrapolation-interpolation formulae for carrying out the integrations required in solution of the energy equation are similar to those required for momentum equation, described in section 3.9 of Chapter III. These formulae are:

$$\bar{S}'_{n+1)_E} = \bar{S}'_n + \frac{\Delta\eta}{24}\left[55\,\bar{S}''_n - 59\bar{S}''_{n-1} + 37\bar{S}''_{n-2} - 9\bar{S}''_{n-3}\right] \qquad (D.1)$$

$$\bar{S}_{n+1)_E} = \bar{S}_n + \frac{\Delta\eta}{24}\left[55\bar{S}'_n - 59\bar{S}'_{n-1} + 37\bar{S}'_{n-2} - 9\bar{S}'_{n-3}\right] \qquad (D.2)$$

and from the energy equation (3.6)

$$\bar{S}''_{n+1)_E} = F\left(\bar{S}'_{n+1)_E}\,,\ \bar{S}_{n+1)_E}\right)$$

where the subscript E denotes "extrapolated".

The interpolated values are obtained from

$$\bar{S}'_{n+1} = \bar{S}'_n + \frac{\Delta\eta}{24}\left[9\bar{S}''_{n+1)_E} + 19\bar{S}''_n - 5\bar{S}''_{n-1} + \bar{S}''_{n-2}\right] \qquad (D.3)$$

$$\bar{S}_{n+1} = \bar{S}_n + \frac{\Delta\eta}{24}\left[9\bar{S}'_{n+1} + 19\bar{S}'_n - 5\bar{S}'_{n-1} + \bar{S}'_{n-2}\right] \qquad (D.4)$$

so that $\bar{S}''_{n+1}$ may now, finally, be obtained from (3.6)

$$\bar{S}''_{n+1} = F(\bar{S}'_{n+1} , \bar{S}_{n+1})$$

APPENDIX E

ERROR INVOLVED IN NUMERICAL INTEGRATION

E.1 Error in Finite-Difference Representation of ξ-derivatives

The errors in the two-point and three-point finite difference approximation of ξ-derivatives have been given in Section 3.3. These are indicated by expressions (3.12) and (3.13). The maximum error involved from this source is given below:

Two Point Formulation: $$\frac{\Delta\xi}{2}\left|\frac{\partial^2 F}{\partial\xi^2}\right|_{max} = 0.00085 \qquad (E.1)$$

Three Point Formulation: $$\frac{(\Delta\xi)^2}{3}\left|\frac{\partial^3 F}{\partial\xi^3}\right|_{max} = 0.00075 \qquad (E.2)$$

E.2 Error in Integration Expressions

E.2.1 Extrapolation Formulae

The errors involved in expressions for $\overline{f}''$, $\overline{f}'$, and $\overline{f}$, respectively, are:

$$E_1 \leq + \frac{251}{720}(\Delta\eta)^5[\overline{f}''(\eta)]^V \qquad (E.3)$$

$$E_2 \leq + \frac{251}{720}(\Delta\eta)^5\,\overline{f}^{VI}(\eta) \qquad (E.4)$$

$$E_3 \leq + \frac{3}{32}(\Delta\eta)^6\,\overline{f}^{VI}(\eta) \qquad (E.5)$$

E.2.2 Interpolation Formulae

The errors involved are

In expression for $\bar{f}''$:

$$E_4 \leq - \frac{19}{720} (\Delta\eta)^5 [\bar{f}''(\eta)]^V \qquad (E.6)$$

In expression for $\bar{f}'$:

$$E_5 \leq - \frac{19}{720} (\Delta\eta)^5 \bar{f}^{VI}(\eta) \qquad (E.7)$$

In expression for $\bar{f}$:

$$E_6 \leq - \frac{17}{1440} (\Delta\eta)^6 \bar{f}^{VI}(\eta) \qquad (E.8)$$

E.3 Accuracy of the Numerical Results

The quantities that affect the accuracy of the numerical results are $\Delta\eta$, η_e, k, $\Delta\xi$ and Q_{max}. Since Cohen and Reshotko's [31] results for the steady state similar flows are the only highly accurate solutions known, these were first used to check the programming of the equations. The four-place accuracy of Cohen and Reshotko's solutions was obtained by choosing the following values for the above mentioned parameters:

$$\Delta\eta = 0.1; \ \eta_e = 5, \ k = 1.0; \ (\xi/\Delta\xi) \leq 25;$$

and

$$Q_{max} = 6 \ .$$

APPENDIX F

CURVES FOR CHAPTERS III AND IV

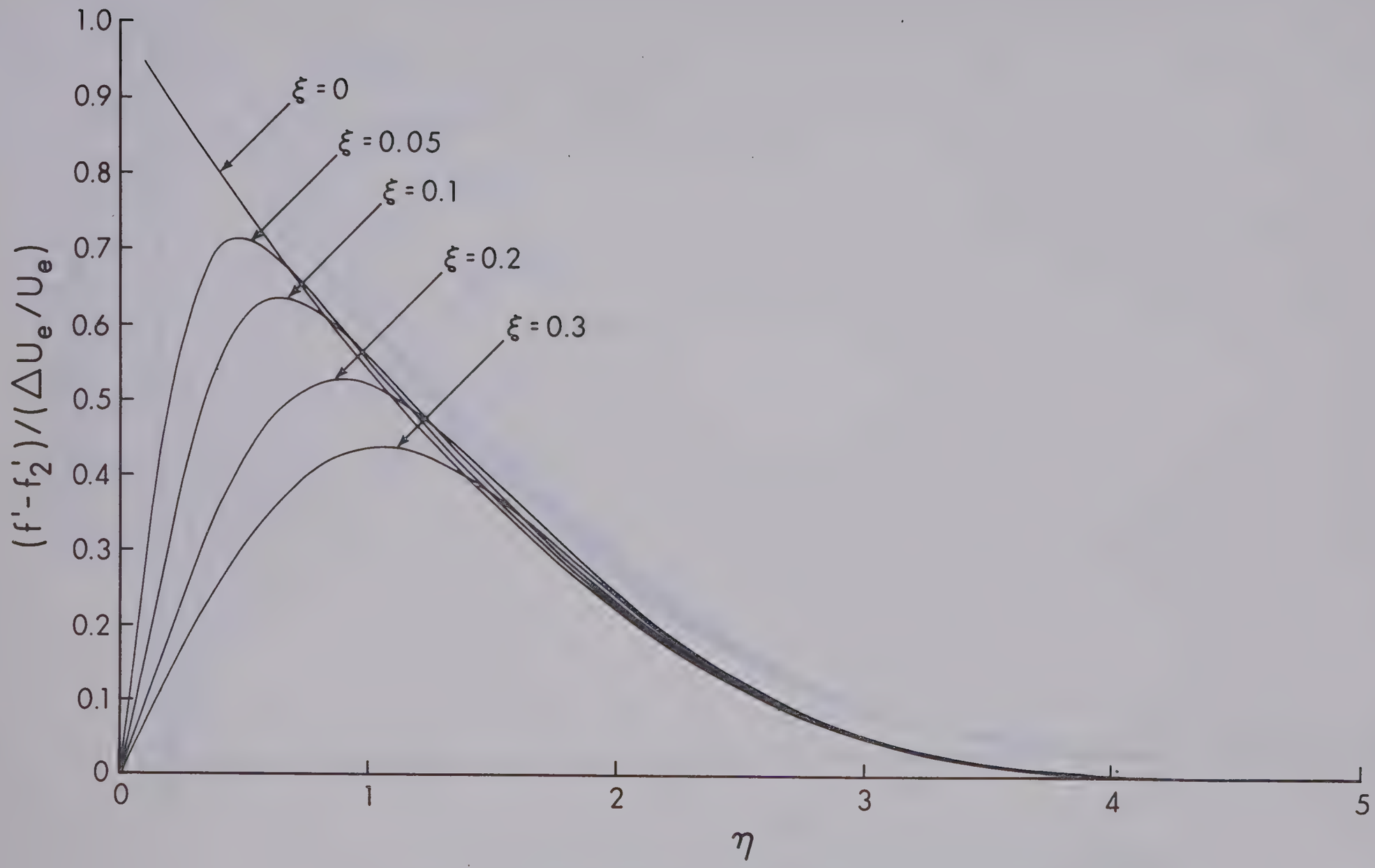

Figure 3 Distribution of the Transient Contribution to the Velocity Function for $S_w = 0$ and $\beta = 0.286$

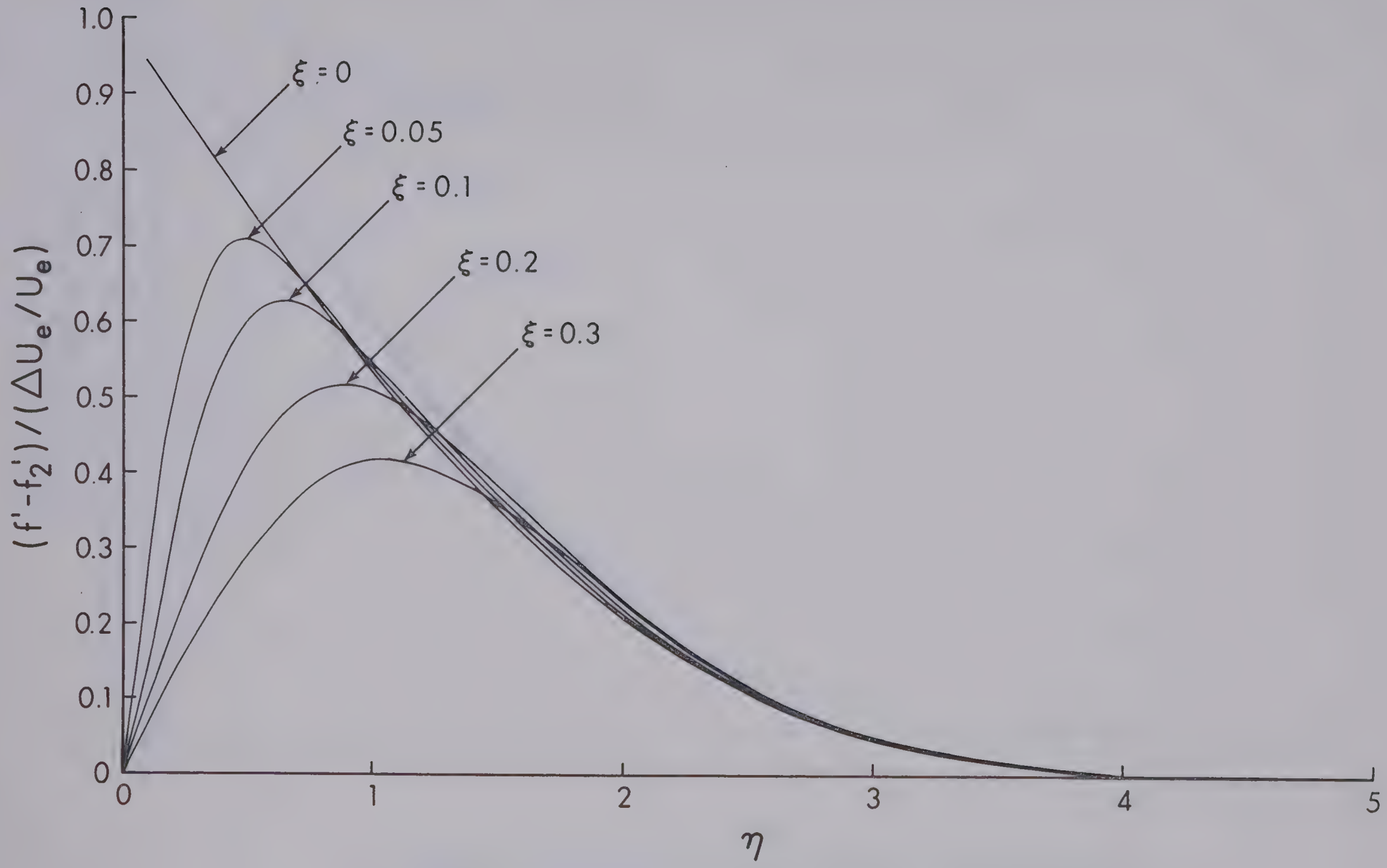

Figure 4 Distribution of the Transient Contribution to the Velocity Function for $S_w = 0.2$ and $\beta = 0.286$

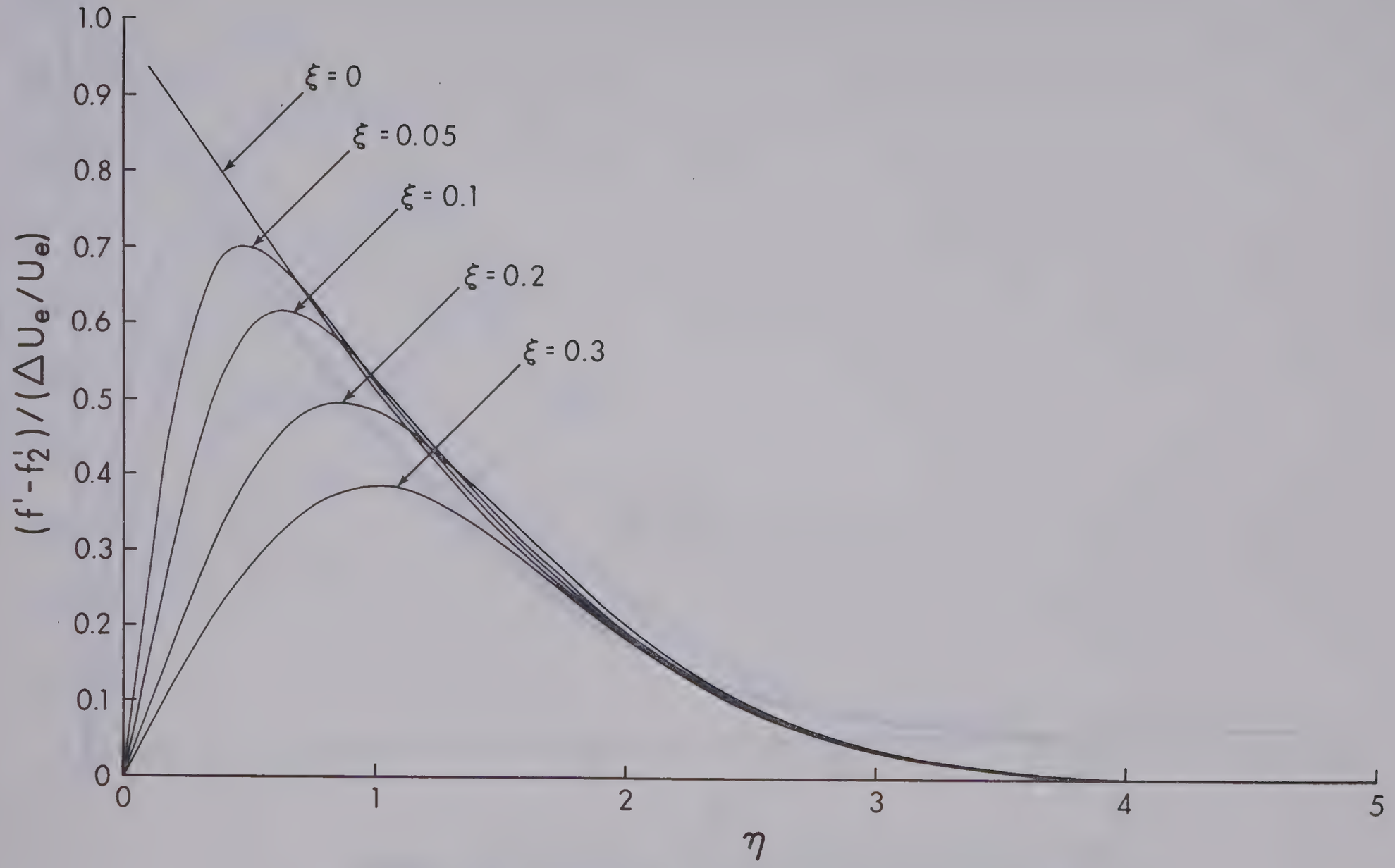

Figure 5 Distribution to the Transient Contribution to the Velocity Function for $S_w = 0.6$ and $\beta = 0.286$

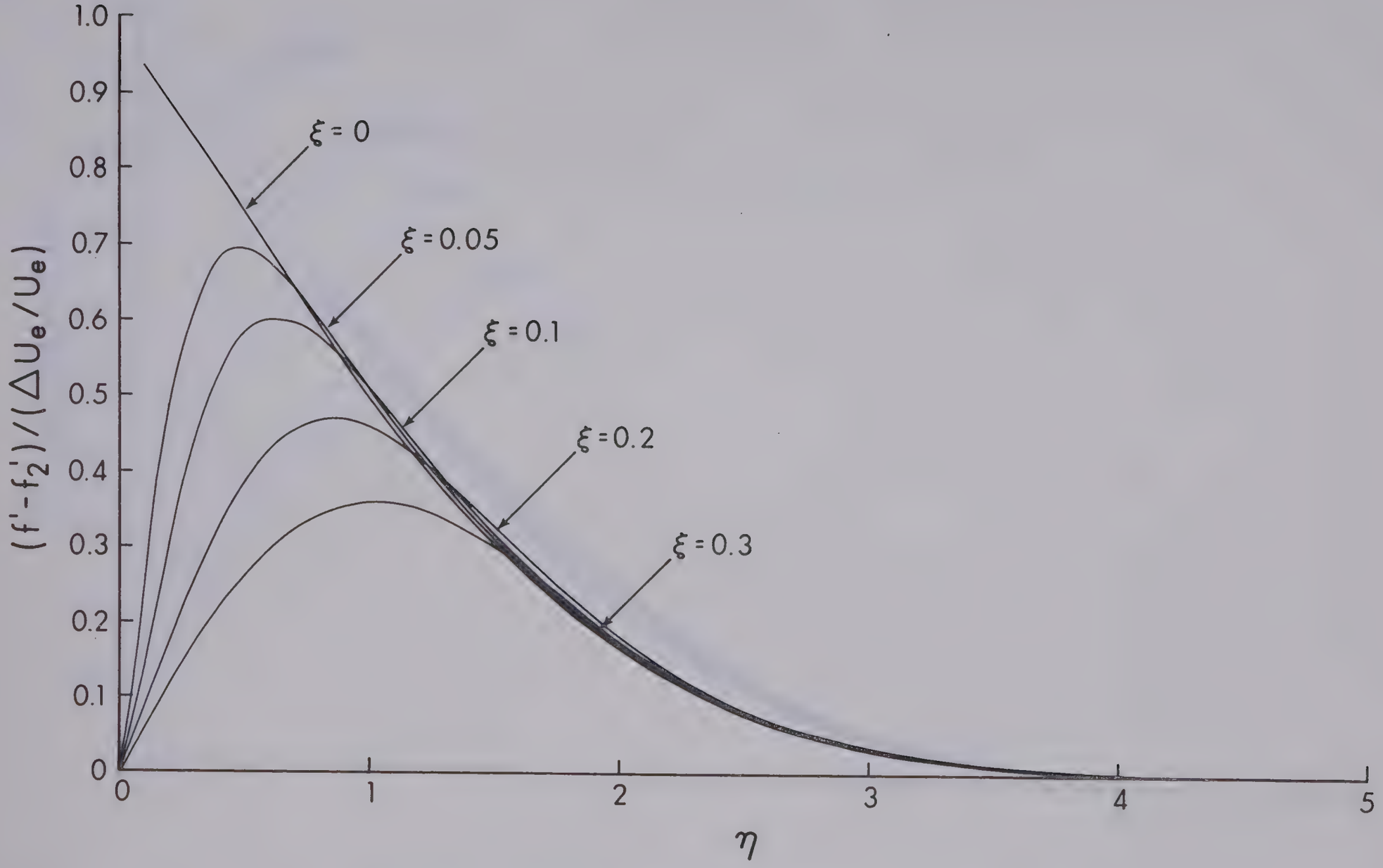

Figure 6 Distribution of the Transient Contribution to the Velocity Function for an Insulated Plate and $\beta = 0.286$

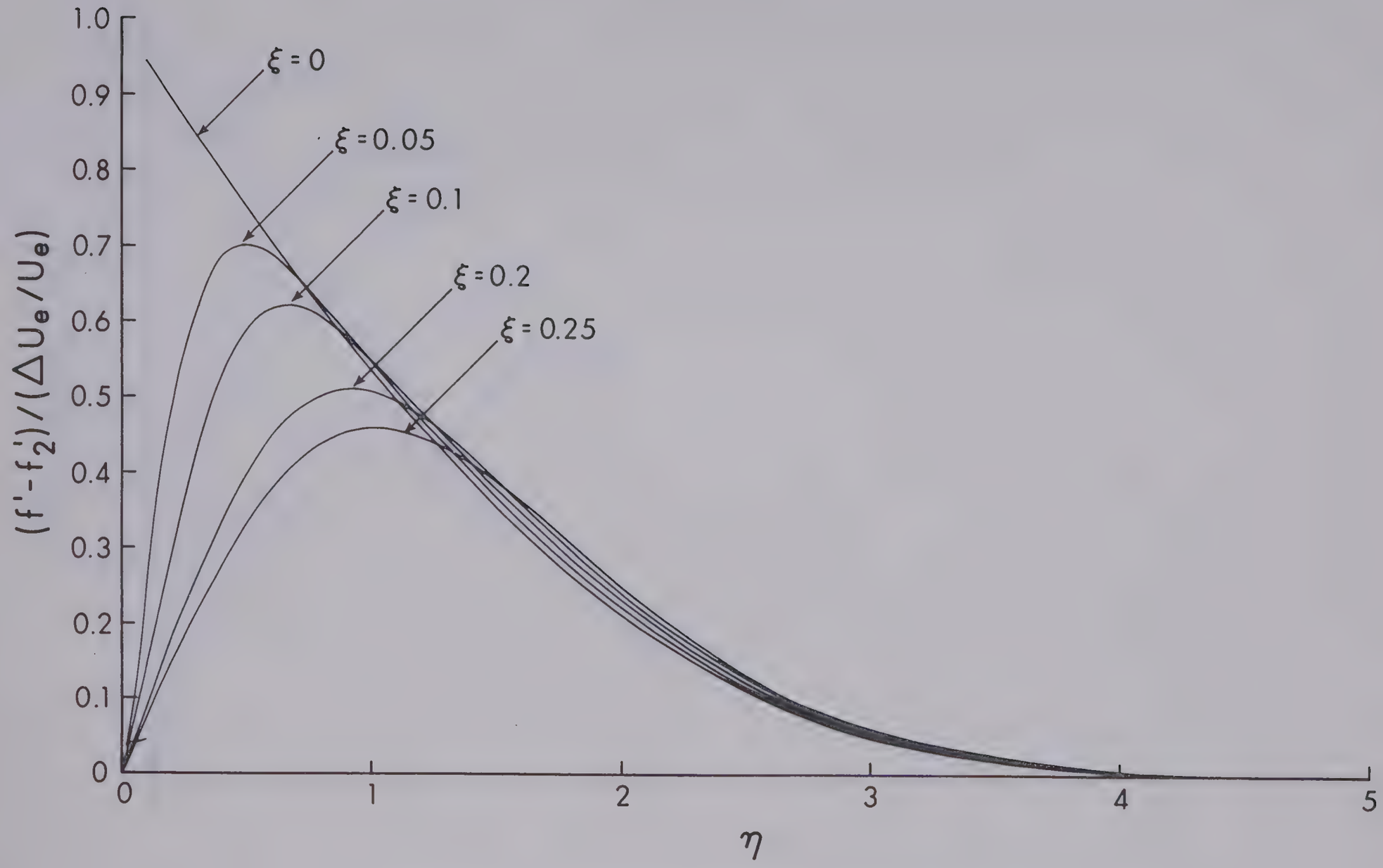

Figure 7 Distribution of the Transient Contribution to the Velocity Function for $S_w = 0$ and $\beta = 0.4$

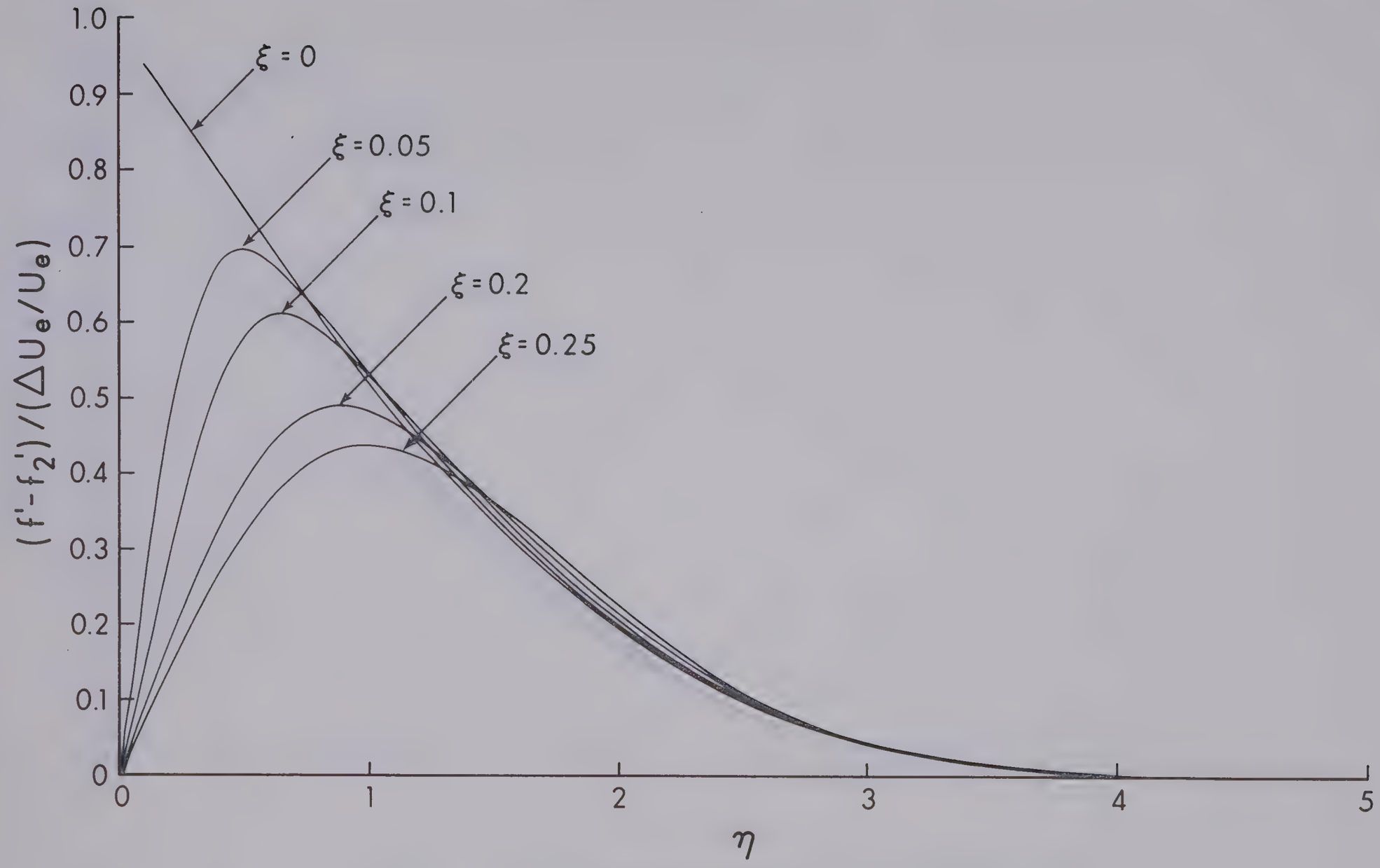

Figure 8 Distribution of the Transient Contribution to the Velocity Function for $S_w = 0.2$ and $\beta = 0.4$

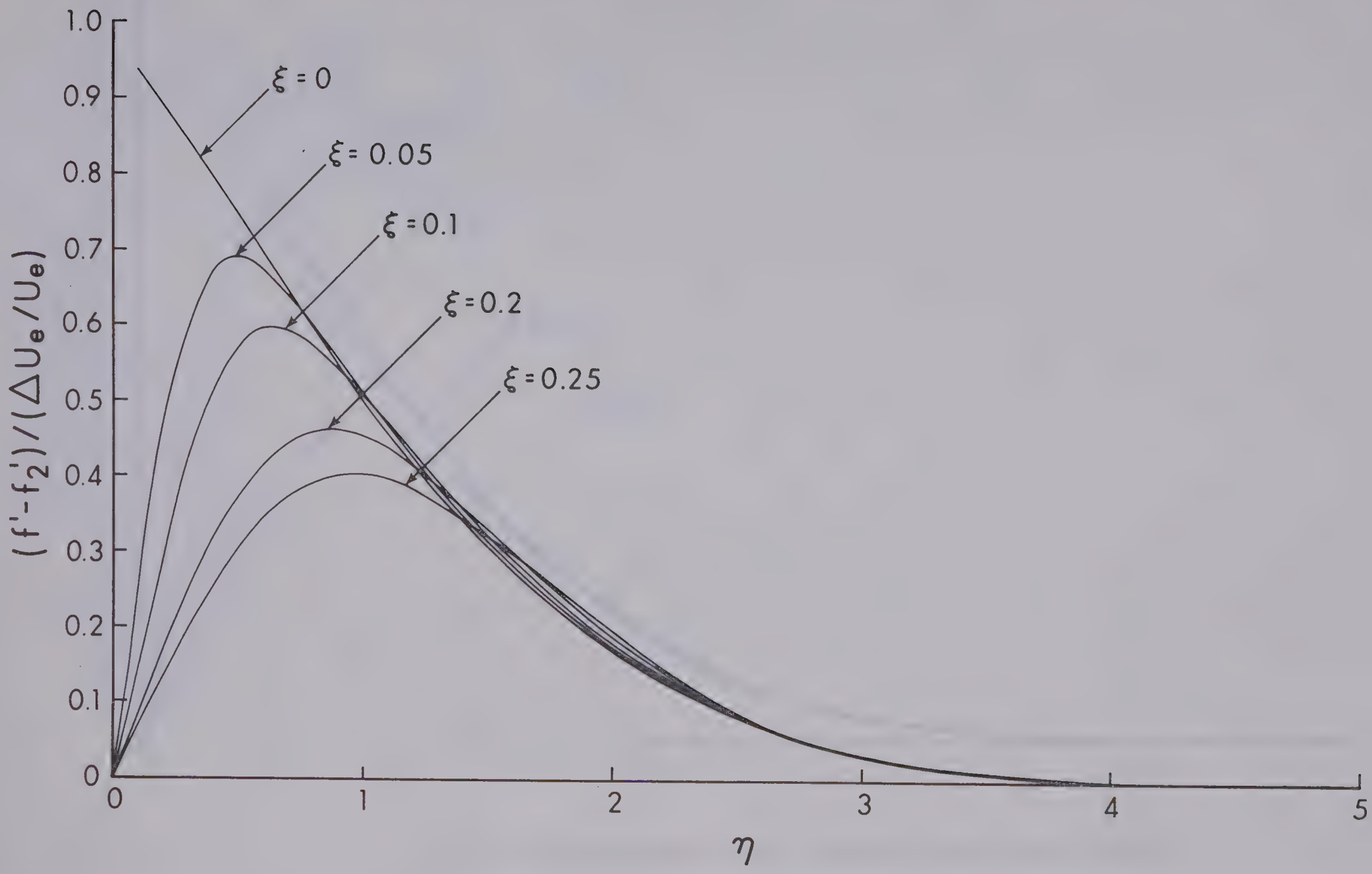

Figure 9 Distribution of the Transient Contribution to the Velocity Function for $S_w = 0.6$ and $\beta = 0.4$

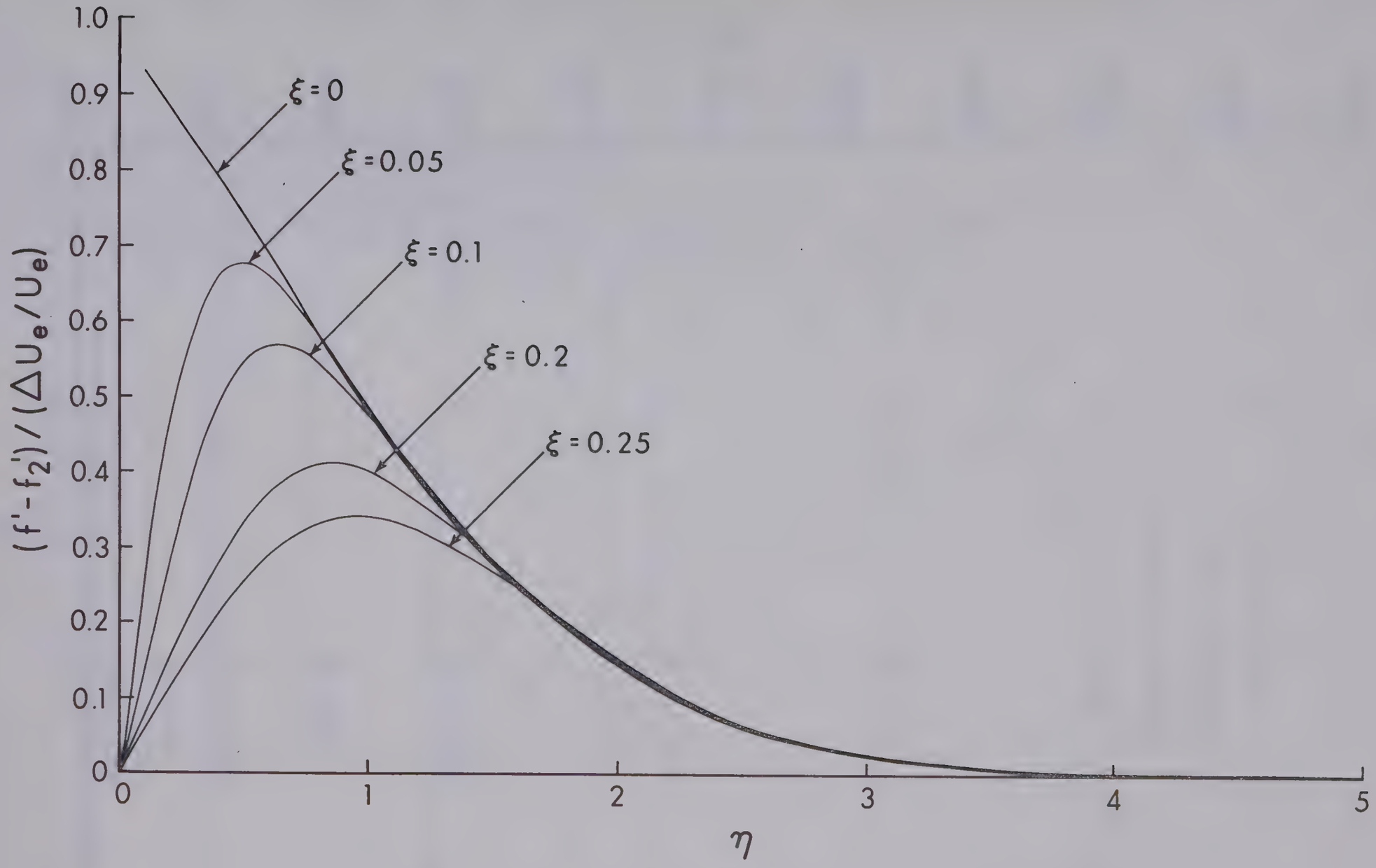

Figure 10 Distribution of the Transient Contribution to the Velocity Function for an Insulated Plate and $\beta = 0.4$

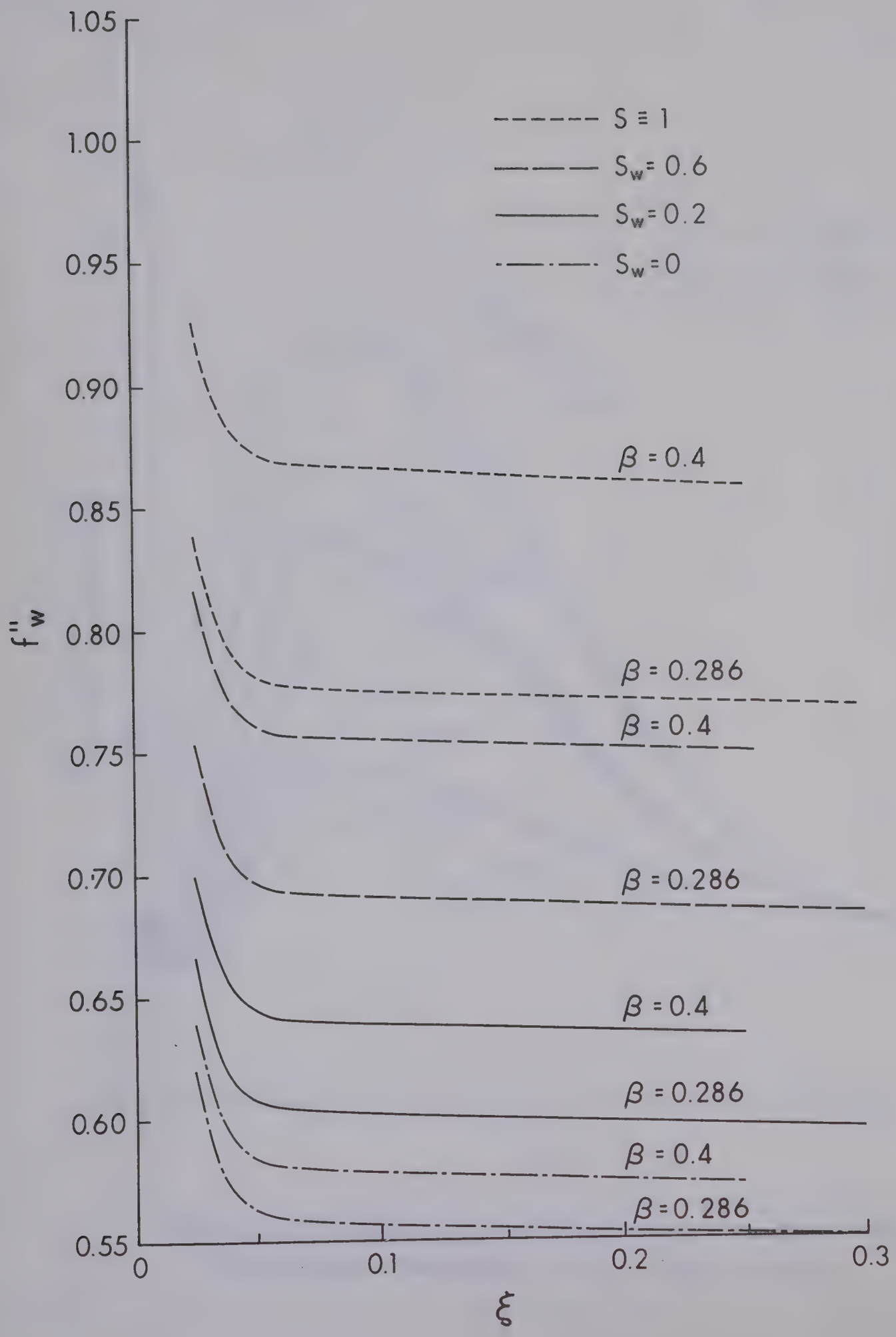

Figure 11 Transient Distribution of Shear Function

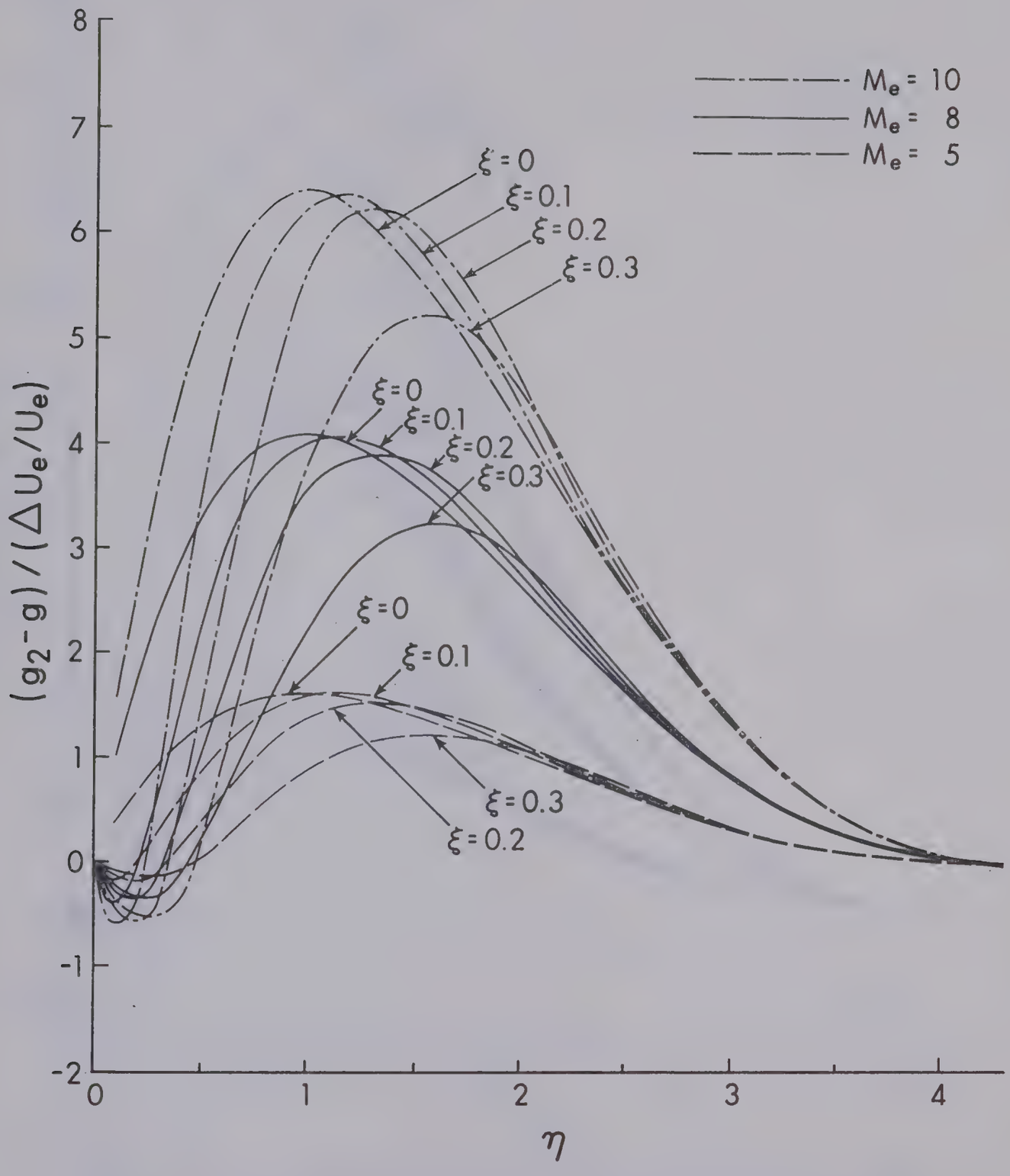

Figure 12 Distribution of the Transient Contribution to the Boundary-Layer Temperature for $S_w = 0$ and $\beta = 0.286$

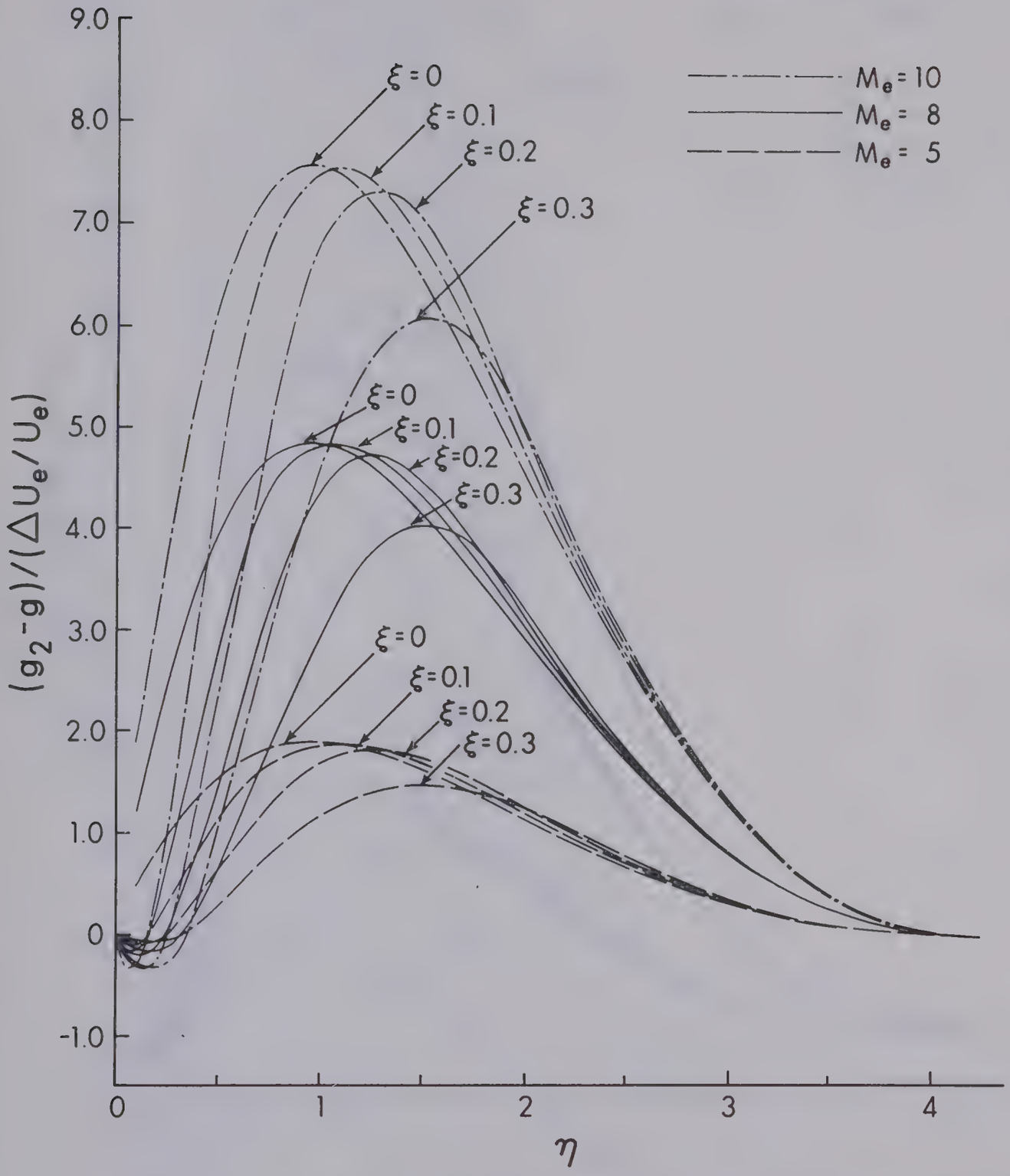

Figure 13 Distribution of the Transient Contribution to the Boundary-Layer Temperature for $S_w = 0.2$ and $\beta = 0.286$

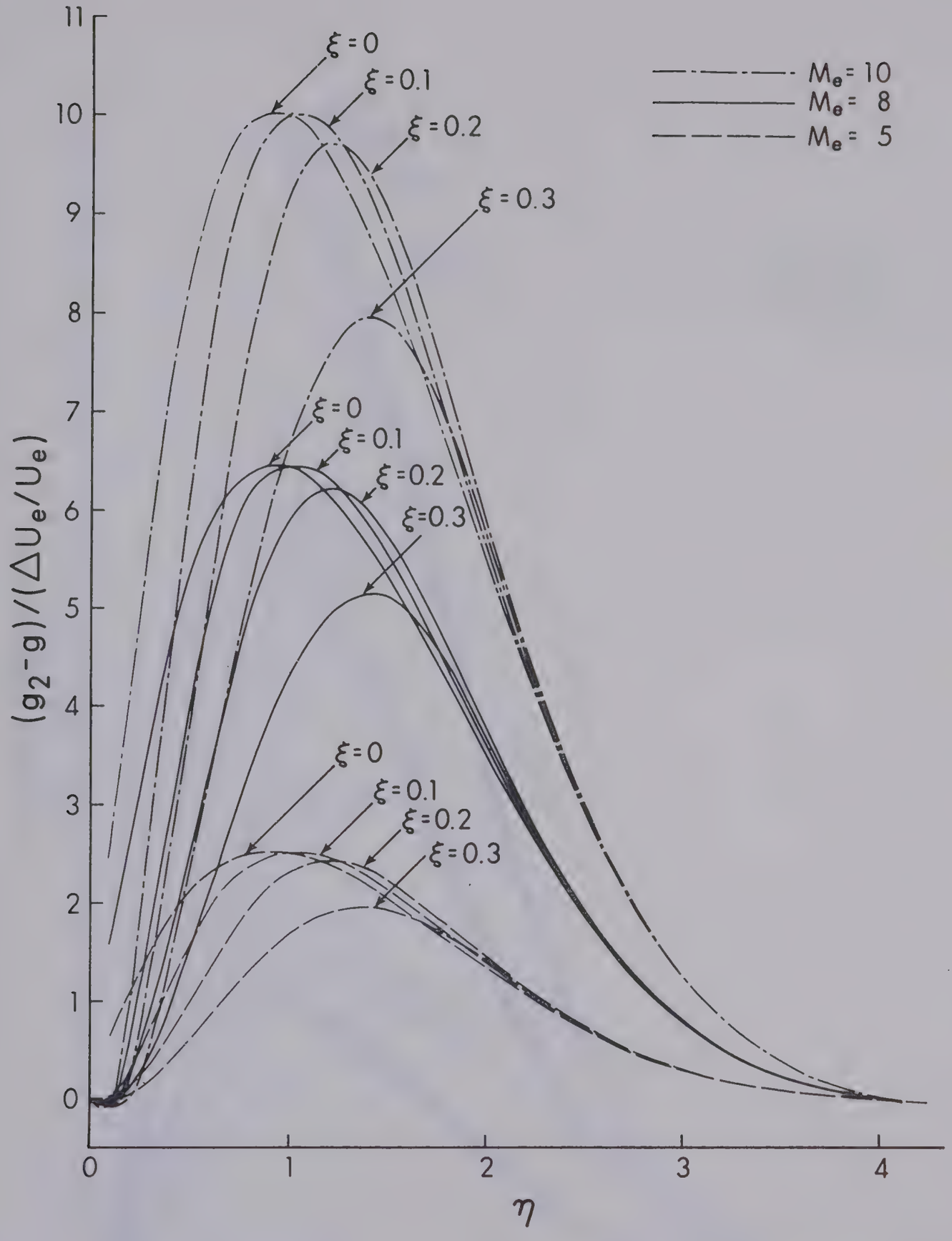

Figure 14 Distribution of the Transient Contribution to the Boundary-Layer Temperature for $S_w = 0.6$ and $\beta = 0.286$

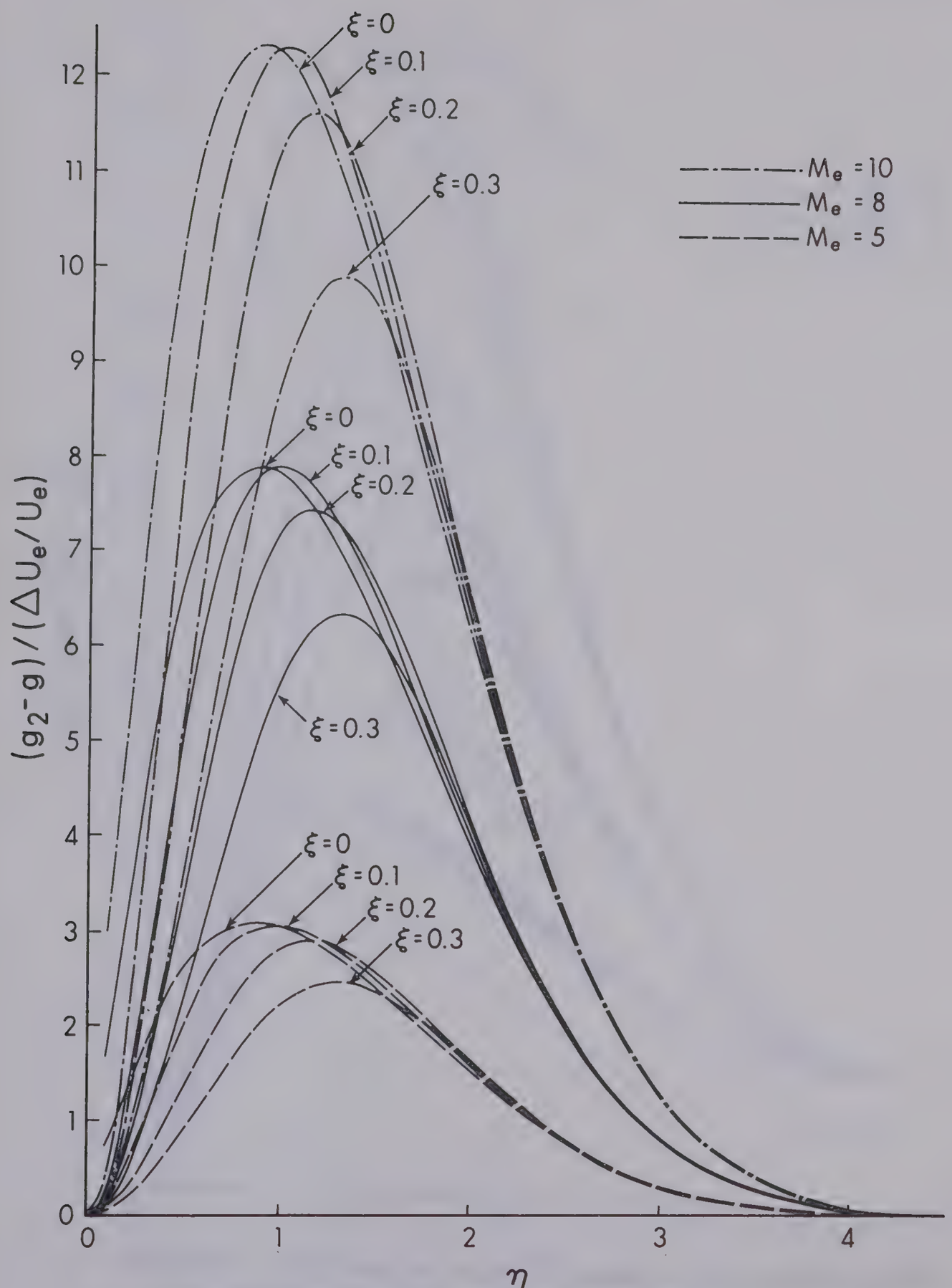

Figure 15 Distribution of the Transient Contribution to the Boundary-Layer Temperature for an Insulated Plate and $\beta = 0.286$

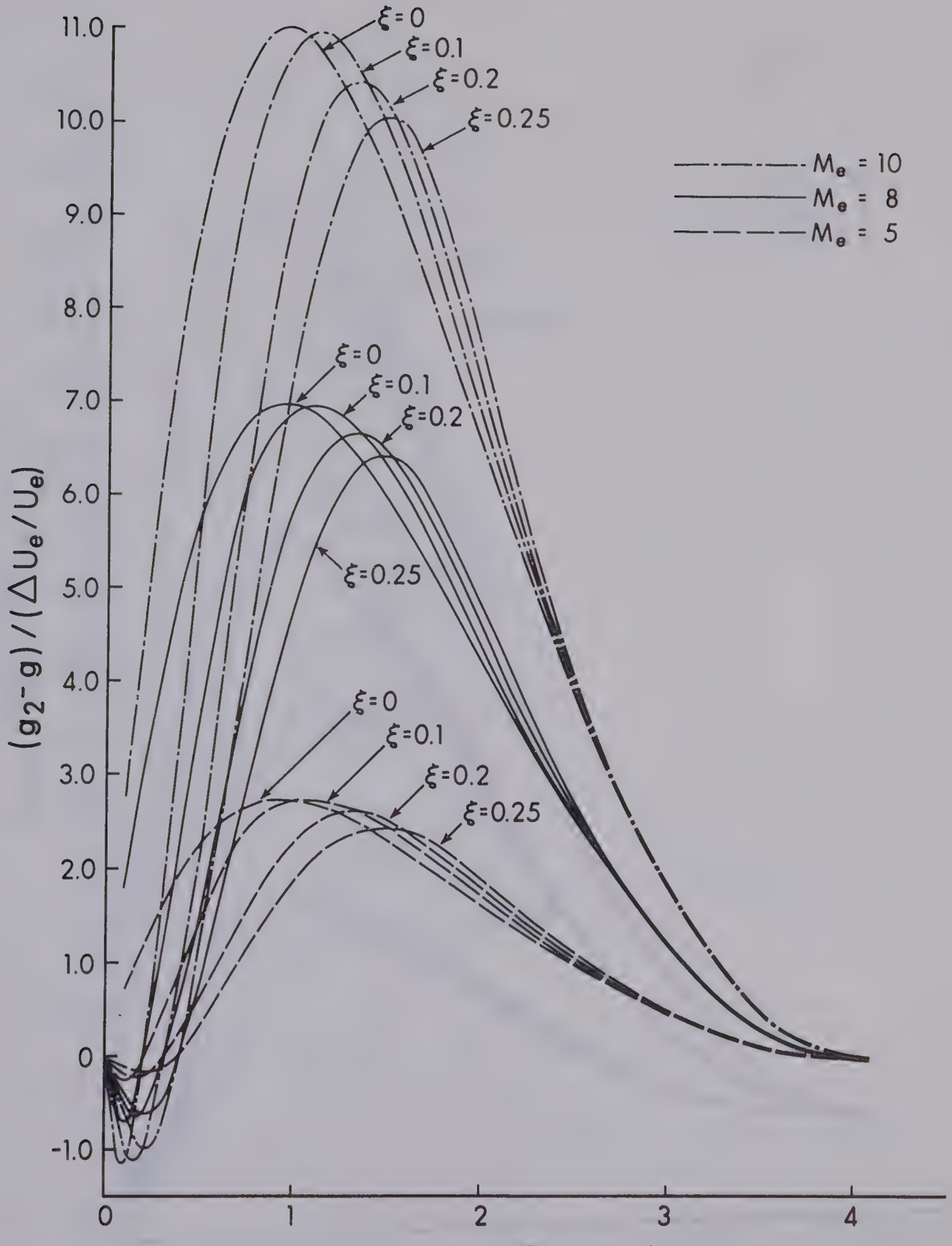

Figure 16 Distribution of the Transient Contribution to the Boundary-Layer Temperature for $S_w = 0$ and $\beta = 0.4$

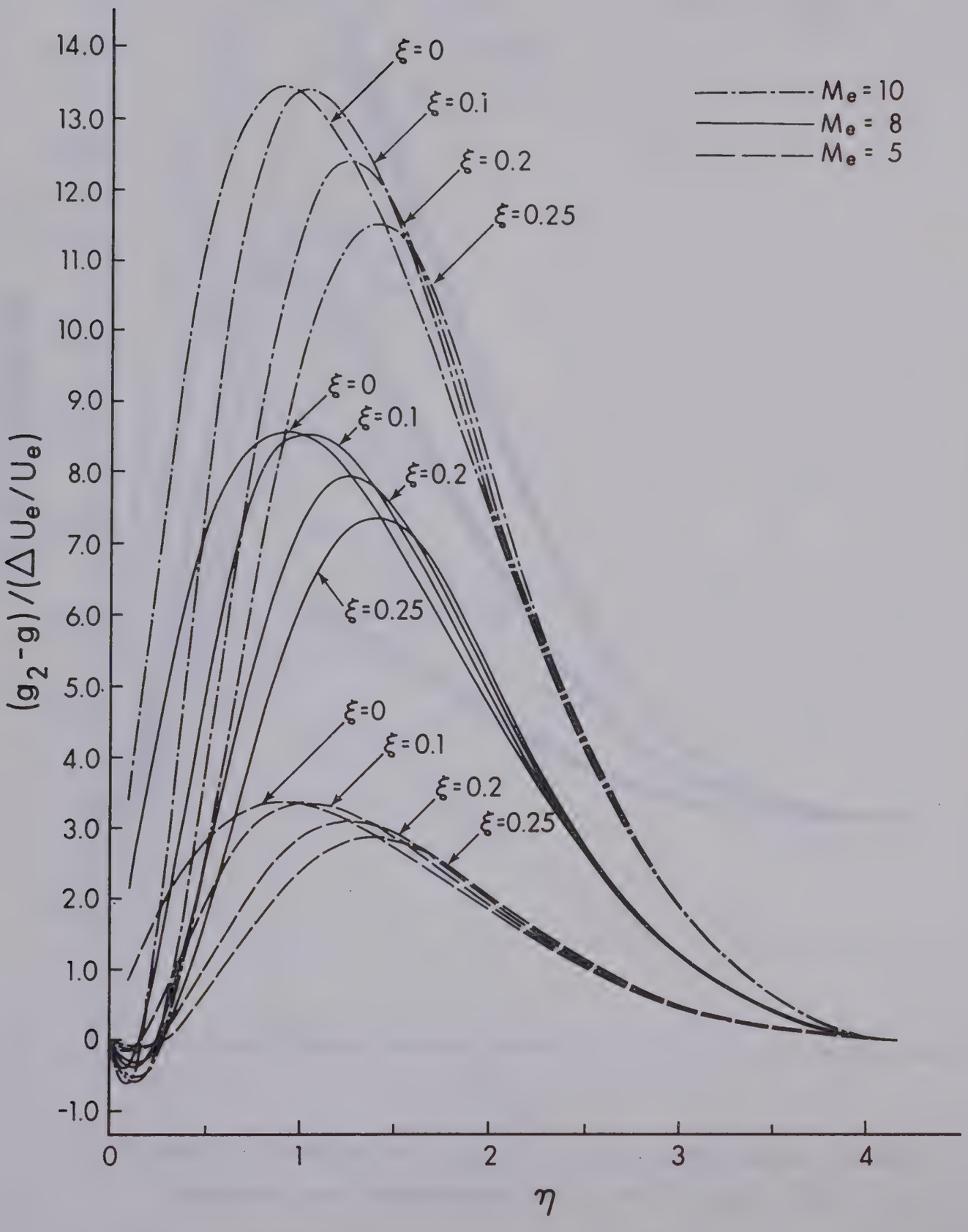

Figure 17 Distribution of the Transient Contribution to the Boundary-Layer Temperature for S_w = 0.2 and β = 0.4

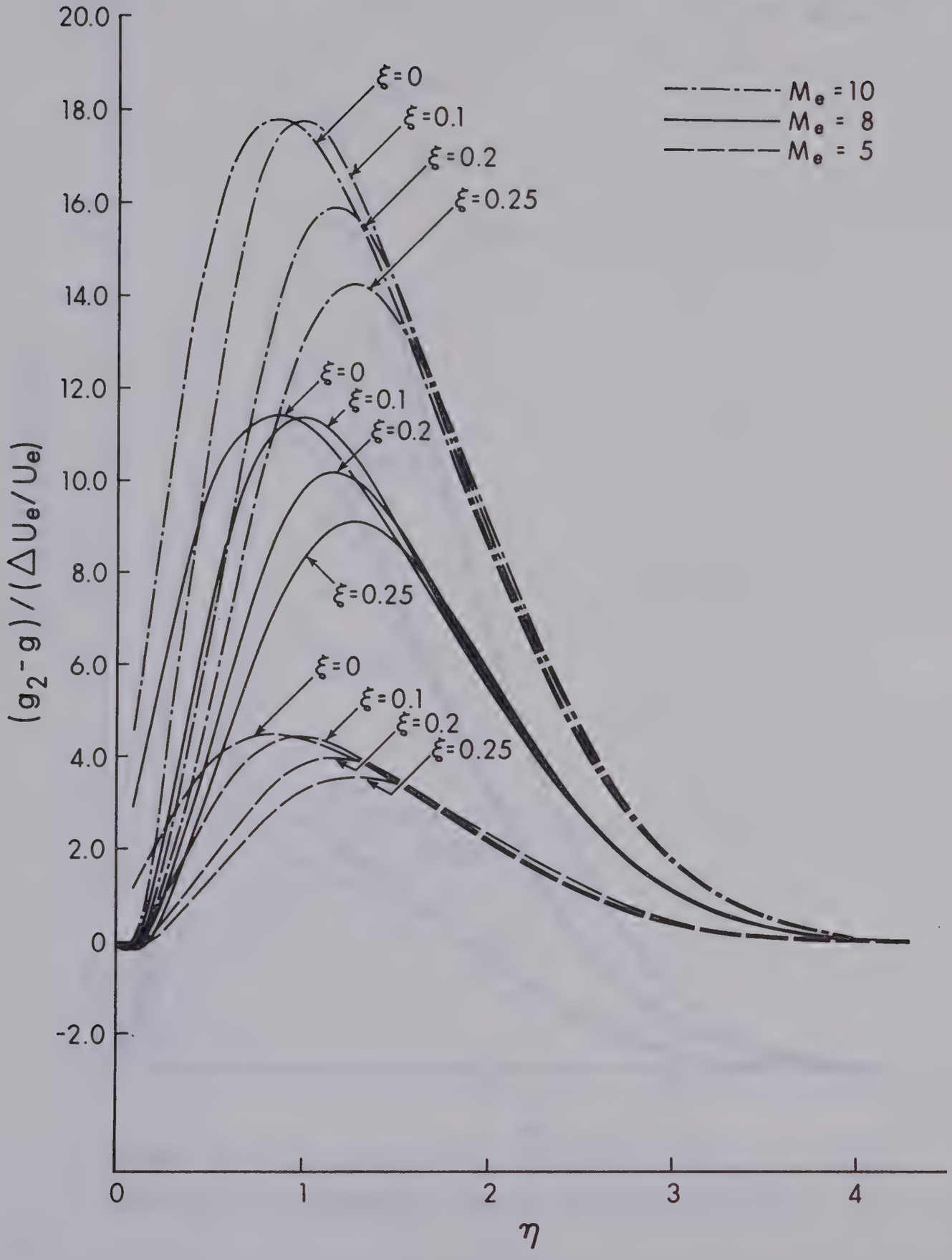

Figure 18 Distribution of the Transient Contribution to the Boundary-Layer Temperature for $S_w = 0.6$ and $\beta = 0.4$

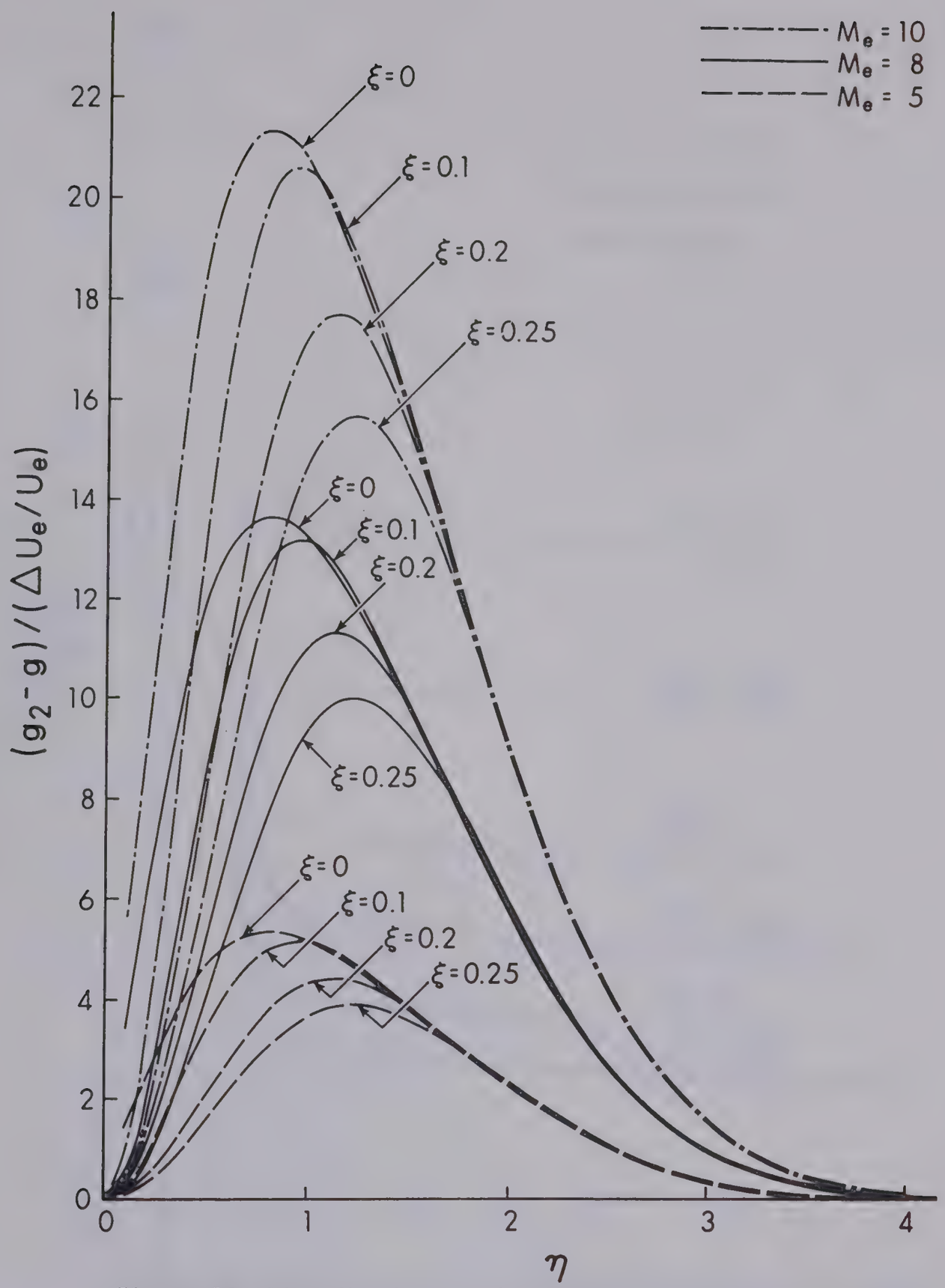

Figure 19 Distribution of the Transient Contribution to the Boundary-Layer Temperature for an Insulated Plate and $\beta = 0.4$

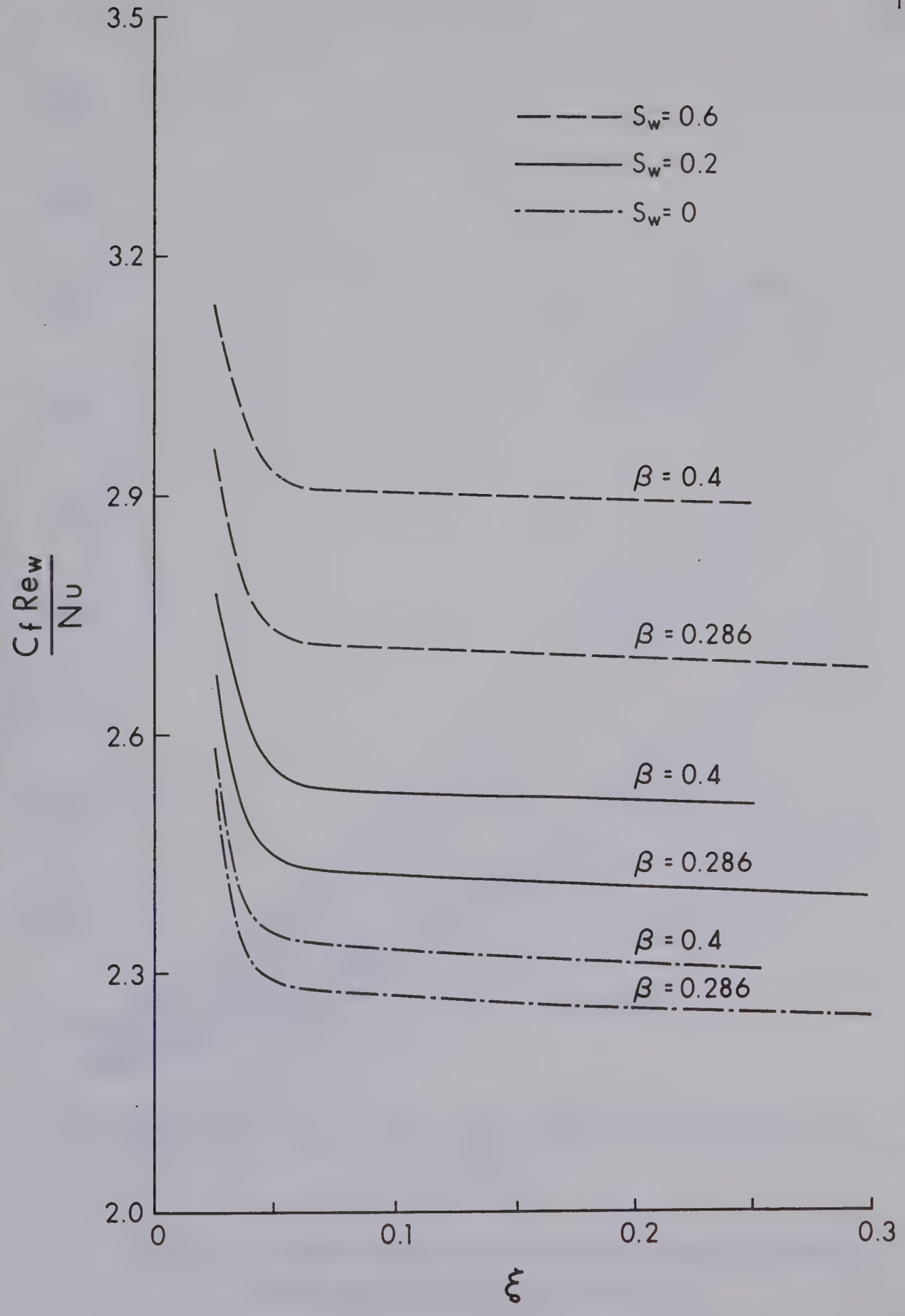

Figure 20 Transient Distribution of Reynolds Analogy Parameter

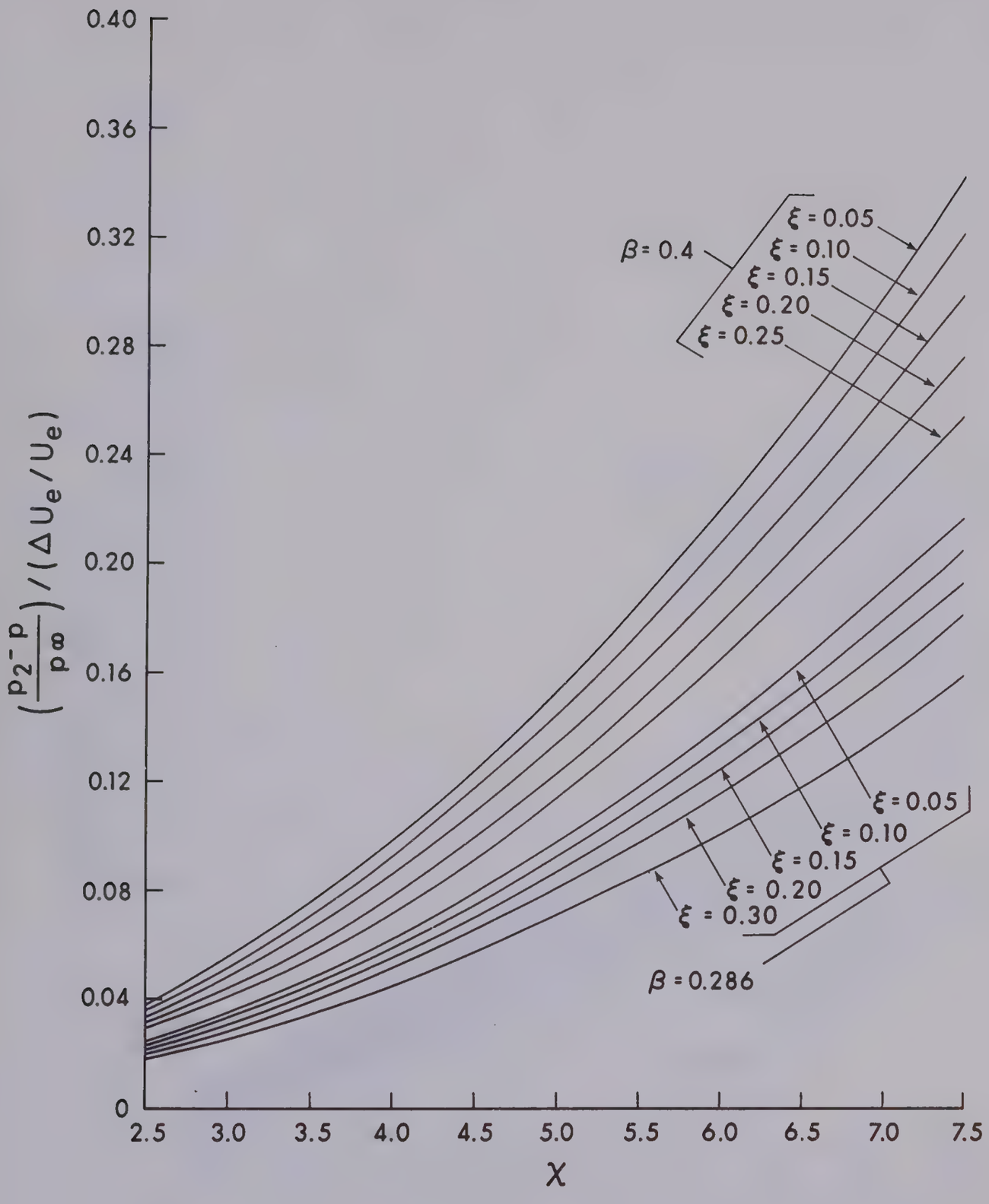

Figure 21 Transient Contribution to the Induced Pressure Distribution for $S_w = 0$ and $M_e = 5$

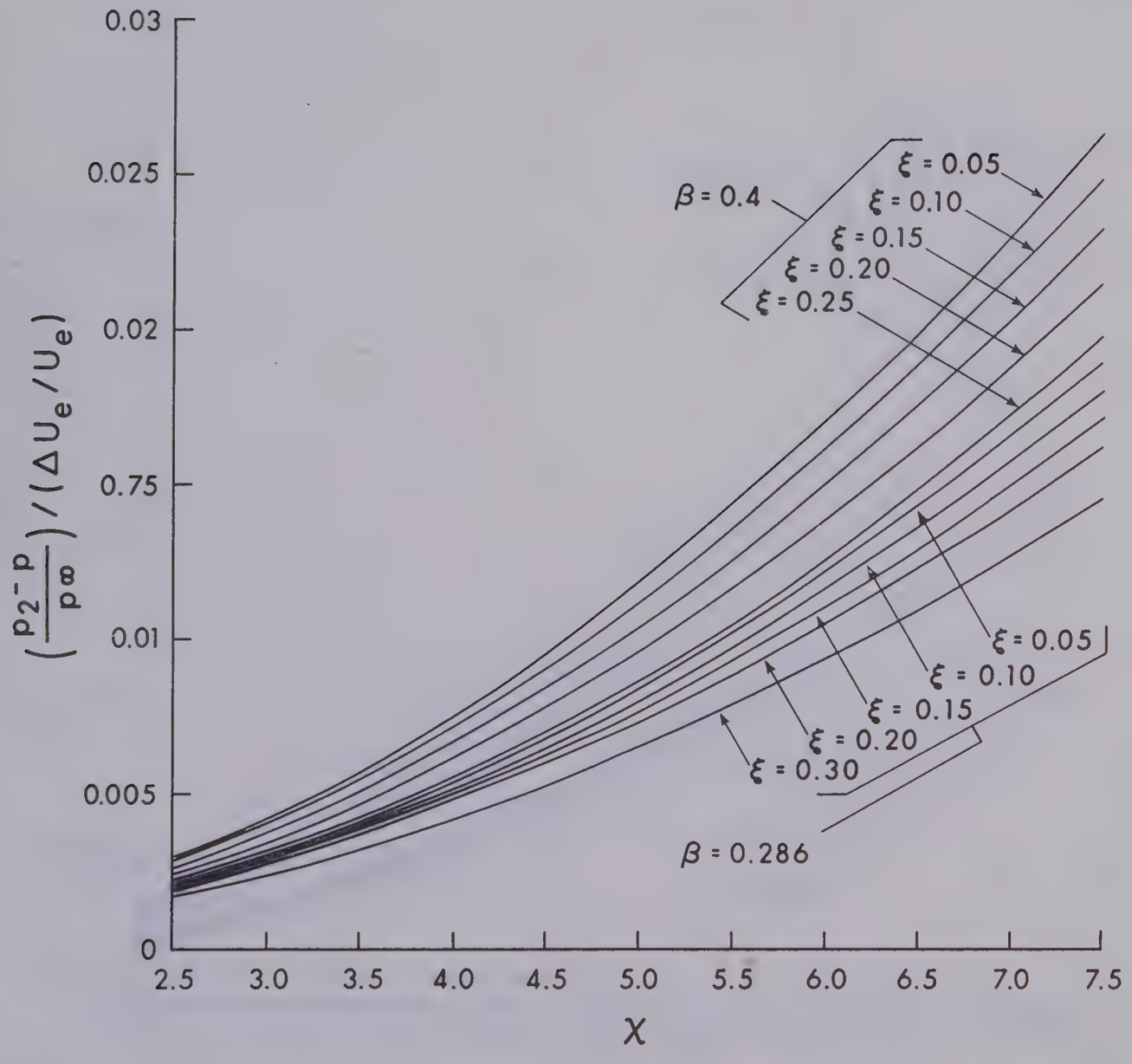

Figure 22 Transient Contribution to the Induced Pressure Distribution for $S_w = 0$ and $M_e = 10$

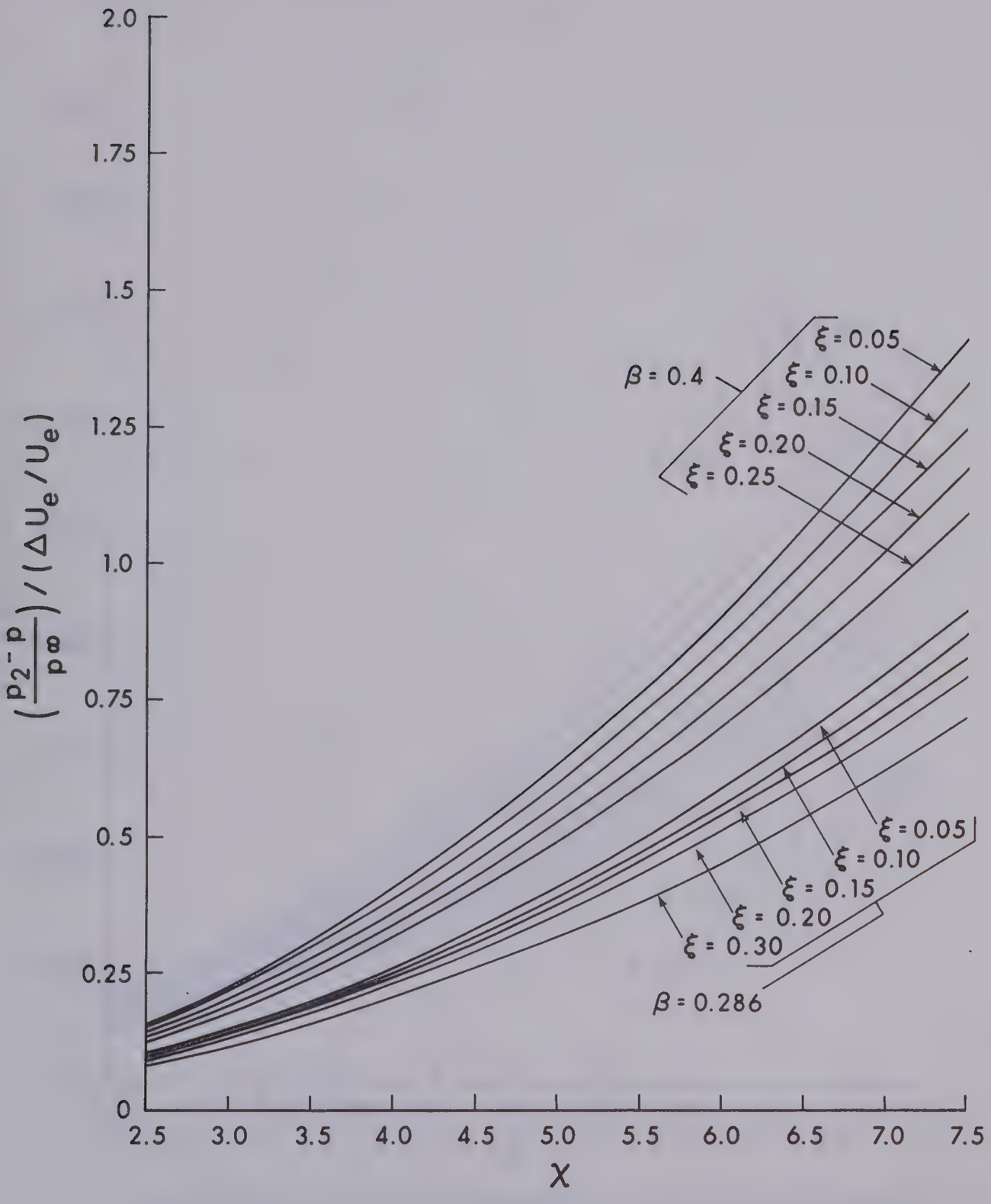

Figure 23 Transient Contribution to the Induced Pressure Distribution for $S_w = 0.6$ and $M_e = 5$

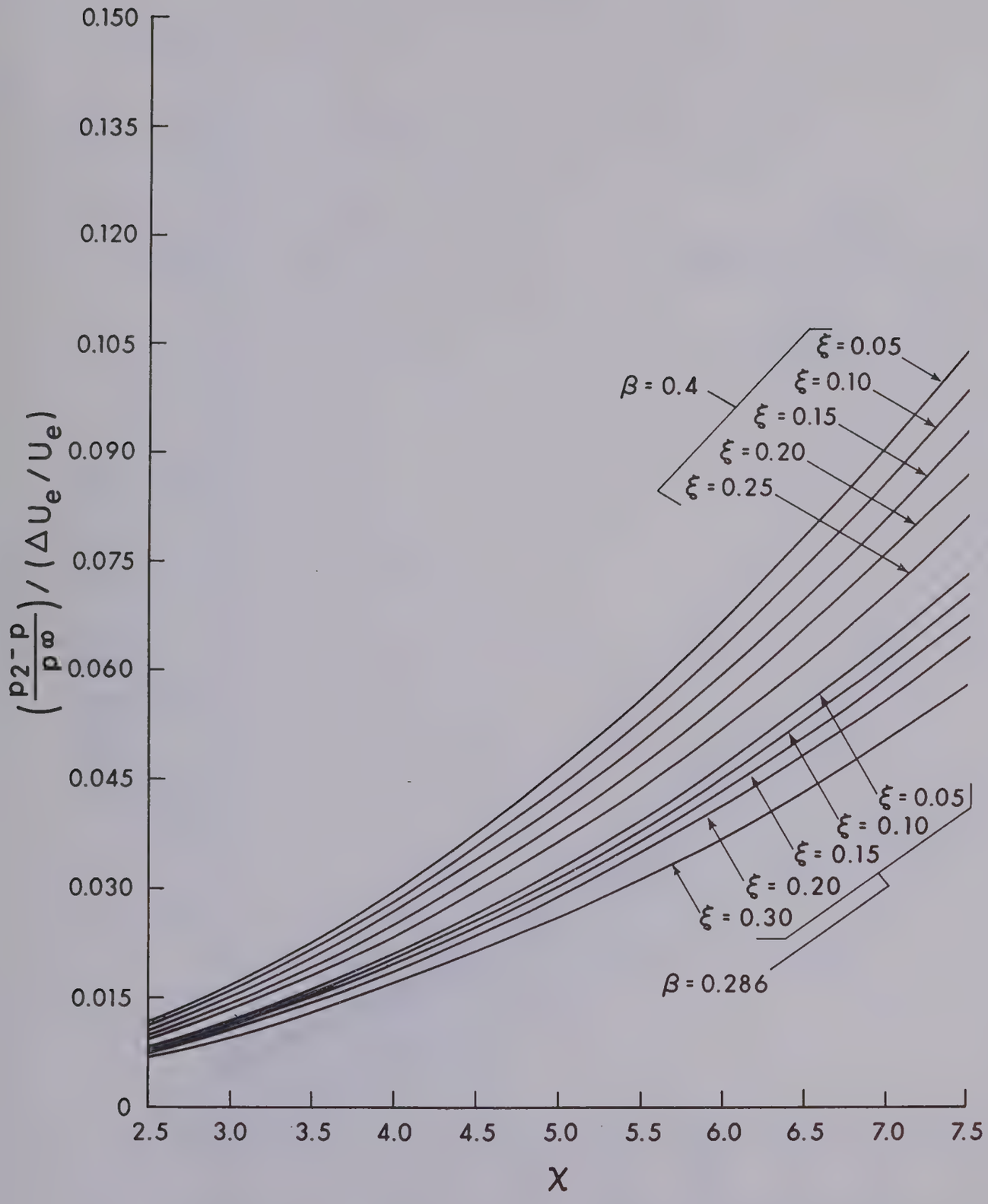

Figure 24 Transient Contribution to the Induced Pressure Distribution for $S_w = 0.6$ and $M_e = 10$

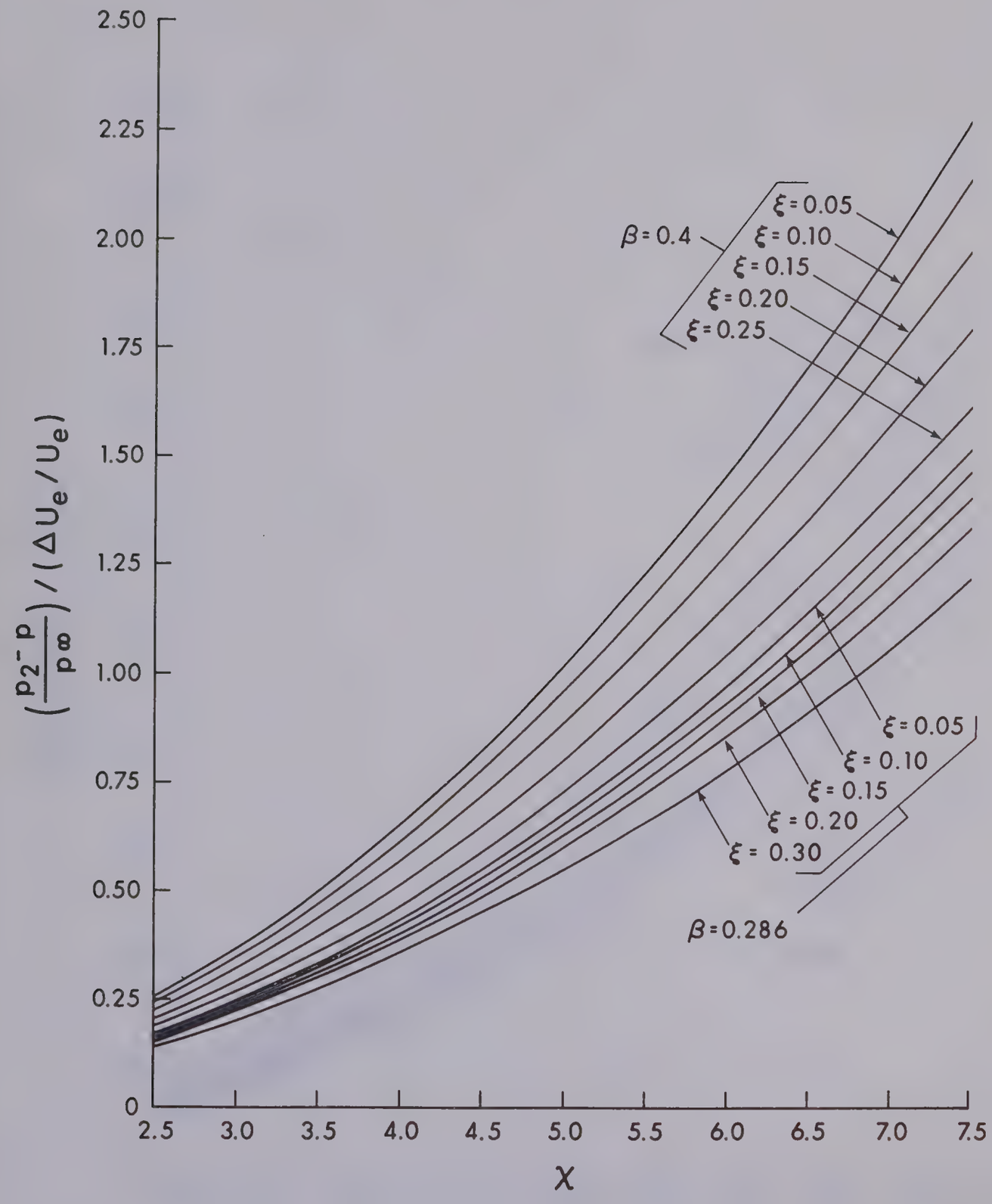

Figure 25 · Transient Contribution to the Induced Pressure Distribution for an Insulated Plate and $M_e = 5$

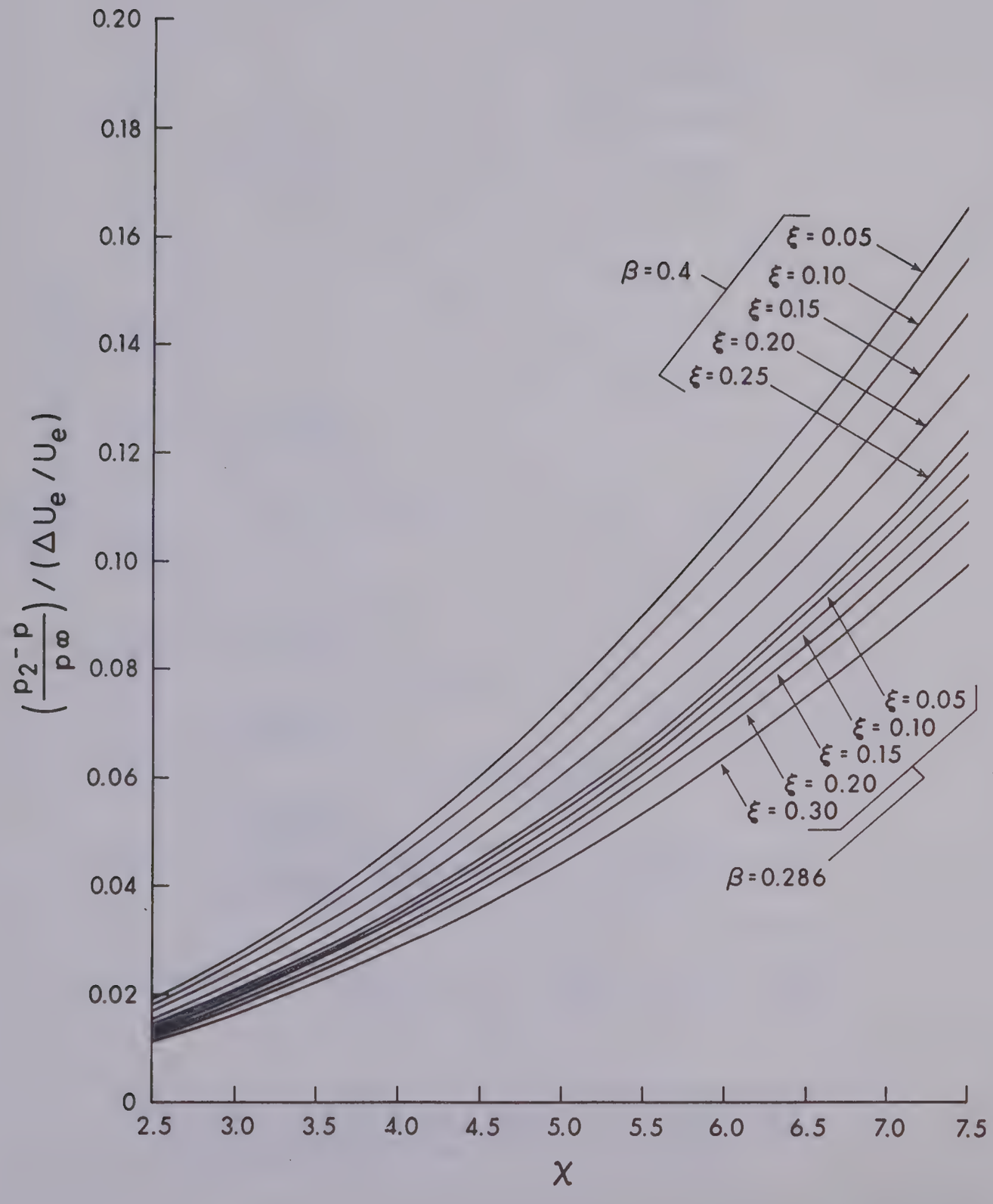

Figure 26 Transient Contribution to the Induced Pressure Distribution for an Insulated Plate and $M_e = 10$

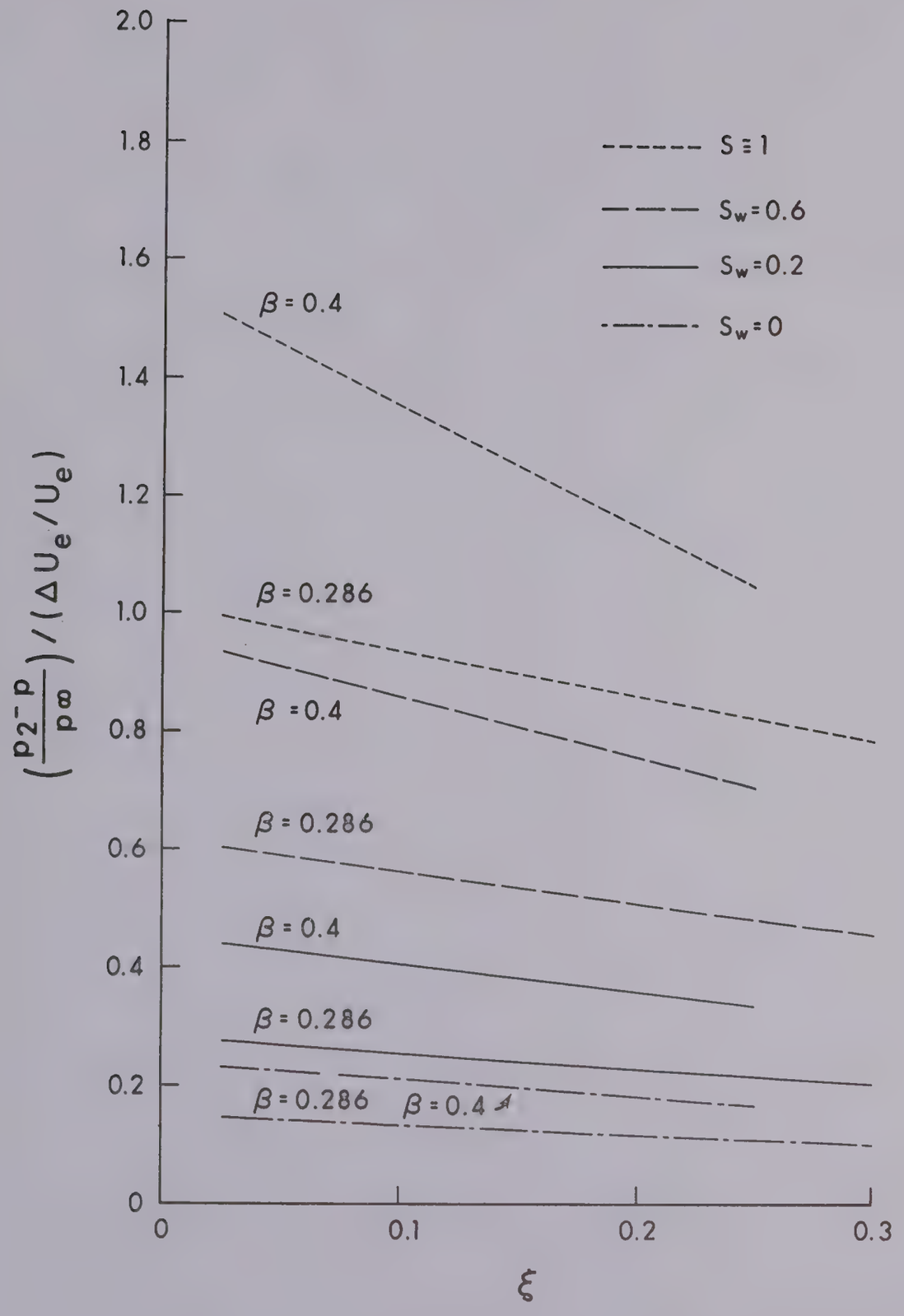

Figure 27 Transient Contribution to the Induced Pressure Distribution for $\chi = 6$ and $M_e = 5$